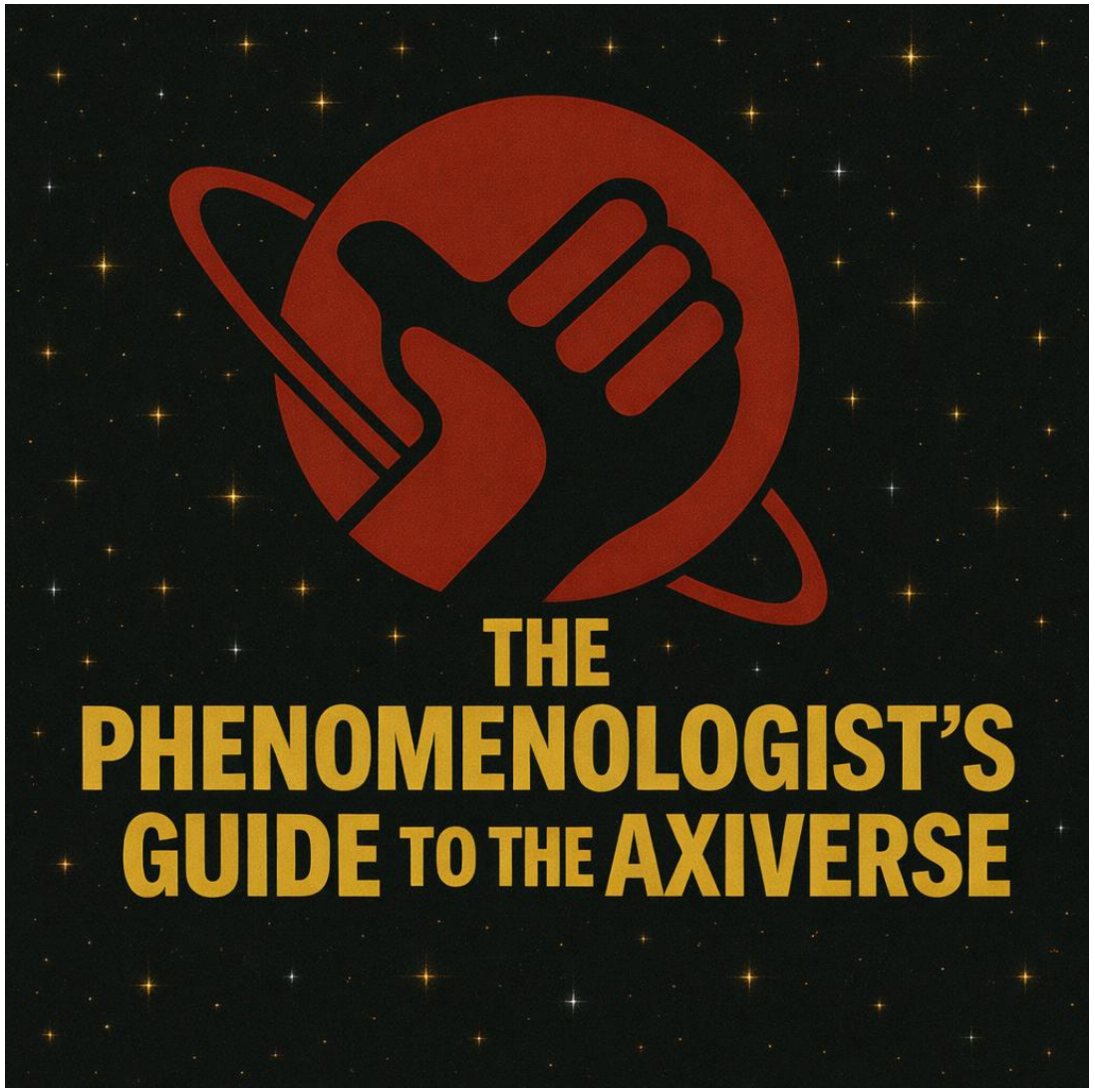

Sokratis Trifinopoulos

3rd March 2026

What is Phenomenology?

"We demand rigidly defined areas of doubt and uncertainty!"
— Douglas Adams, The Hitchhiker's Guide to the Galaxy

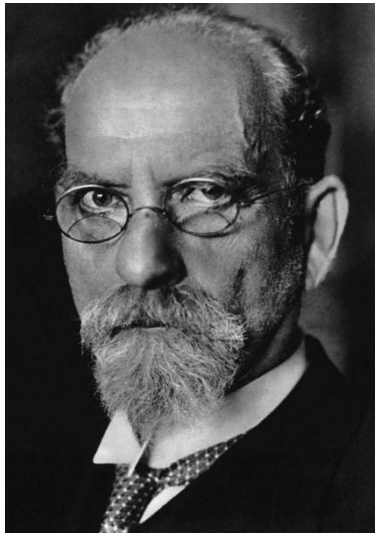

ChatGPT 5.2

What is Phenomenology?

Phenomenology is a philosophical approach that investigates conscious experience as it is directly lived and perceived. It focuses on how phenomena appear in awareness, while setting aside background assumptions about what might underlie or cause that experience.

What is the etymology of the term?

The term *phenomenology* comes from the Greek words *phainómenon*, meaning "that which appears," and *lógos*, meaning "study" or "discourse." It entered the English language in the late 18th century and became closely tied to Husserl's philosophy in a 1907 article in *The Philosophical Review*.

What is Phenomenology (in Physics)?

Phenomenology (in physics) is the application of theoretical models to make predictions that can be directly tested by experiments. In modern usage, phenomenology often operates at the level of effective theories, describing physics across multiple scales without requiring a complete microscopic or fundamental description.

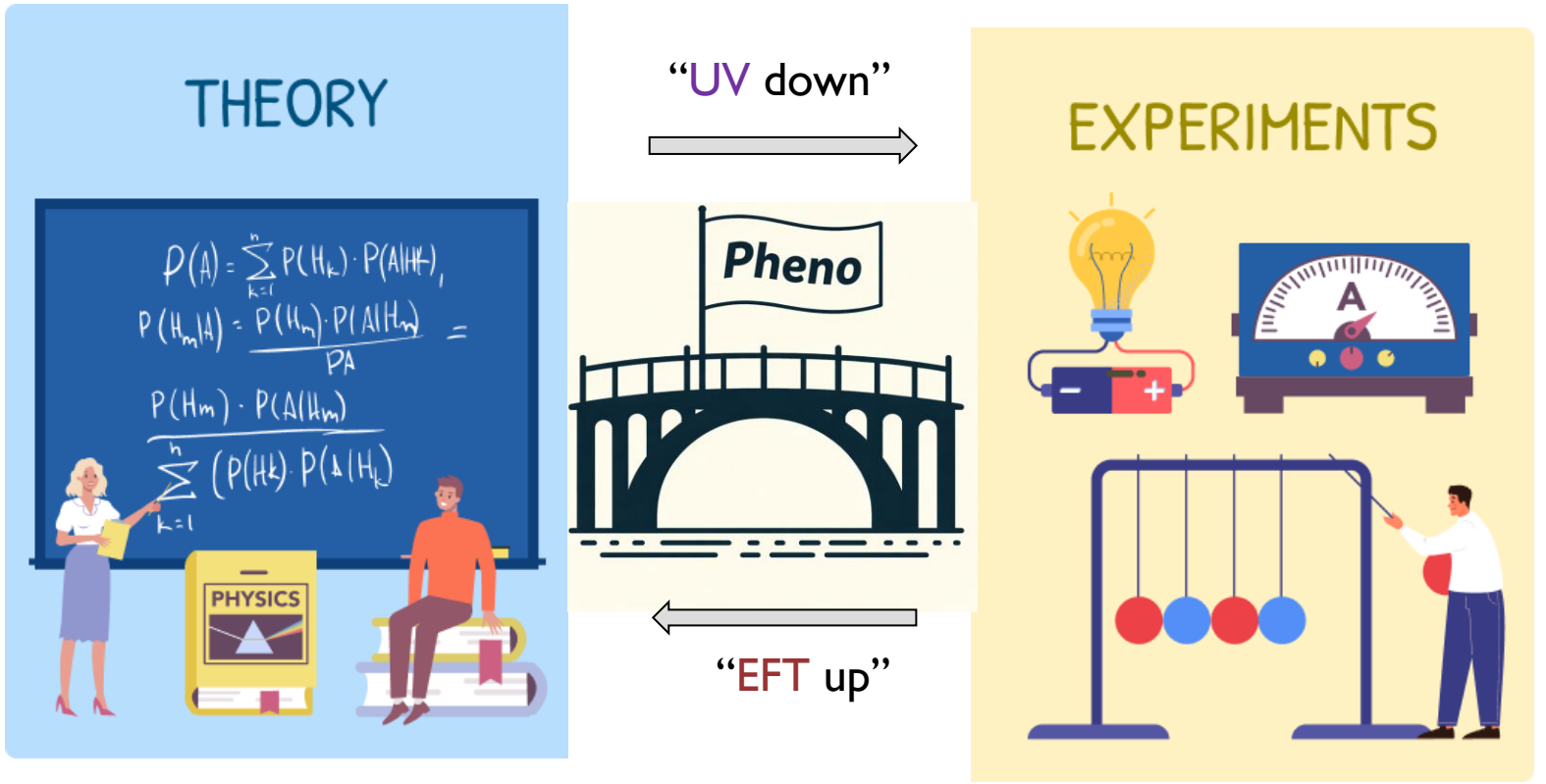

Sokratis Trifinopoulos

A broad and growing field

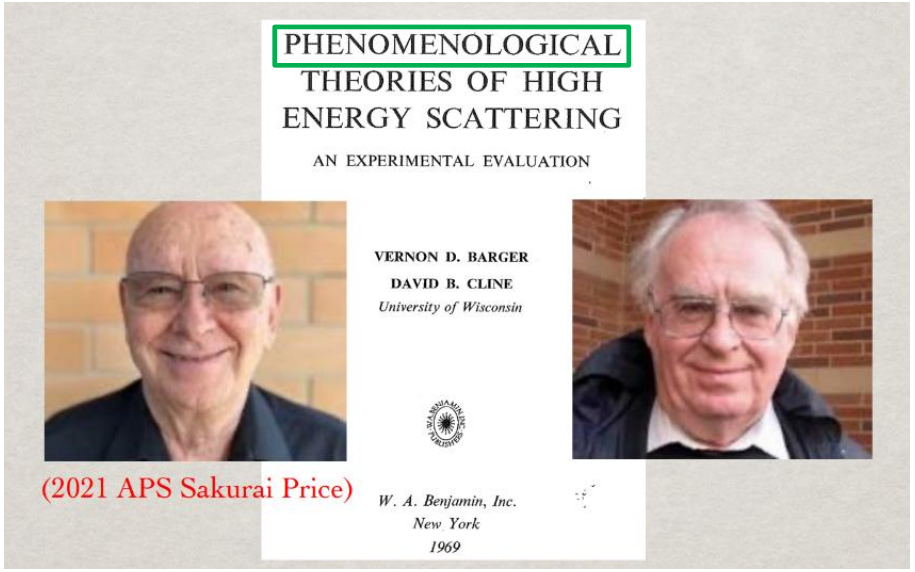

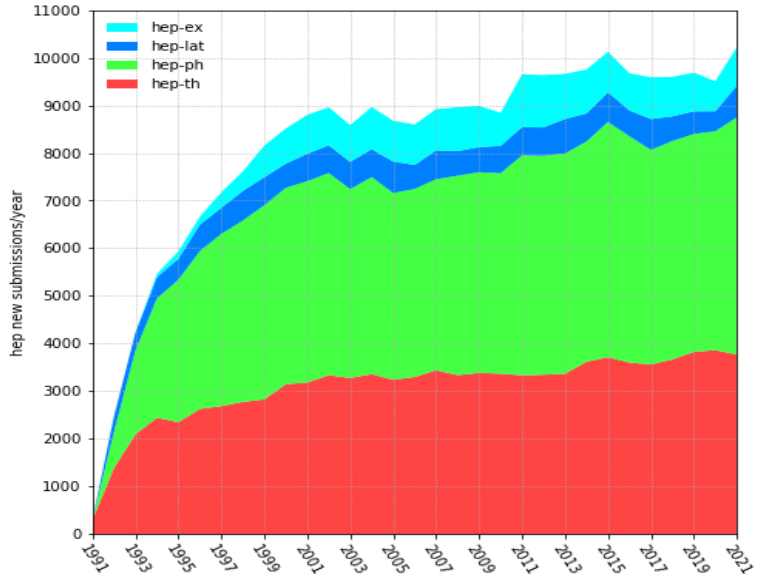

arXiv.org > **category taxonomy**

Search... All fields Search

Help | Advanced Search

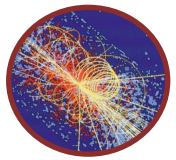

HIGH ENERGY PHYSICS - PHENOMENOLOGY
(HEP-PH)

hep-ph (High Energy Physics - Phenomenology)

Theoretical particle physics and its interrelation with experiment. Prediction of particle physics observables: models, effective field theories, calculation techniques. Particle physics: analysis of theory through experimental results.

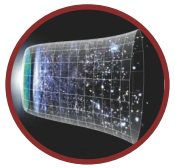

ASTROPHYSICS
(ASTRO-PH)

astro-ph.CO
(Cosmology and Nongalactic Astrophysics)

Phenomenology of early universe, cosmic microwave background, cosmological parameters, primordial element abundances, extragalactic distance scale, large-scale structure of the universe. Groups, superclusters, voids, intergalactic medium. Particle astrophysics: dark energy, dark matter, baryogenesis, leptogenesis, inflationary models, reheating, monopoles, WIMPs, cosmic strings, primordial black holes, cosmological gravitational radiation

CERN

A journey across cosmic scales

- A prime example of a broad phenomenological endeavor that spans $O(10^{70})$ in mass is the search for **dark matter**.

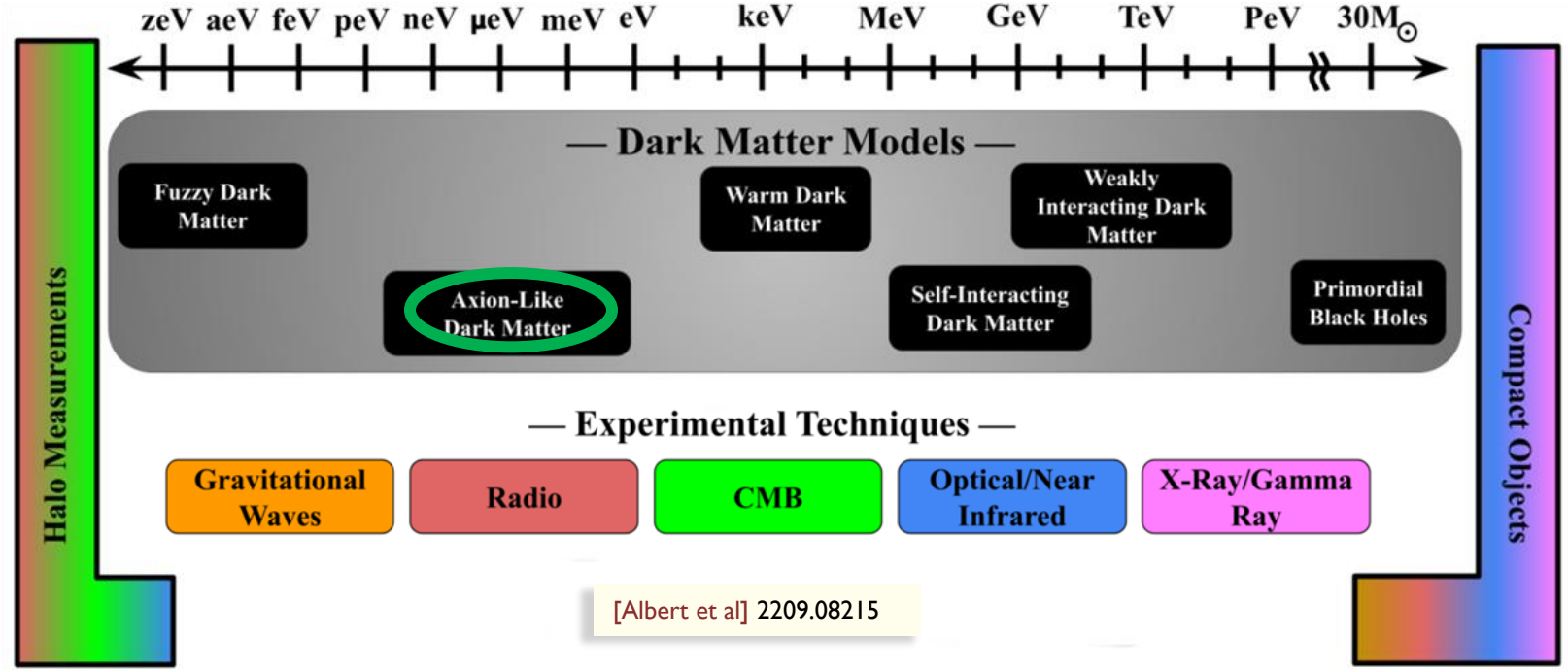

- Axions are one of the most well-motivated and sought-after **New Physics** particles.

Axions clean up many problems

- The QCD axion a famously solves the strong CP problem:

  QCD allows a CP-violating term: $\mathcal{L}_\theta \supset \frac{\alpha_s}{8\pi}\theta\, G^{\mu\nu}\tilde{G}_{\mu\nu}$, with $\theta \sim O(1)$.

  However, experimentally we find $|\theta| \leq 10^{-10}$. Why?

  Minimal elegant solution: global Peccei-Quinn symmetry $U(1)_{\rm PQ}$, which is spontaneously broken at high scale f_a, and introduces the axion field $a(x)$:

$$\theta \to \theta + \frac{a(x)}{f_a}$$

  Non-perturbative QCD generates: $V(a) \sim \Lambda_{\rm QCD}^4 \left[1 - \cos\left(\theta + \frac{\langle a\rangle}{f_a}\right)\right]$, whose minimum $\langle a\rangle = -\, f_a\, \theta$ dynamically sets $\boxed{\theta \to 0}$ and $m_a \approx \Lambda_{\rm QCD}^2 / f_a$.

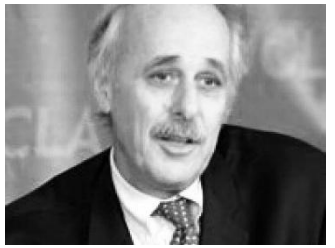

[Peccei, Quinn]
PRL 38 (1977) 1440-1443

- Unexpected bonus: Axions are stable + weakly-interacting $\sim f_a^{-1}$ + non-thermal

  ✓ excellent **cold dark matter (CDM)** candidates

What is the Axiverse?

What is the Axiverse?

> A scenario in which fundamental theory predicts a large spectrum of light pseudoscalar fields — axion-like particles — with masses distributed logarithmically over many orders of magnitude.

[Svrček, Witten] hep-th/0605206
[Arvanitaki et al] 0905.4720
[Kim] PRL 43(1979)103
[Musco] 1809.02127
[Giudice, McCullough] 1610.07962
[Choi, Im] 1511.00132

Examples: i) string compactifications: ALPs = zero-modes of higher-D tensor fields, ii) new strong confinging sectors: ALPs = pseudo-Goldstone bososns (similar to pions), iii) Clockwork mechanism, iv) Electroweak relaxation, *etc.*

String Axiverse

Asimina Arvanitaki, Savas Dimopoulos, Sergei Dubovsky, Nemanja Kaloper, John March-Russell

String theory suggests the simultaneous presence of many ultralight axions possibly populating each decade of mass down to the Hubble scale 10^-33eV. Conversely the presence of such a plenitude of axions (an "axiverse") would be evidence for string theory, since it arises due to the topological complexity of the extra-dimensional manifold and is ad hoc in a theory with just the four familiar dimensions. We investigate how upcoming astrophysical experiments will explore the existence of such axions over a vast mass range from 10^-33eV to 10^-10eV. Axions with masses between 10^-33eV to 10^-28eV cause a rotation of the CMB polarization that is constant throughout the sky. The predicted rotation angle is of order \alpha~1/137. Axions in the mass range 10^-28eV to 10^-18eV give rise to multiple steps in the matter power spectrum, that will be probed by upcoming galaxy surveys. Axions in the mass range 10^-22eV to 10^-10eV affect the dynamics and gravitational wave emission of rapidly rotating astrophysical black holes through the Penrose superradiance process. When the axion Compton wavelength is of order of the black hole size, the axions develop "superradiant" atomic bound states around the black hole "nucleus". Their occupation number grows exponentially by extracting rotational energy from the ergosphere, culminating in a rotating Bose-Einstein axion condensate emitting gravitational waves. This mechanism creates mass gaps in the spectrum of rapidly rotating black holes that diagnose the presence of axions. The rapidly rotating black hole in the X-ray binary LMC X-1 implies an upper limit on the decay constant of the QCD axion f_a<2*10^17GeV, much below the Planck mass. This reach can be improved down to the grand unification scale f_a<2*10^16GeV, by observing smaller stellar mass black holes.

ALPs and Dark Sectors

- For the QCD axion the CDM window is: $\underbrace{10^9}_{\text{stellar \& SN}} \lesssim \frac{f_a}{\text{GeV}} (\lesssim H_{\text{inf}}) < \underbrace{10^{17}}_{M_{\text{Pl}}}$ and $m_a \simeq 6\mu\text{eV}\left(\frac{10^{12}\text{GeV}}{f_a}\right)$.
- More general ALPs have *generic* masses $m_a \approx \Lambda^2 / f_a$ and dominant couplings to the SM particles (e.g. photons $g_{a\gamma\gamma}$, gluons g_{agg}, fermions g_{af} etc)
- Ultralight ALPs: proxies for dark sector that communicates to us only via gravity (*nightmare scenario*)
- Heavy ALPs: motivated by the quality problem, axion-gluon portals etc.

[Dimopoulos] PLB84(1979)435–439 [Holdom, Peskin] NPB 208(1982)397–412 [Agrawal, Hower] 1710.04213 [Gaillard et al] 1809.02127 [Hook et al] 1911.12364 [Fitzpatrick et al] 2306.03128

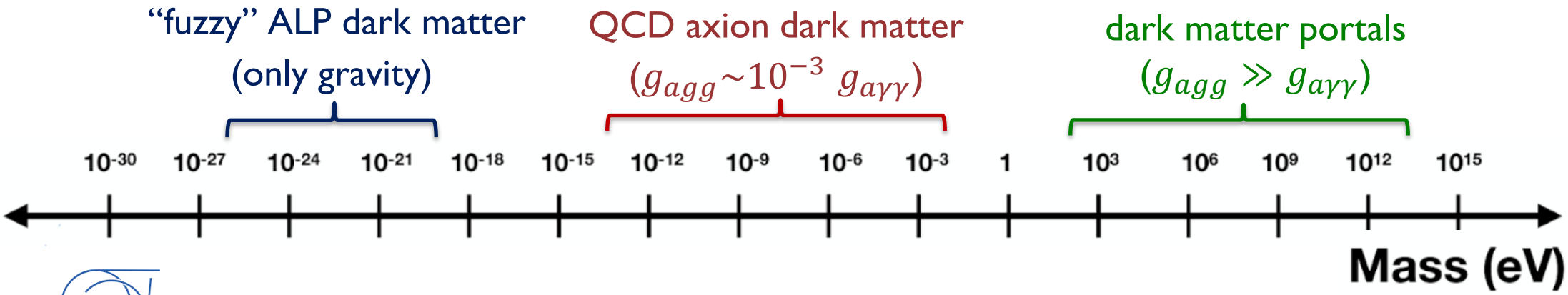

Exploring the *Axiverse*

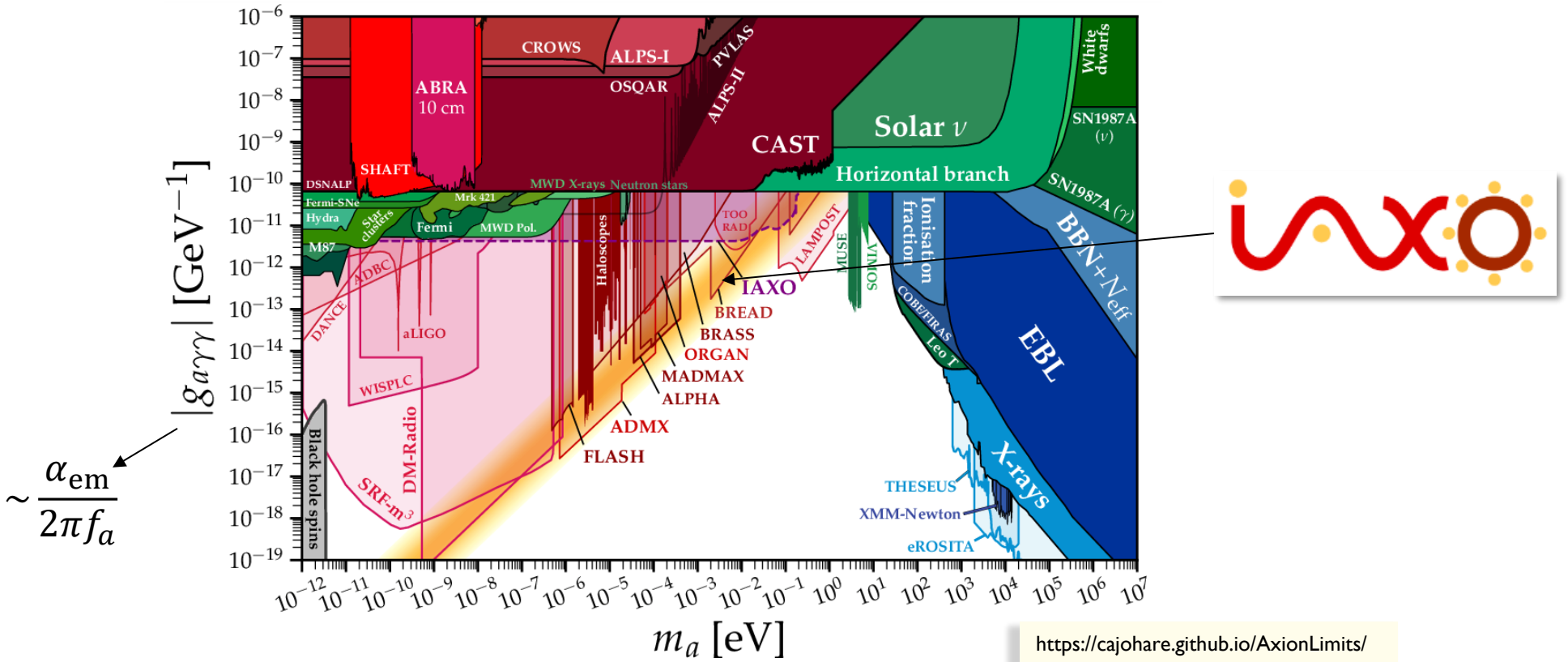

$$\sim \frac{\alpha_{\rm em}}{2\pi f_a}$$

https://cajohare.github.io/AxionLimits/

Many probes (large competition)

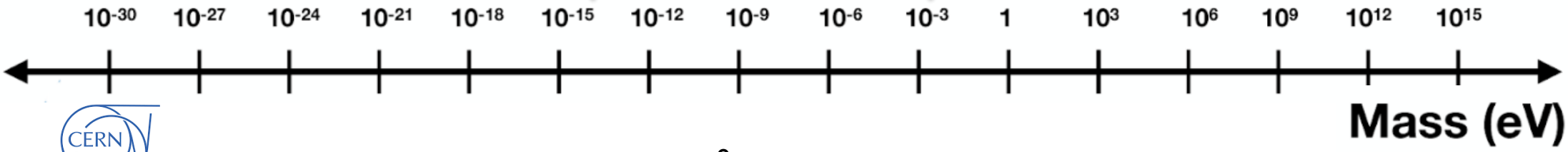

Exploring the *Axiverse*

[Ivanov, **Trifinopoulos**] 2508.04767

[Gorghetto, **Trifinopoulos**, Valogiannis] 2511.04734

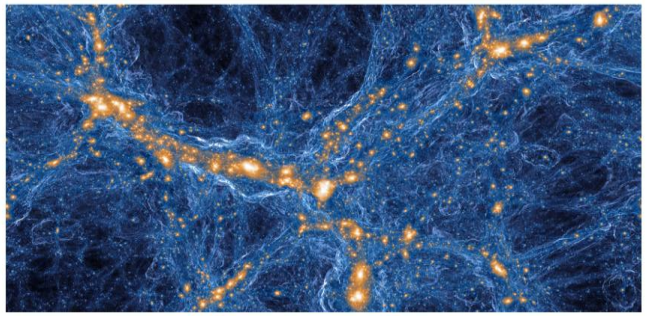

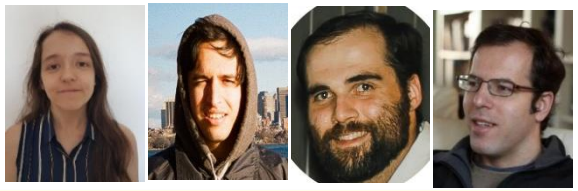

[Baruch, Fitzpatrick, Menzo, Soreq, **Trifinopoulos**, Zupan] 2502.12314

[Balkin, Coren, Jentsch, Liu, Ovchynnikov Soreq, **Trifinopoulos**] 2601.00068, 2601.XXXXX

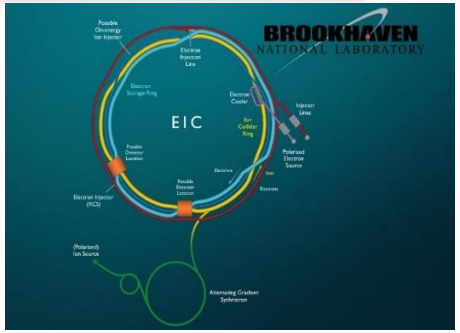

Davoudiasl, Liu, Marcarelli, Soreq, **Trifinopoulos**] 2412.13289

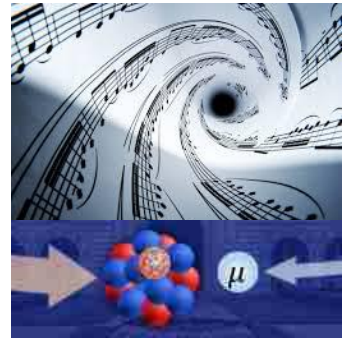

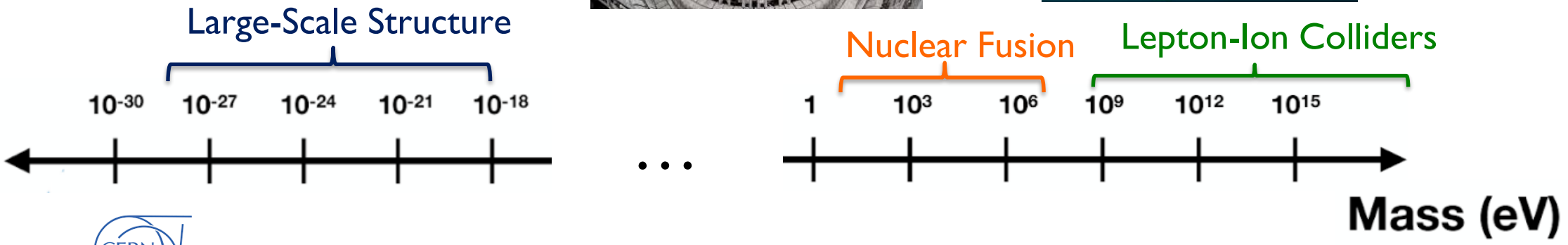

Outline

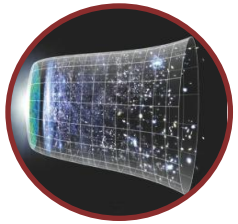

I. Large-Scale Structure bounds

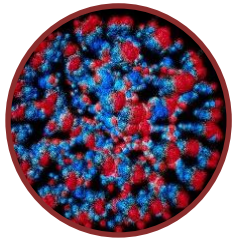

II. Production at Fusion Reactors

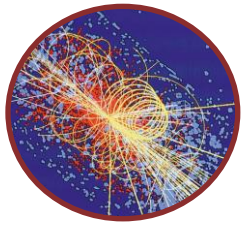

III. Searches at Colliders

Post-inflationary Axions

- The initial conditions for the axion field are inhomogeneous if $H_{\rm inf} > f_a$.

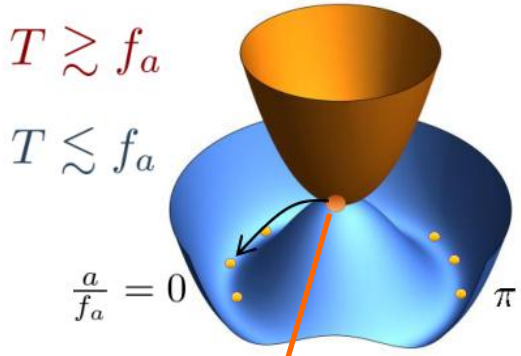

after inflation

Courtesy of Marco Gorgettho

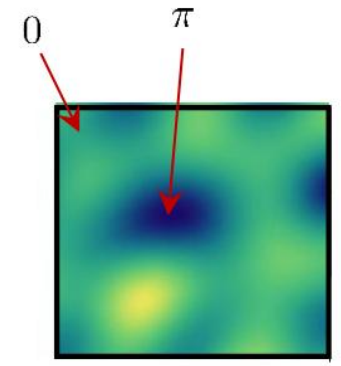

spatial inhomogeneities

[Buschmann et al] 1906.00967
[O'Hare et al] 2112.05117 [Gorgettho et al] 2007.04990, 2101.1100

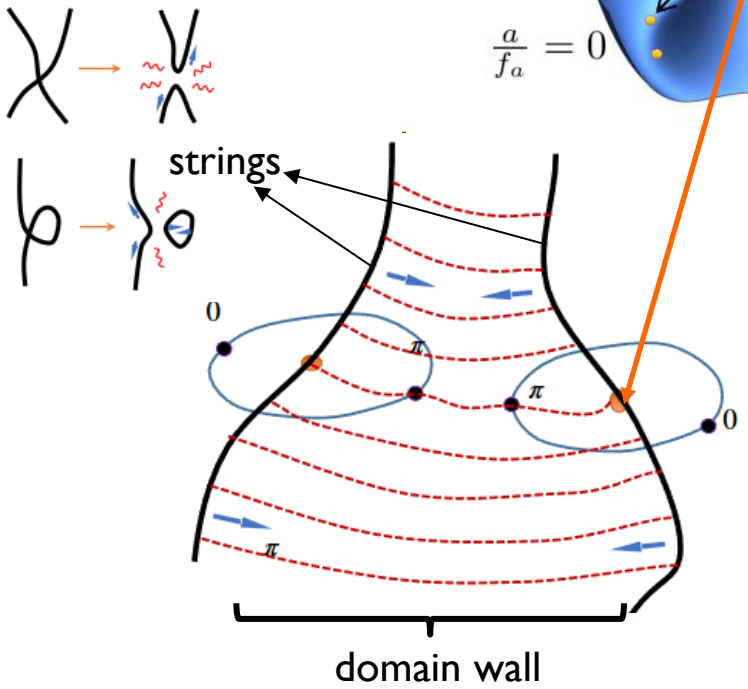

- The e.o.m. admit non-trivial solutions: **axion strings**, which form a network with an attractor solution (*scaling regime*):

  # local strings per Hubble patch $\xi \simeq 0.24 \log(f_a/H)$ H^{-1}

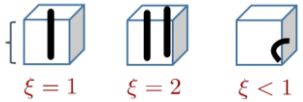

- To sustain the regime, the network radiates energy into axions at rate $\Gamma = \xi\, \mu / t^3$ and gravitational waves.
  string tension $\mu = E/L$
- When $H_* \sim m_a$, **domain walls** bounded by the strings form.

Seeds of accelerated structure formation

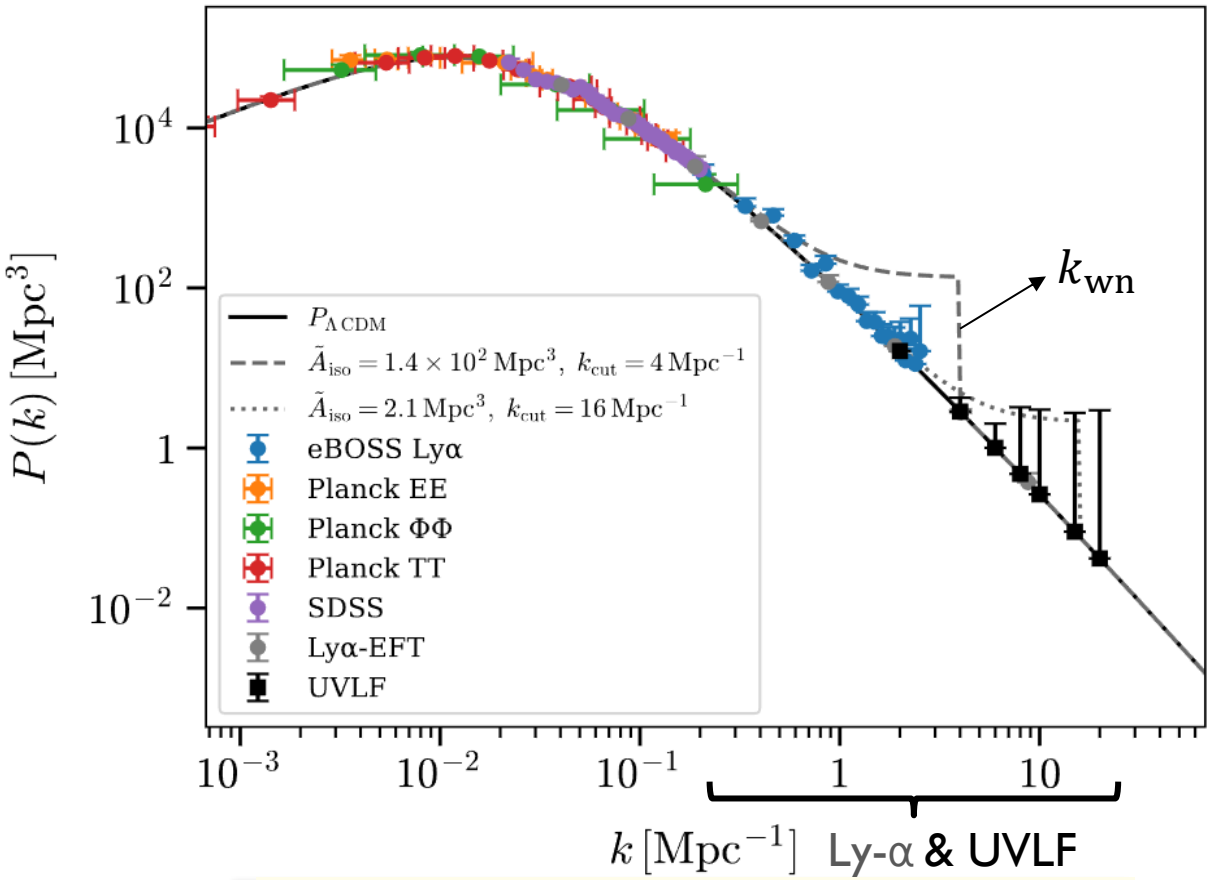

[Gorghetto, **Trifinopoulos**, Valogiannis] 2511.04734

- The string-wall system is unstable and collapses in one Hubble time. On length scales $\sim 1/H_*$, the axion field develops $O(1)$ isocurvature fluctuations δ_{iso}.
- The fluctuations in the CDM overdensity field δ define the **matter-power spectrum**:

$$\langle \delta^*(k)\,\delta(k')\rangle = \frac{2\pi^2}{k^3}\,(2\pi)^3\delta^3(k-k')\,\mathcal{P}(k)$$

- If axions are a sub-component of total CDM with fraction f_{DM}, then we can write

$$\mathcal{P}(k) = \mathcal{P}_{\mathrm{ad}}(k) + \mathcal{P}_{\mathrm{iso}}(k)\,,$$

$$\mathcal{P}_{\mathrm{iso}}(k) = \begin{cases} f_{\mathrm{DM}}^2 (k/k_{\mathrm{wn}})^3\,, & \text{if } k \lesssim k_{\mathrm{wn}} \\ 0\,, & \text{otherwise} \end{cases}$$

where $k_{\mathrm{wn}} \equiv C k_*$ and $k_* = H_* a_* \simeq 54 \sqrt{\frac{m_a}{10^{-20}\mathrm{eV}}}\ \mathrm{Mpc}^{-1}$

$C \sim O(10)$ according to simulations

[Gorgettho, Hardy, Nicolaescu] 2101.11007

Pheno Pipeline

Primordial source of white-noise $\mathcal{P}_{\rm iso}$ at $z_{\rm eq} \simeq 3400$

transfer functions

Enhancement of matter power at late times $(4 \lesssim z \lesssim 10)$

cosmo/astro modeling

Modification of Large-Scale Structure Observables

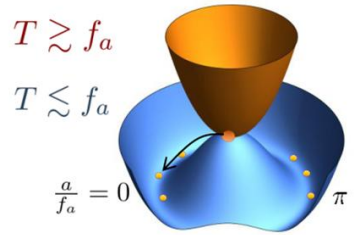

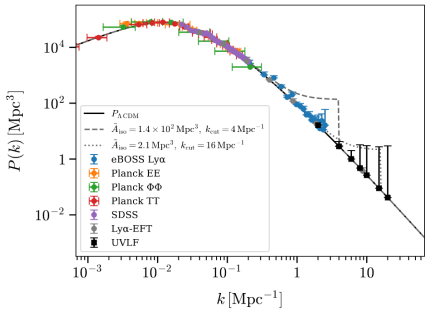

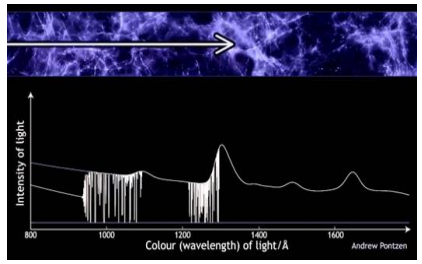

Large-Scale Structure Observations

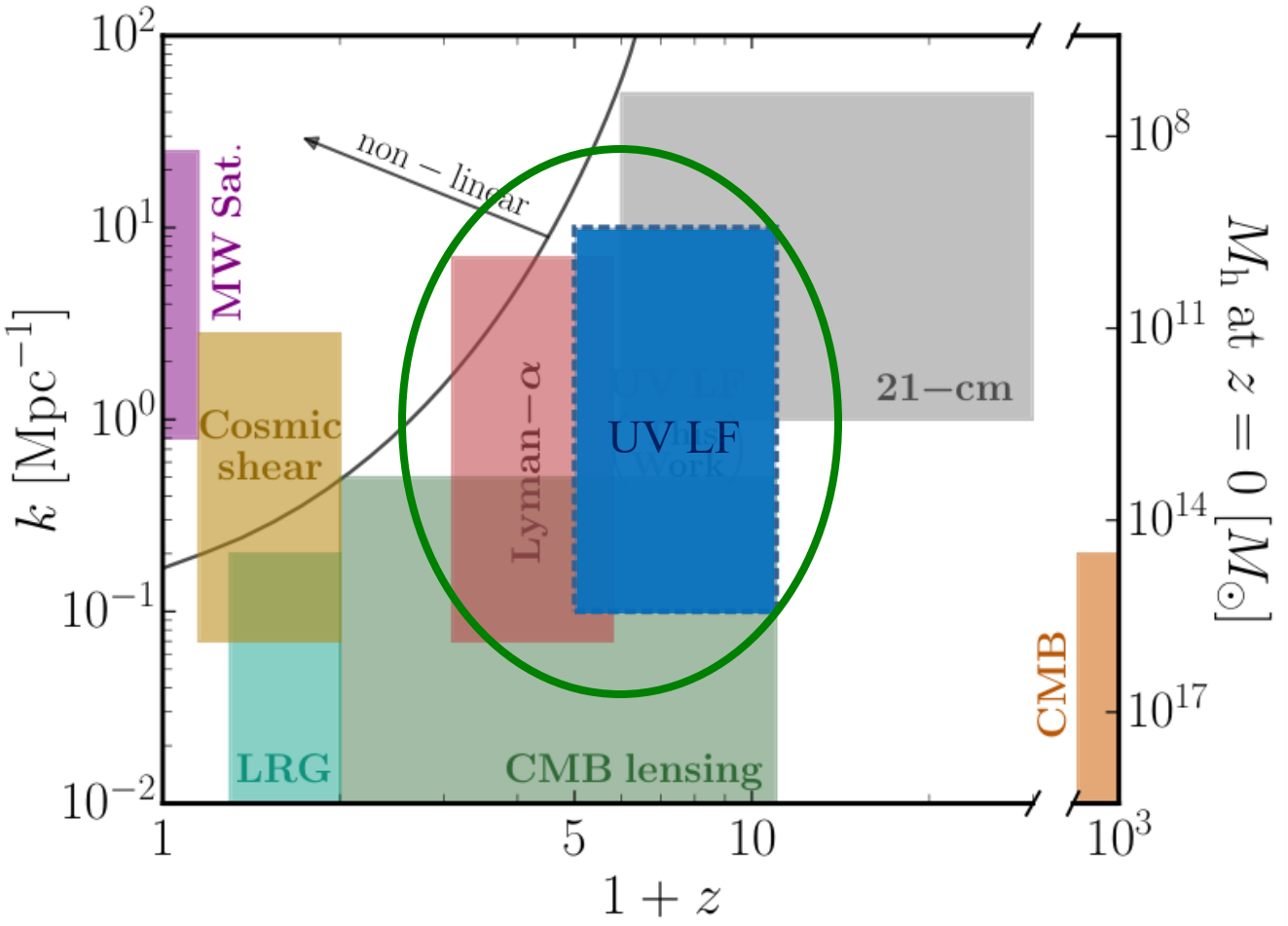

[Sabti, Munoz, Blas] 2110.13161

The Lyman-α forest

- The Ly-α forest arises from the $\mathrm{n} = 2 \rightarrow n = 1$ electron transition of the H-atom ($\lambda_0 = 1216\ \text{Å}$) observed at a range of redshifts due to multiple absorptions inside clouds of intergalactic gas in superclusters.

- It is a powerful tool for tracing the dark matter distribution at (sub)galactic scales.

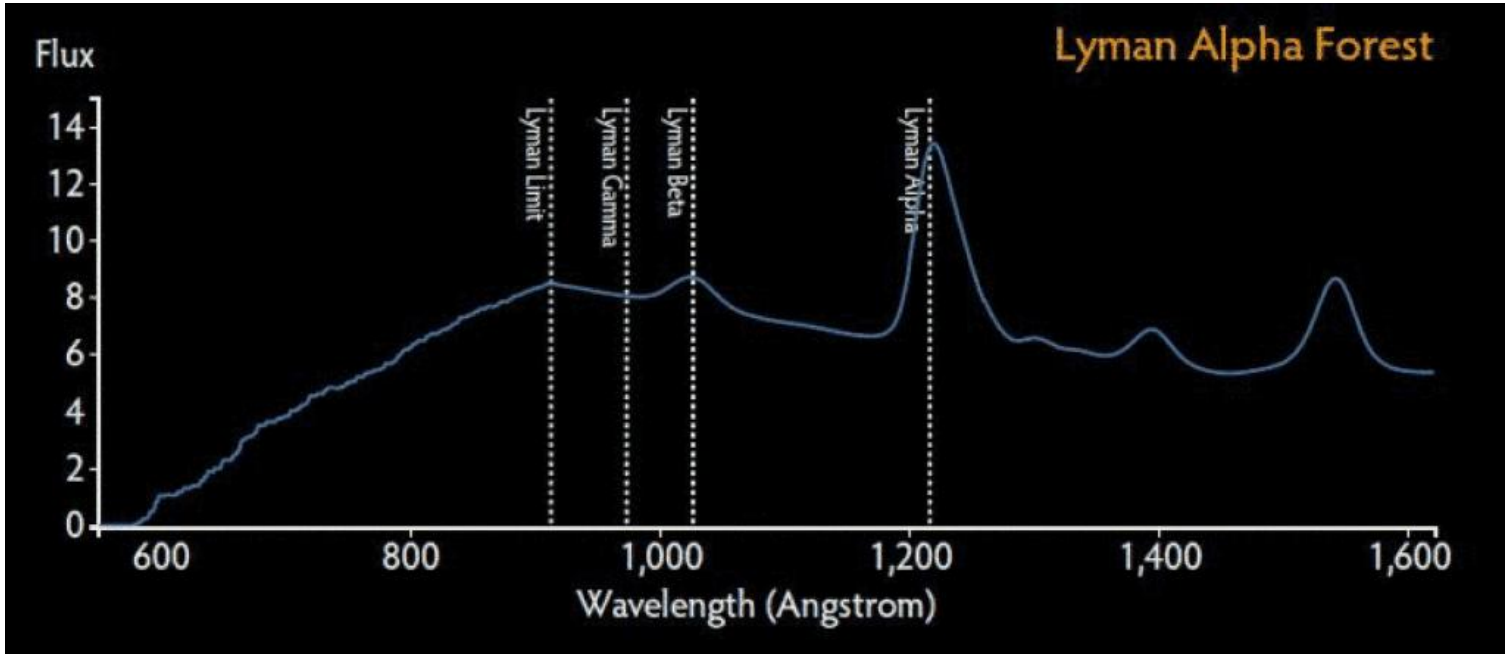

An Effective Field Theory (EFT) approach

effective fluid — *full N-body + hydro simulations*

$k_{\rm NL} \sim 5$ $\qquad$ $k_J \sim 10\ h\ {\rm Mpc}^{-1}$

[Ivanov] 2309.10133

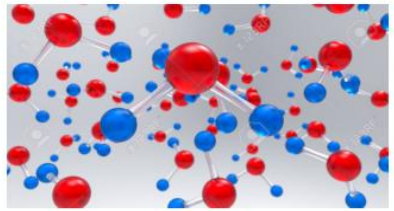

- The EFT exploits the existing symmetries, i.e. SO(2) invariance around the line-of-sight (denoted by ||) and the equivalence principle:

$$\eta \equiv \partial_\parallel v_\parallel/(aH)$$

$$\delta_F(\mathbf{x}) \equiv \frac{F(\mathbf{x})}{\langle F\rangle} - 1 = b_1\,\delta_m(\mathbf{x}) + b_\eta\,\eta(\mathbf{x}) + \sum_i b_{\mathcal{O}_i}\,\mathcal{O}_i(\mathbf{x})$$

15 nuisance parameters for Ly-α EFT at one-loop level

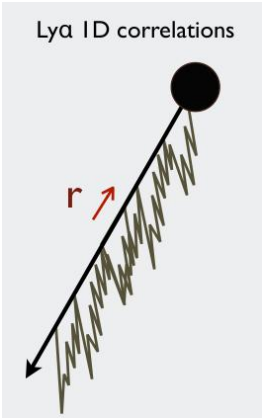

- At tree-level: $P_{\rm tree}(k,z) = \left(b_1 - b_\eta \mu^2 \frac{d\ln D_+(z)}{d\ln a}\right)^2 P(k)$

$$\mu = k_\parallel/k$$

[Kaiser] Mon. Not. Roy. Astron. Soc. 227 (1987)

1D spectra at small scales

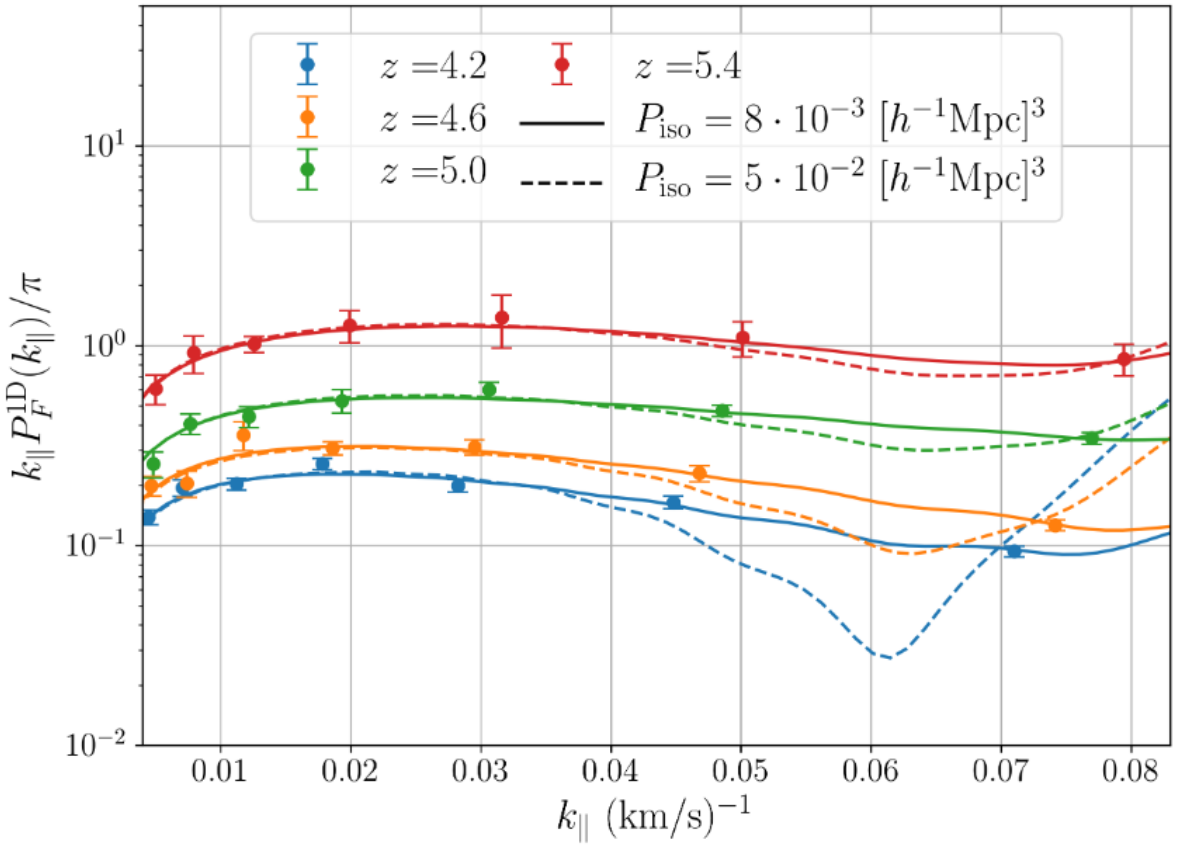

[Ivanov, **Trifinopoulos**] 2508.04767

- The EFT models the full 3D spectrum. Then the 1D spectra are:

$$P_{\rm 1D}(k_\parallel) = \frac{1}{2\pi}\int_{k_\parallel}^{k_{\rm max}} dk\ k P_{\rm 3D}(k, k_\parallel) + \underbrace{\mathcal{C}_0 + \mathcal{C}_1 k_\parallel^2 + \mathcal{C}_2 k_\parallel^4}$$

UV-sensitive contributions captured by the EFT!

- The 1D power spectra are available from HIRES/MIKE surveys for $z \lesssim 5.4$.

- We use the MontePython sampler to perform likelihood analysis of the enhanced power-spectrum with a modified code of CLASS. [Chudaykin, Ivanov, Philcox, Simonovic] 2004.10607 [Brinckmann, Lesgourgues] 1804.07261

UV light from Early Stars

- Young massive stars emit primarily in the ultraviolet region.
- The Hubble Space Telescope (HST) has discovered $O(10^4)$ of UV-bright galaxies.

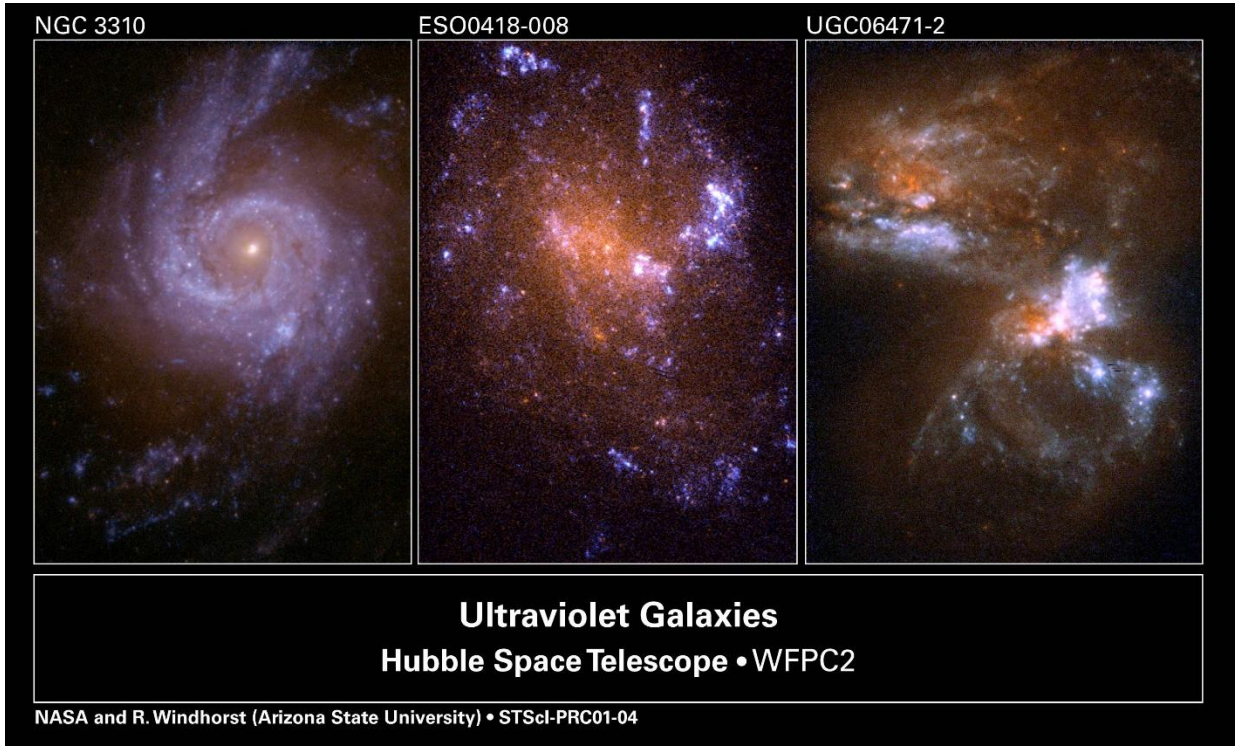

HST UV Luminosity Function (UV LF)

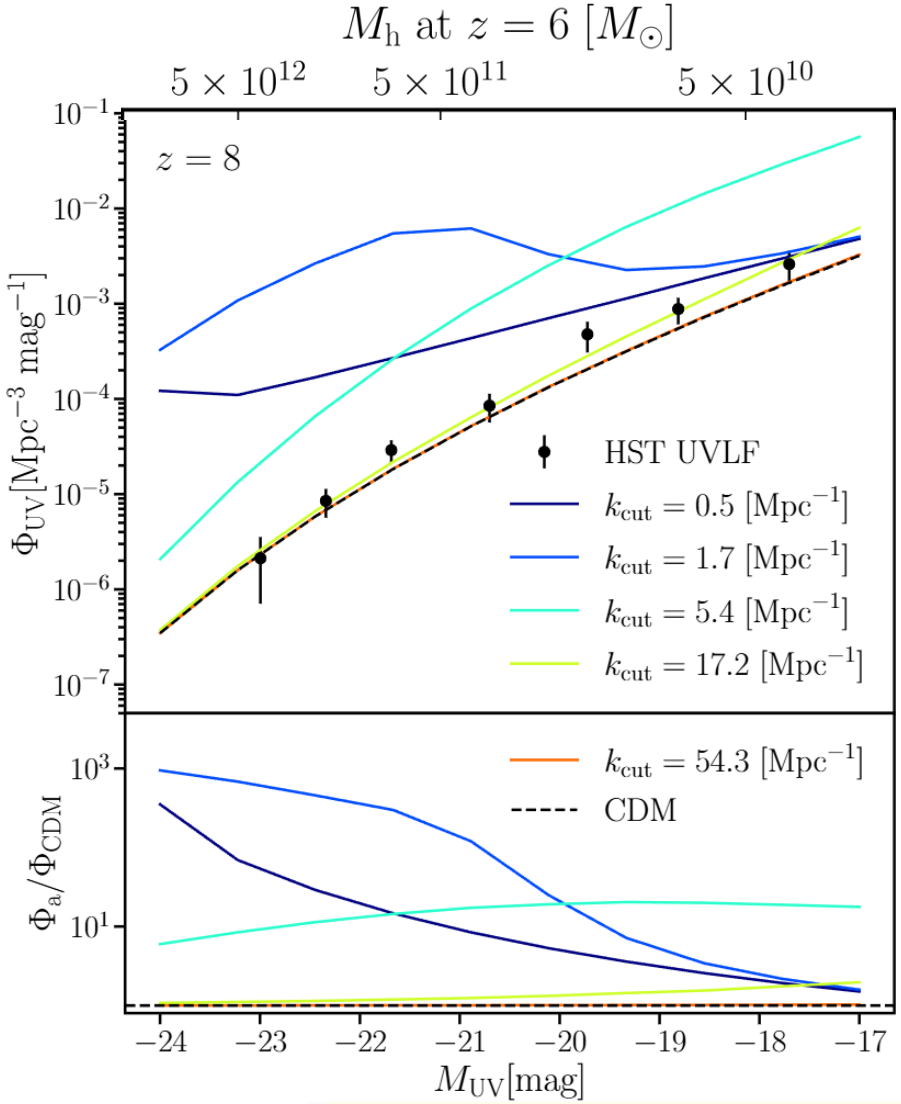

[Gorghetto, **Trifinopoulos**, Valogiannis] 2511.04734

- In Press-Schechter theory, halos correspond to regions where δ exceeds a critical collapse threshold.
- So, knowing $P(k)$ one can calculate the Halo-Mass Function (HMF) dn_h/dM_h.
- The HST catalogues probe the range $7 < z < 10$ via the UV LF:

$$\Phi_{\rm UV} = \underbrace{\frac{{\rm d}n_{\rm h}}{{\rm d}M_{\rm h}}}_{\text{cosmology (7 params)}} \times \underbrace{\frac{{\rm d}M_{\rm h}}{{\rm d}M_{\rm UV}}}_{\text{astrophysics (8 params)}}$$

[Sabti, Munoz, Blas] 2110.13161
[Sabti, Munoz, Kamionkowski] 2305.07049

- We use the likelihood code `GALLUMI` to constrain modifications to UVLF due to $\mathcal{P}_{\rm iso}$.

Novel Constraints on Ultralight DM!

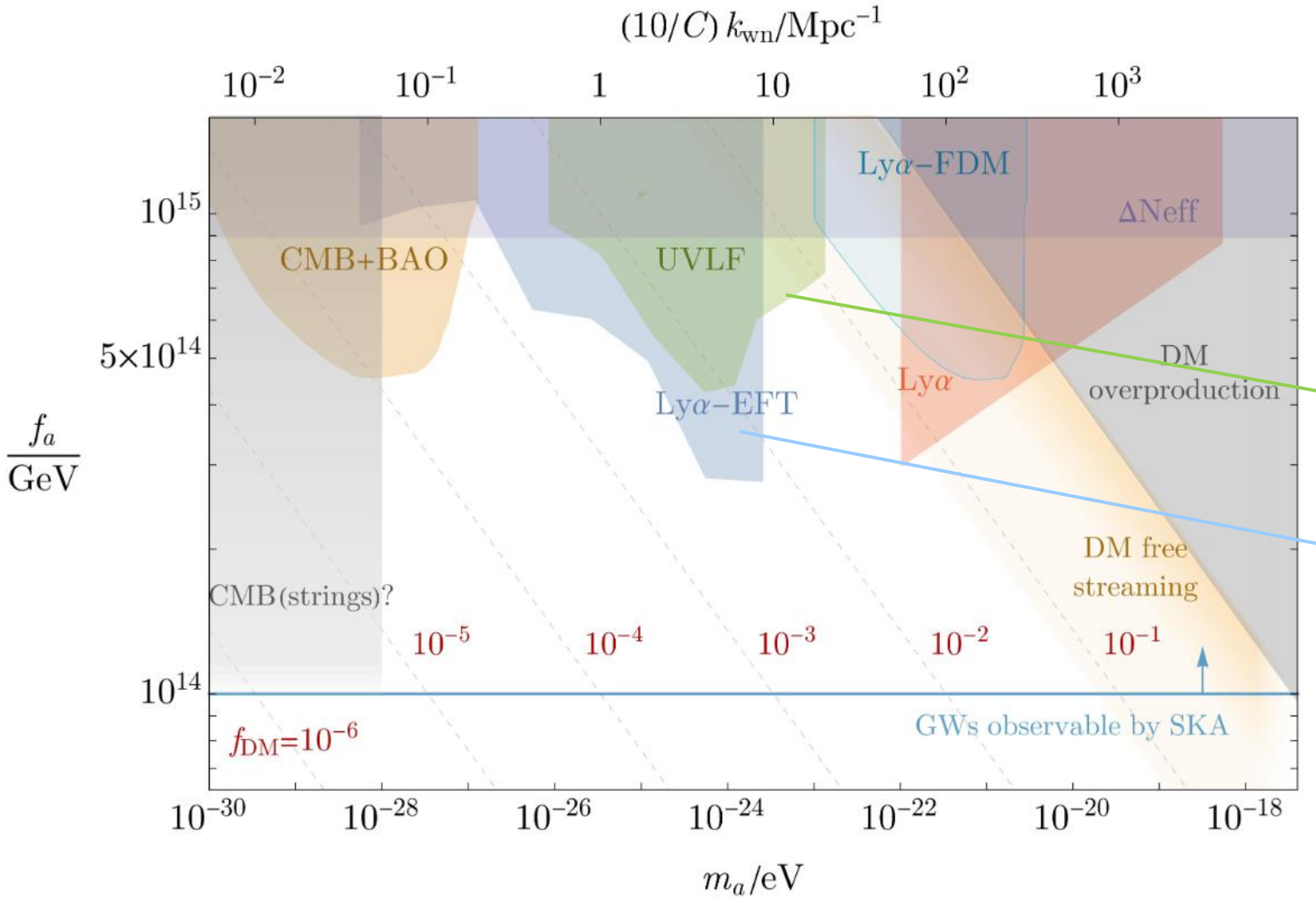

[Gorghetto, **Trifinopoulos**, Valogiannis] 2511.04734

[Ivanov, **Trifinopoulos**] 2508.04767

Novel Constraints on Supermassive DM!

Primordial Black Holes generate also isocurvuture fluctuations.

[Murgia et al]
1903.10509

Simulation-based analysis
(previous SOTA)

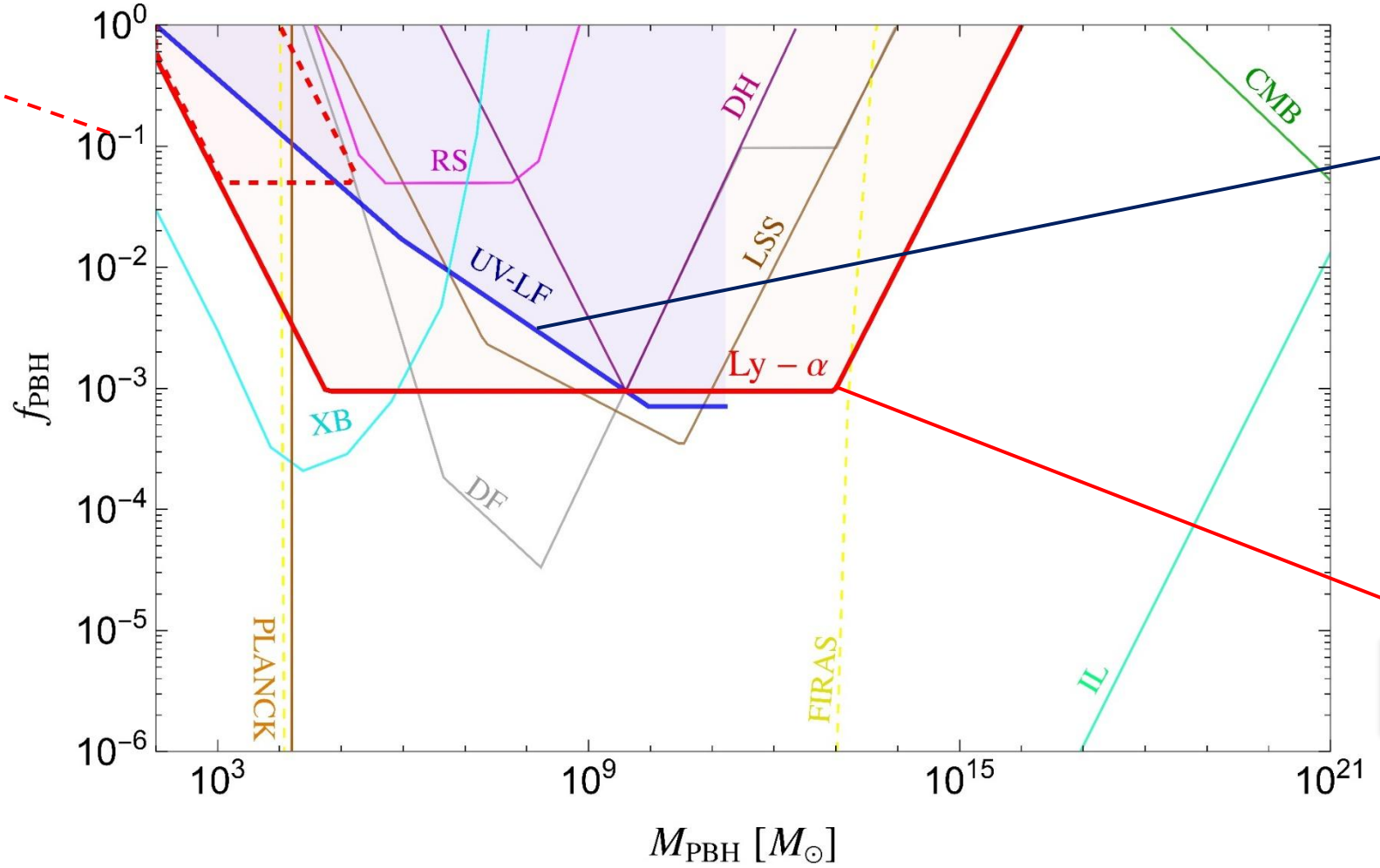

[Gouttenoire, **Trifinopoulos**, Valogiannis, Vanvlasselaer]
2307.01457

[Ivanov, **Trifinopoulos**]
2508.04767

EFTs:

✓ precision & accuracy

✓ fast/cheap BΛCDM

Simulations:

✓ non-linear reach

✗ resource-intense

Outline

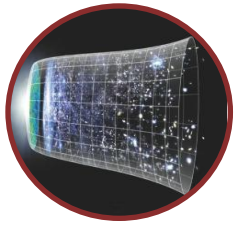

I. Large-Scale Structure bounds

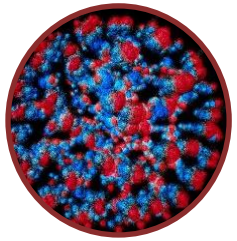

II. Production at Fusion Reactors

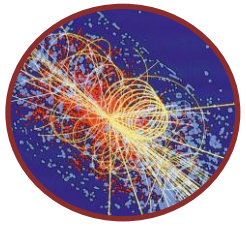

III. Searches at Colliders

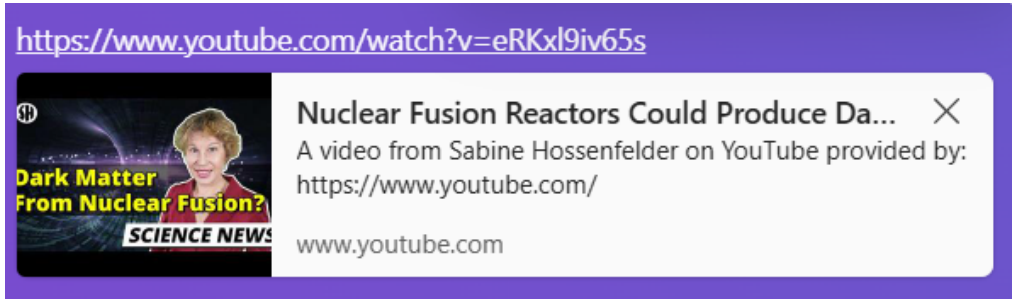

✅ Achievement Unlocked

Nuclear Fusion: "it's just 30 years away"

- We are entering a new era of fusion: moving from proof-of-principle to realistic machines!
- Fusion is achieved in a tokamak, where magnetic fields confine an extremely hot (~10^5K) , toroidal plasma.

[Meschini et al] Frontiers in Energy Research 11 (2023)

ITER (International Thermonuclear Experimental Reactor)

$P = 500 - 2000$MW, $B = 5$ T, R = 6m

ARC (Affordable Robust Compact reactor)

$P = 400$ MW, $B = 9$ T, R = 3m

Operational Principle in a nutshell

[Baruch, Fitzpatrick, Menzo, Soreq, **Trifinopoulos**, Zupan] 2502.12314

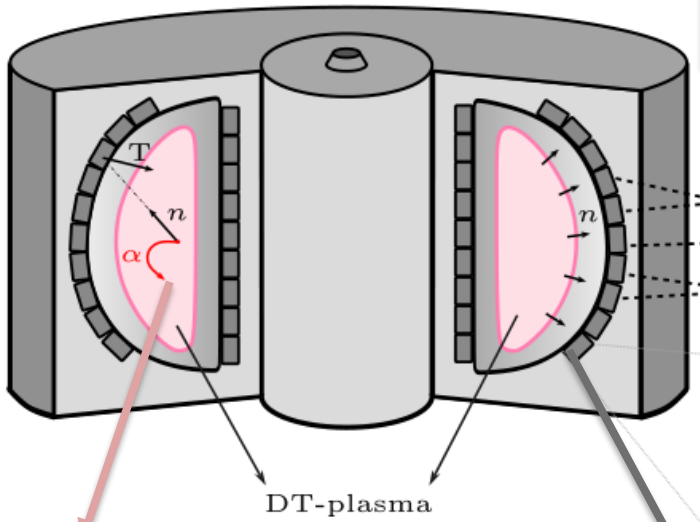

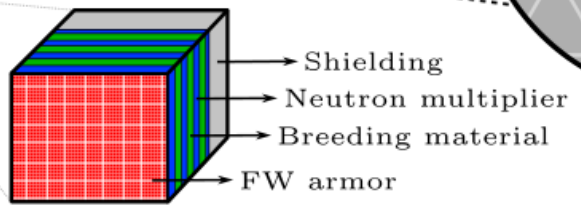

WCLL: 84% Pb, 16% Li

a

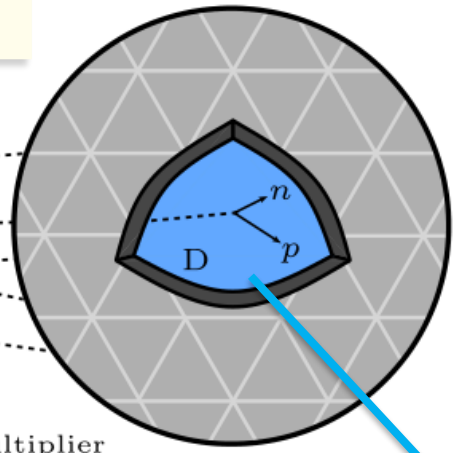

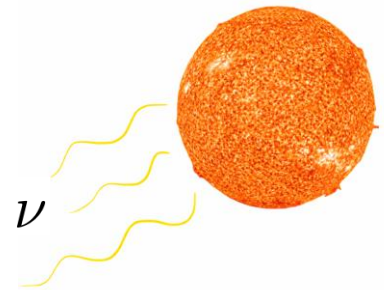

Background

$\nu + d \to n + p + \nu$

$N_{\rm bkg}$~5000 events/year

Main Reaction

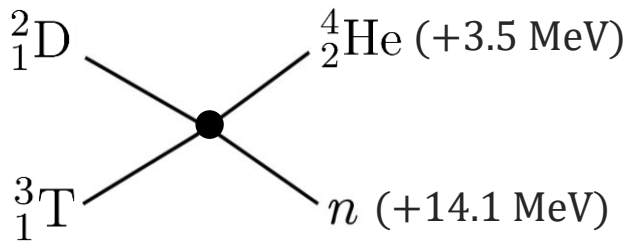

$$\Phi_n^{\rm total} \simeq 10^{15}\ \text{neutrons cm}^{-2}\text{s}^{-1} \left(\frac{P}{2000\ \text{MW}}\right)$$

Production ($E_a = E_n + S_n$)

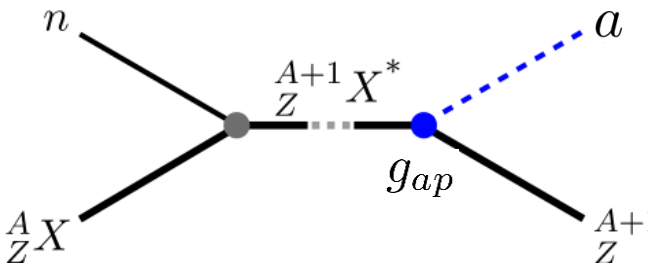

resonant capture + de-excitation

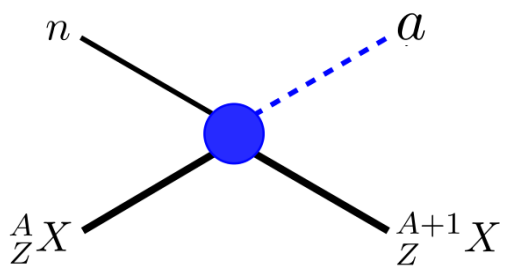

non-resonant capture + de-excitation

Detection

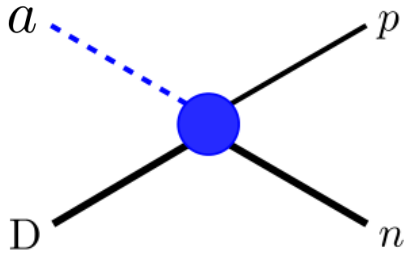

deuterium-dissociation
(above $E_D = 2.2$ MeV)

Leading prospects for ALP-proton coupling

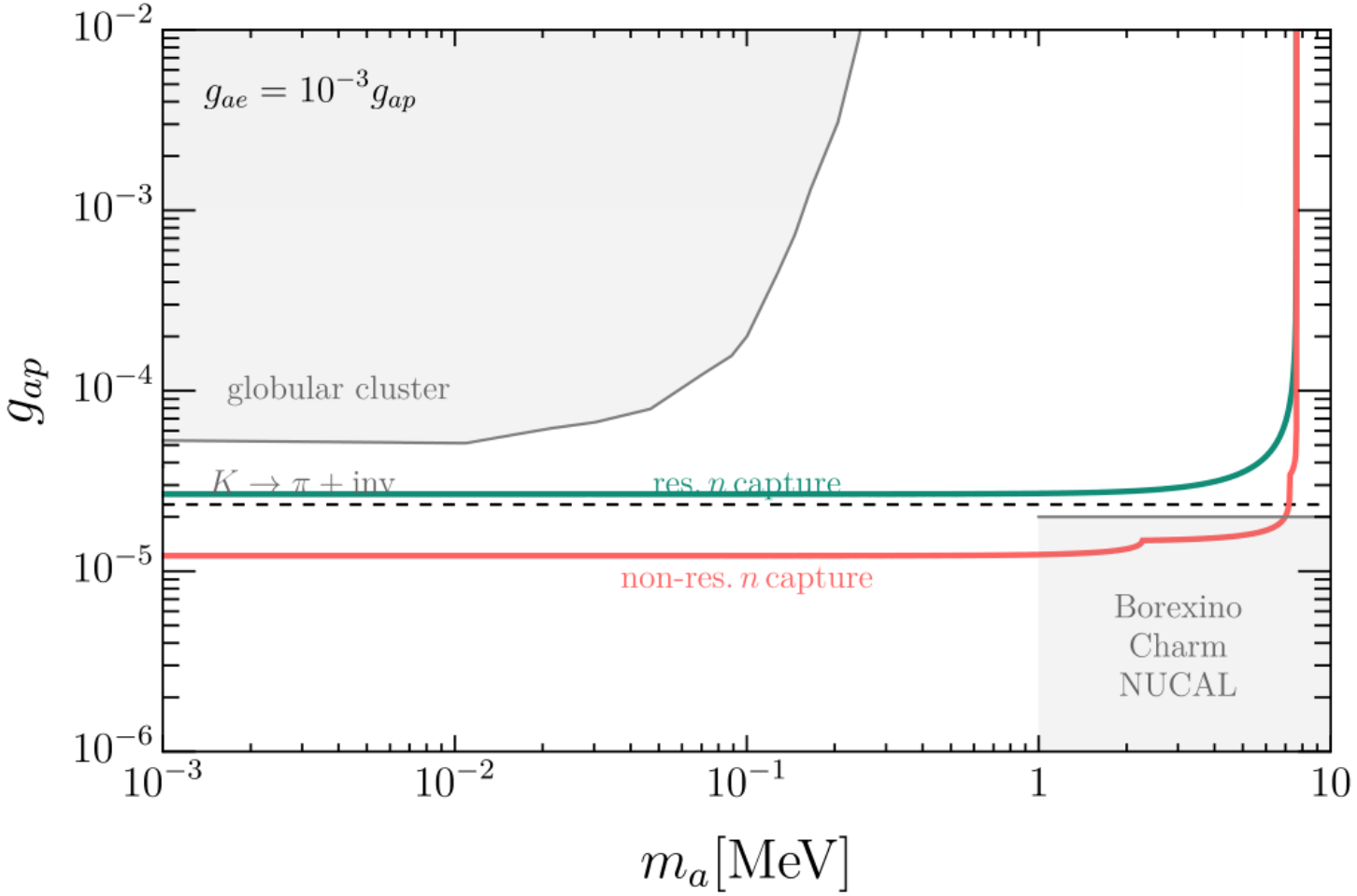

- Expected number of dissociation events:

$$N_a^{\text{res.}} \approx 2 \times 10^{20}\, g_{ap}^4 \left(\frac{T}{1\,\text{y}}\right) \left(\frac{L}{10\,\text{m}}\right)^2$$

$$N_a^{\text{non-res.}} \approx 4 \times 10^{21}\, g_{ap}^4 \left(\frac{T}{1\,\text{y}}\right) \left(\frac{L}{10\,\text{m}}\right)^2$$

[Baruch, Fitzpatrick, Menzo, Soreq, **Trifinopoulos**, Zupan] 2502.12314

Nuclear transitions

- The resonant production of ALPs can be related to magnetic nuclear de-excitations:

$$\sigma_{a;\mathrm{M1}} = \mathcal{B}_{a/\gamma;\mathrm{M1}}\sigma_{\gamma;\mathrm{M1}}, \quad \mathcal{B}_{a/\gamma;\mathrm{M1}} \equiv \left(\frac{\Gamma_a}{\Gamma_\gamma}\right)_{\mathrm{M1}} = \left(\frac{p_a}{E_\gamma}\right)^3 \frac{1}{2\pi\alpha}\frac{1}{1+\delta^2}\left(\frac{(1+\beta)\,g_{ap}}{\left(\mu_0-\frac{1}{2}\right)\beta+\mu_3-\eta}\right)^2$$

[Donnelly et al] PRD 18(1978)1607

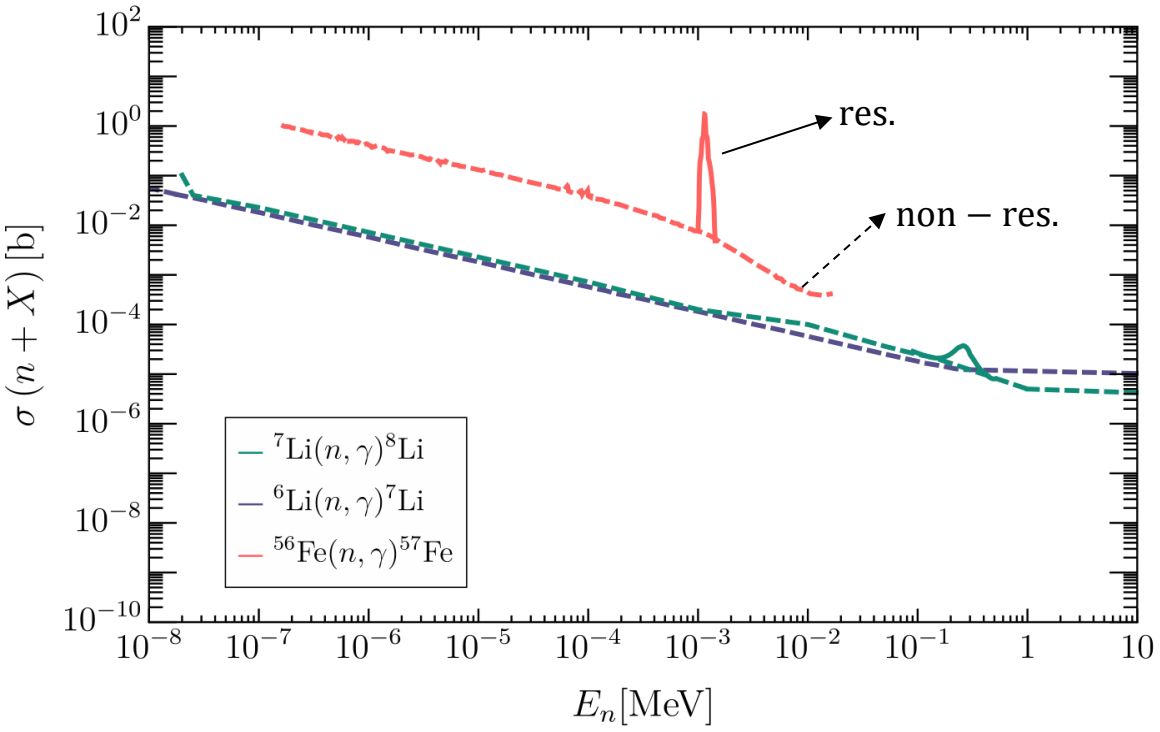

Nuclear structure parameters

	^{7}Li [5]	^{8}Li [55]	^{57}Fe [17]
η	0.5	−0.1034	0.8
β	1.0	1.0	−1.19
δ	0	0	0.002

- The NDA estimate for the non-resonant is:

$$\sigma_{\gamma;\mathrm{M1}}^{\mathrm{non-res.}} \sim (Q/m_N)^2 \sigma_{\gamma;\mathrm{E1}}^{\mathrm{non-res.}}$$

[Kopecky et al] ATLAS of neutron capture cross sections

(Un)available Nuclear Input

- We used for target elements (e.g. ^{7}Li,^{8}Li and ^{57}Fe) that exist in the breeding blanket and for which we found available nuclear data.

Process	$S_n(^{A+1}_{Z}X)$	Transition	Multipolarity	E_γ
$^{6}\mathrm{Li}(n,\gamma)^{7}\mathrm{Li}$	7.25 MeV	$\|1/2^+\rangle \to \|3/2^-\rangle$	E1 (non-res.)	7.25 MeV
		$\|1/2^+\rangle \to \|1/2^-\rangle$	E1 (non-res.)	6.77 MeV
$^{7}\mathrm{Li}(n,\gamma)^{8}\mathrm{Li}$	2.03 MeV	$\|3/2^-\rangle \to \|2^+\rangle$	E1 (non-res.)	2.03 MeV
		$\|3/2^-\rangle \to \|3^+\rangle$	M1 (res.)	2.26 MeV
$^{56}\mathrm{Fe}(n,\gamma)^{57}\mathrm{Fe}$	7.65 MeV	$\|1/2^+\rangle \to \|1/2^-\rangle$	E1 (non-res.)	7.65 MeV
		$\|1/2^+\rangle \to \|3/2^-\rangle$	E1 (non-res.)	7.63 MeV
		$\|1/2^-\rangle \to \|1/2^-\rangle$	M1 (res.)	7.64 MeV
		$\|1/2^-\rangle \to \|3/2^-\rangle$	M1 (res.)	7.63 MeV

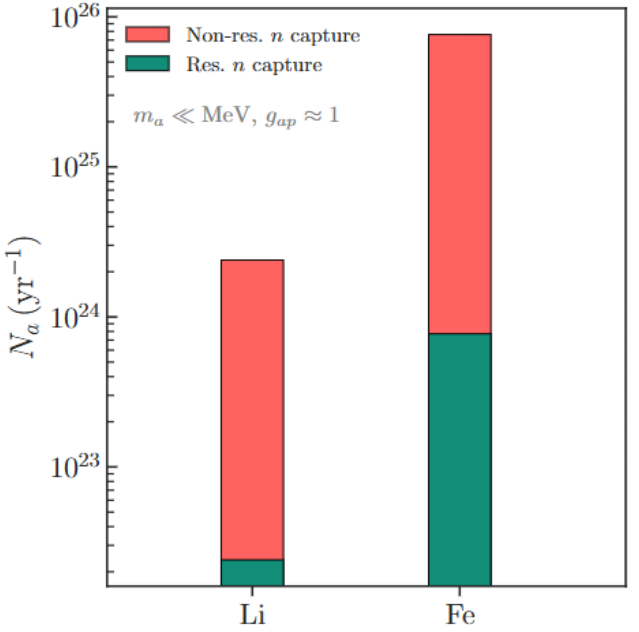

HCBS (% composition):

Elements	Li_2TiO_3	Beryllium	IN-RAFMS
6Li	7.578	0.000 2775	—
7Li	5.052	0.000 0225	—
Be	—	99.2073	—
Cu	0.0005	0.0031	0.002
Nb	—	—	0.001
Zn	0.0008	—	—
Fe	0.002	0.08	88.1
Cr	0.0009	0.0037	9.2
Mn	0.001	0.0015	0.6
Mo	—	0.002	0.002
Ni	0.0028	0.0106	0.005
V	—	—	0.24
Si	0.008	0.06	0.05
Al	0.0025	0.06	0.005
Sn	—	—	0.01
W	—	0.01	1.5
As	—	—	0.01
Se	—	—	—
S	—	0.001	0.002
Cd	0.0005	—	—
Ti	43.63	0.006	0.005
K	0.001	—	—
Co	0.004	0.0006	0.005
Ca	0.01	0.002	—
Mg	0.003	0.06	—
B	0.001	0.0002	0.001
Zr	0.001	0.0043	—
Na	0.003	0.0015	—
O	43.698	0.37	0.01
C	—	0.1	0.12
Ta	—	0.001	0.08
N	—	0.0114	0.04
P	—	—	0.002
Sb	—	—	0.01
Pb	—	0.002	—
F	—	0.0005	—
Cl	—	0.001	—

- What if there are better options? *E.g.* elements with higher M_1 rates in WCLL or other blanket designs.

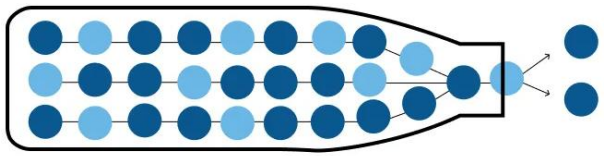

limited knowledge of nuclear structure parameters

Modern Pheno Solution: Use AI!

- Nuclear Co-Learnt Representations (NuCLR) is an *interpretable* deep-learning model that predicts various nuclear observables.

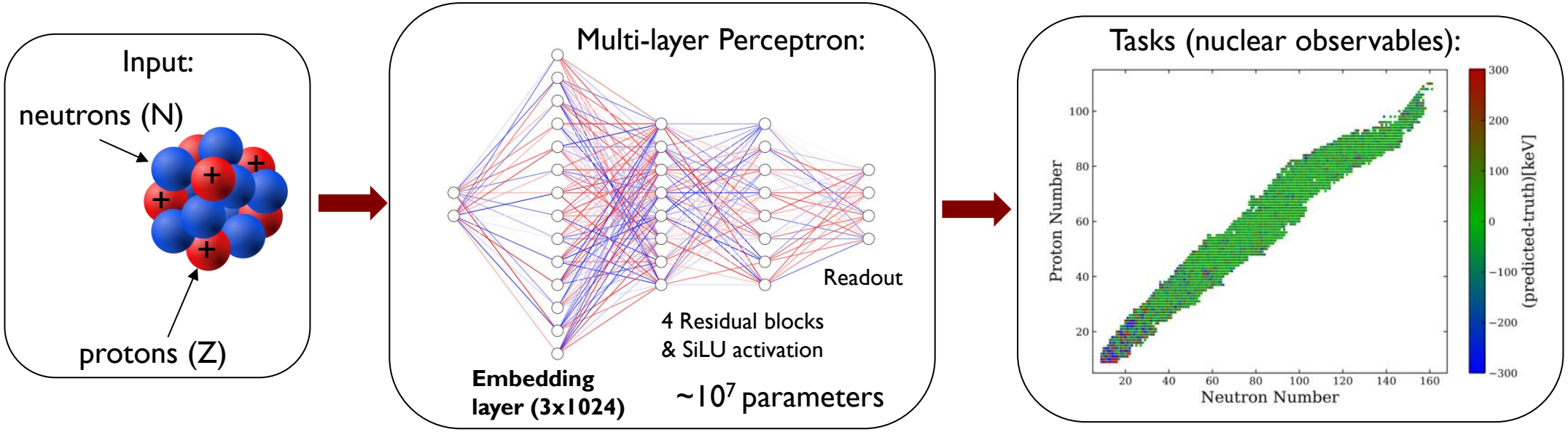

[Kitouni, Nolte, **Trifinopoulos**, Kantameni, Williams] 2307.01457
[Kitouni, Nolte, Perez-Diaz, **Trifinopoulos**, Williams] 2405.17425
[Richardson, **Trifinopoulos**, William] 2508.08370

- **Multi-task Learning (MTL):** The model is trained with data from multiple tasks simultaneously, using shared representations to learn the common ideas between them.

Interpretable AI for Theoretical Physics

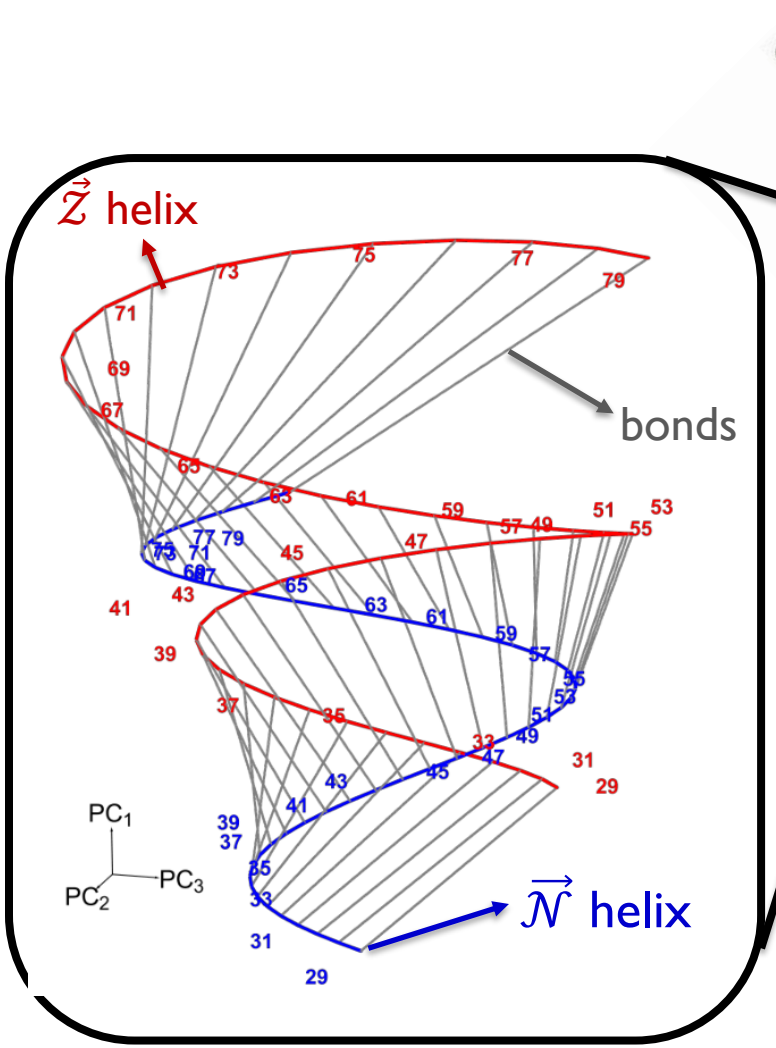

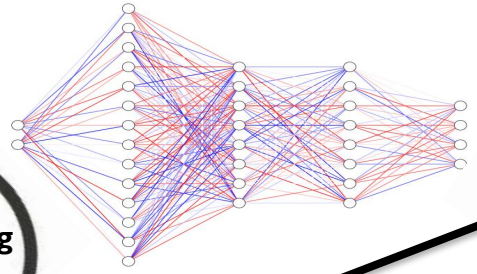

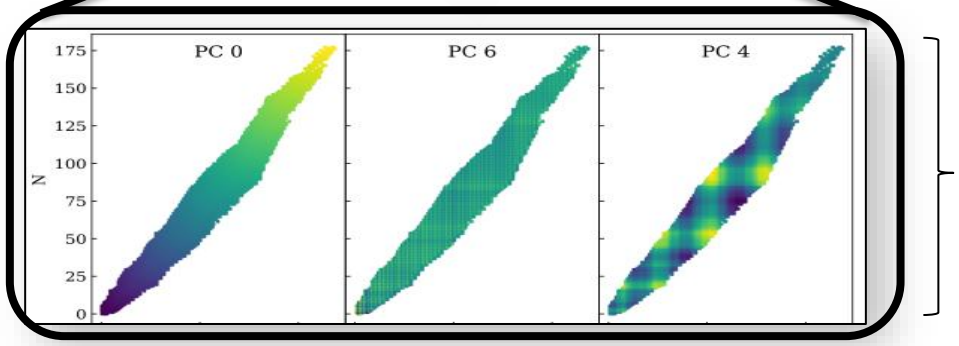

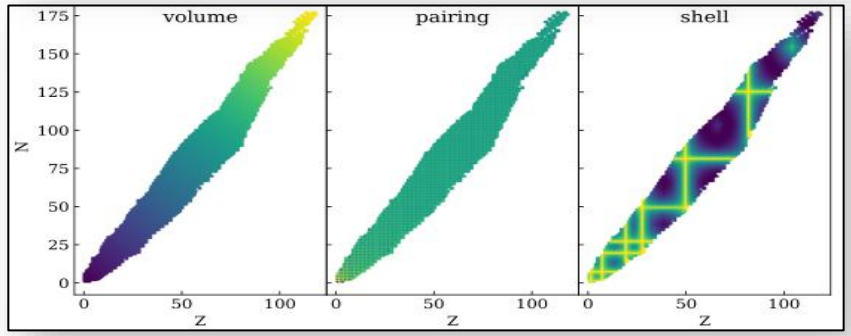

Weizsäcker, Bethe (Nobel 1967)
Gamow, Goeppert-Mayer (Nobel 1963)

Physics for AI & AI for Physics

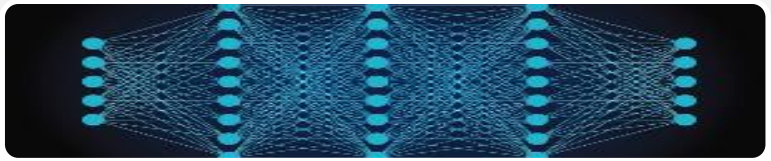

Artificial Intelligence

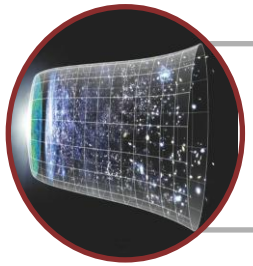

Cosmology

r-process nucleosynthesis

Neutron Stars

AI Interpretability

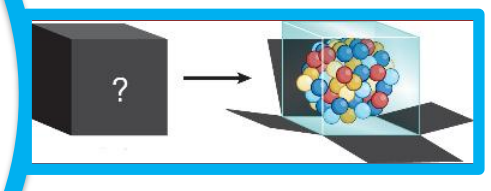

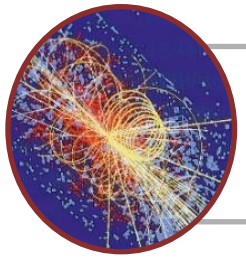

Particle Physics

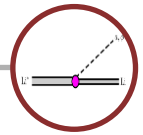

New Physics Searches

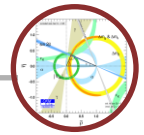

CKM unitarity

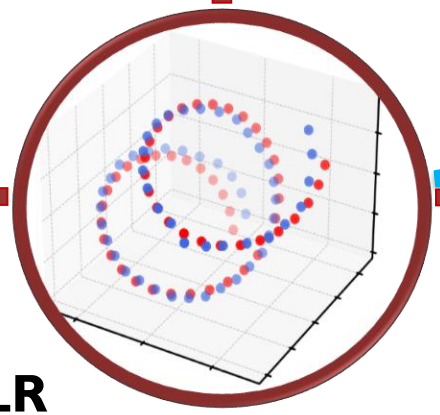

NuCLR

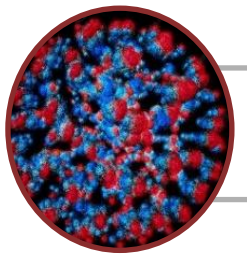

Nuclear Physics

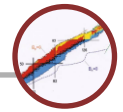

Drip lines

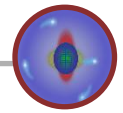

Exotic Nuclei

CERN

Sokratis Trifinopoulos

Outline

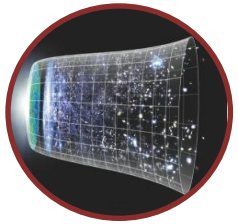

I. Large-Scale Structure bounds

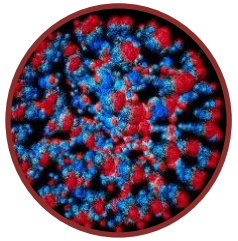

II. Production at Fusion Reactors

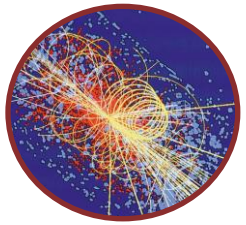

III. Searches at Colliders

The Large-Hadron Collider (LHC)

- LHC has already provided ground-breaking results:
  - ✓ completion of the SM spectrum (**Higgs** boson discovery)
  - ✓ exquisite precise measurements of a huge number of other SM processes
  - ✓ fundamentally challenged our expectations for BSM Physics at the electroweak scale

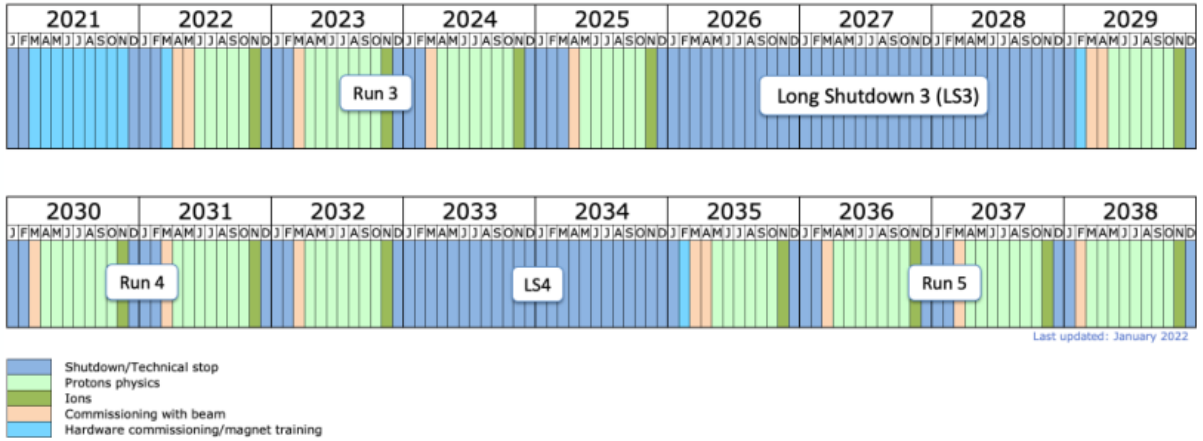

High-Luminosity LHC

increased Lumi ×10

- We are moving towards the HL-phase and there is still lots of data to collect!

Still no direct evidence for New Physics!

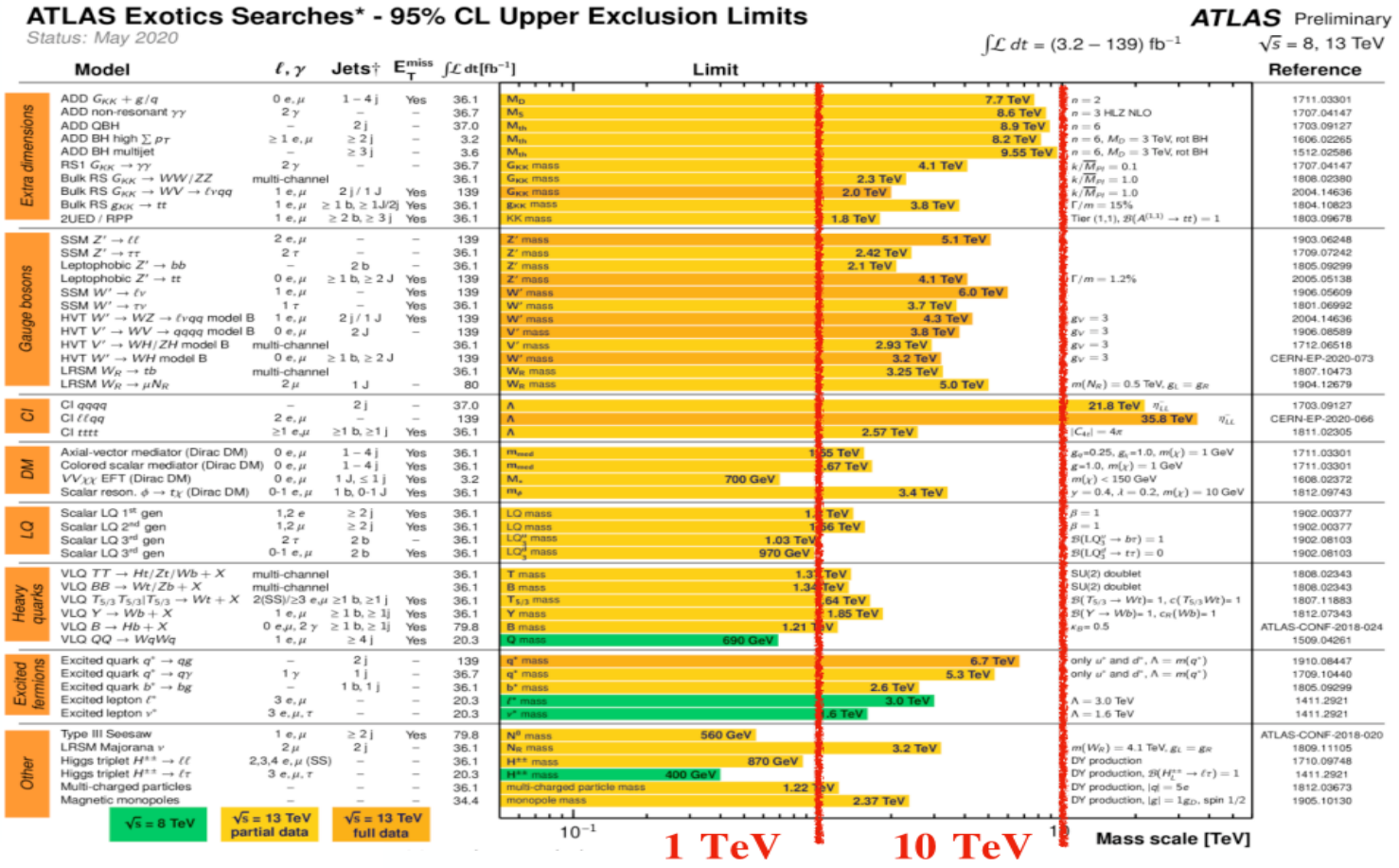

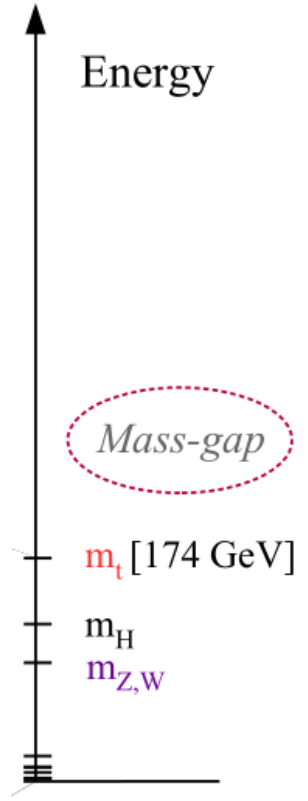

Who is the successor?

- Various options! FCC-ee seems to be the current favorite (but still no sooner than 2045 😔)

Project	Scope	TRL	R&D	Test facilities	Performance	Site preparation	Schedule	Cost	Risk
CLIC 380 GeV, 1.5 TeV		4 - 6 / 5.2							
FCC-ee 91-365 GeV		4 - 7 / 6.0							
FCC-hh 85 TeV		4 - 7 (Nb_3Sn) / 4.3 2 - 7 (HTS) / 3.2							
FCC-hh - SA 85 TeV		4 - 7 (Nb_3Sn) / 5					Nb_3Sn		
LCF 250 - 550 GeV		5 - 7 / 5.5							
LEP3 91 - 230 GeV		3 - 6 / 4.0							
LHeC: HL-LHC + 50 GeV ERL		3 - 6 / 4.5							
MC 3.2 TeV, 7.6 TeV		3.2 TeV: 3 - 5 7.6 TeV: 2 - 5							

https://cds.cern.ch/record/2947728

Is BSM Physics at Colliders in crisis?

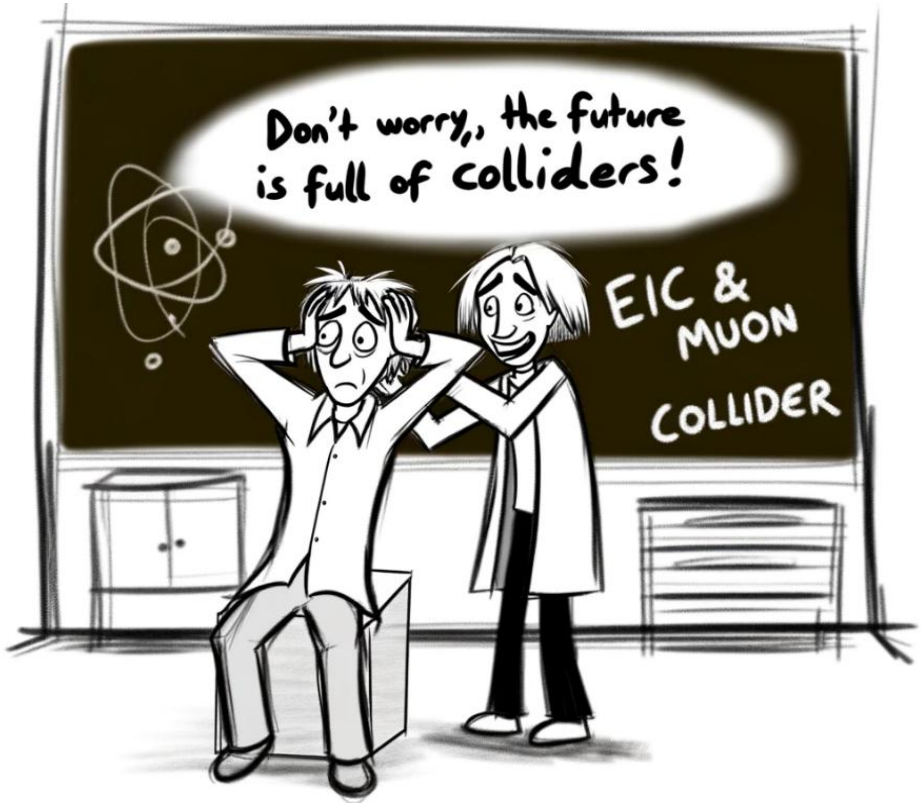

- BSM physics at colliders has a bright future: there is rich pheno to explore at machines designed to study the QCD frontier.

Electron-Ion Collider (EIC)

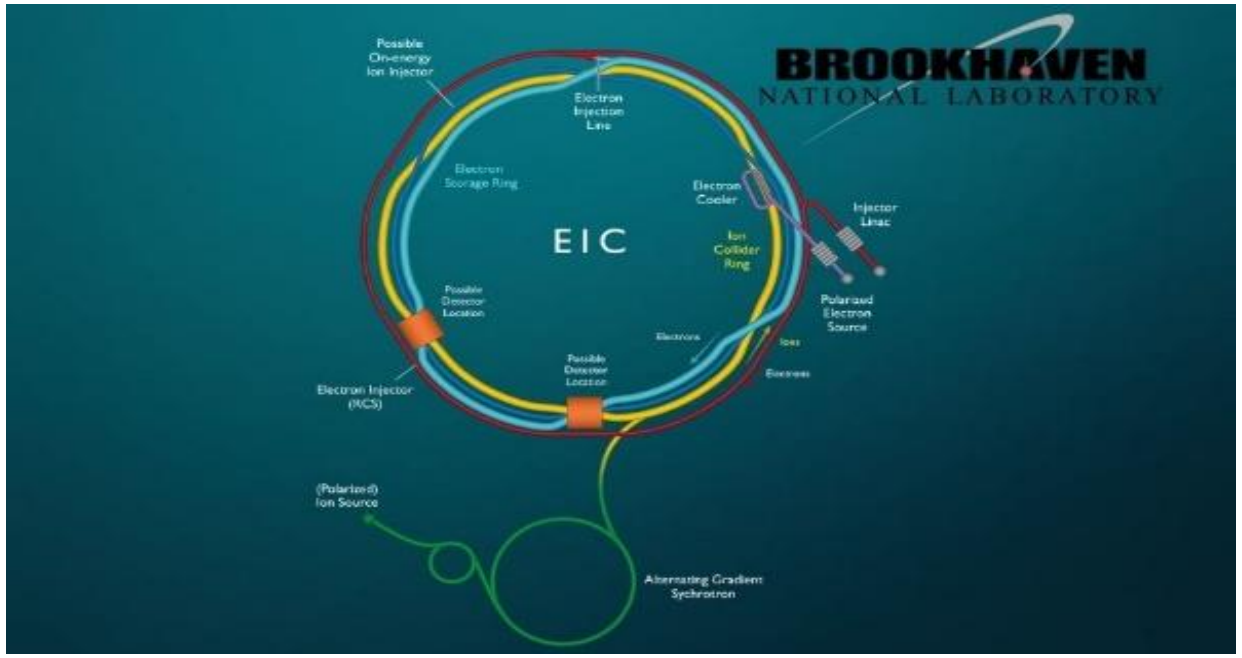

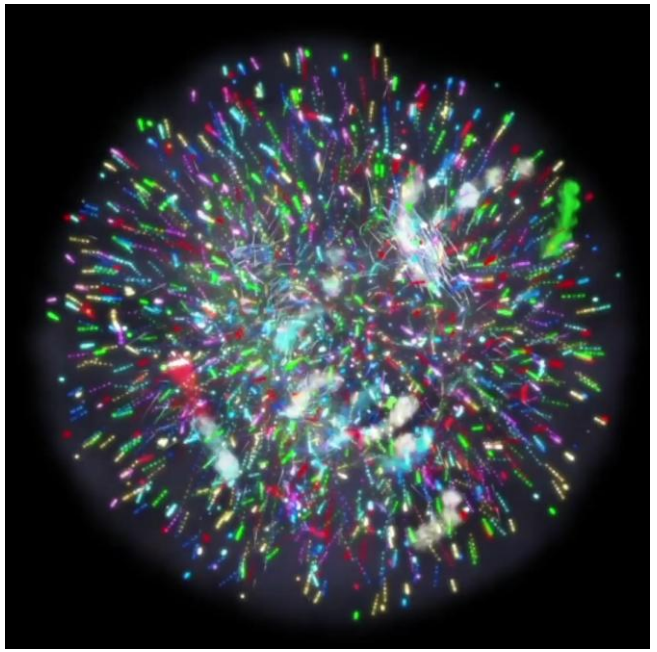

MIT/Jefferson Lab/Sputnik Animation

- Scientific purpose: study the properties of nuclear matter, e.g. 3D structure of protons & nuclei, origin of nucleon mass and spin, nuclear PDFs etc as well as a rich BSM program

The EIC Detector

$E_p \approx 40 - 275$ GeV

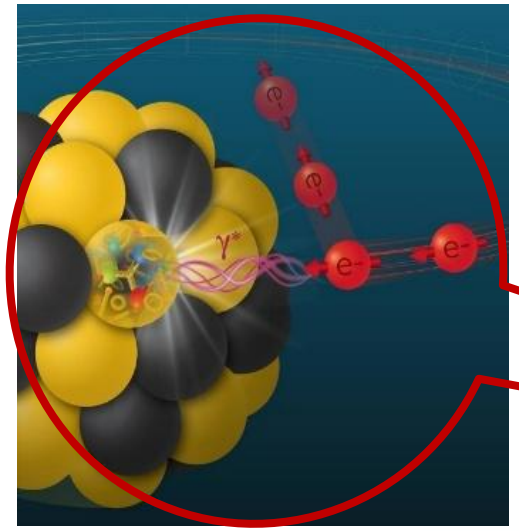

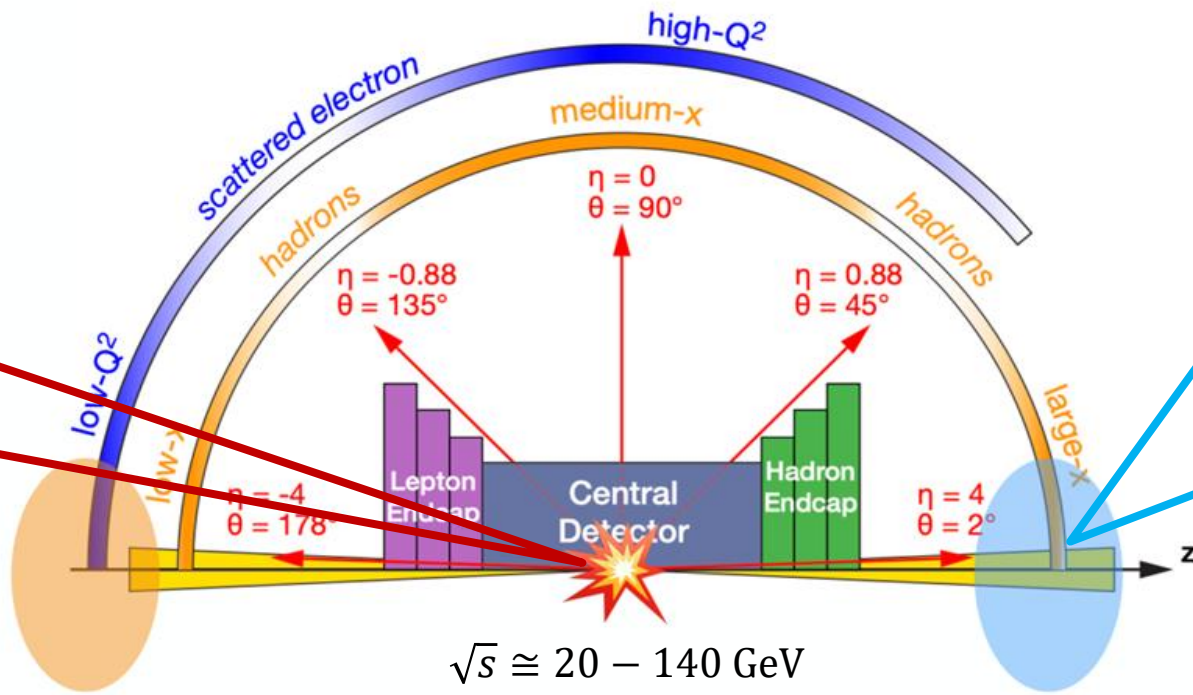

$E_e \approx 18$ GeV

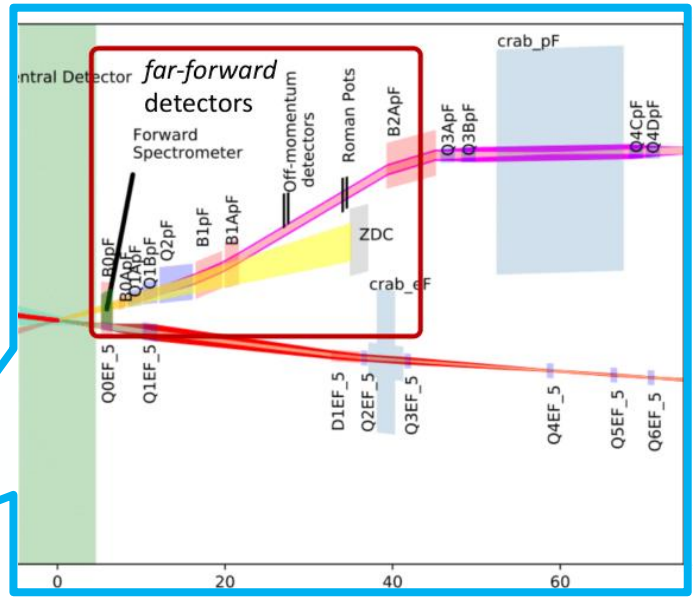

$\sqrt{s} \cong 20 - 140$ GeV

Far-backward detector:
Measure scattered electrons with very low Q^2 and luminosity

Ideal for studying coherent scattering

[EIC Report] 2103.0541]

Far-forward detector:
Can select the coherent collision vetoing spectator neutrons from nuclear breakup

BSM at EIC?

- The EIC is a **very powerful machine**. Can we use it for BSM physics?

1. Axion-like particles (**ALPs**) with couplings to the photons.

   [Balkin et al] 2310.08827 [Liu, Yan] 2112.02477
2. Lepton-Flavour-Violating ALPs

   [Davoudiasl, Marcarelli, Neil] 2112.04513 2402.17821 [Cirigliano et al] 2102.06176
3. Light Leptoquarks

   [Gonderinger, Ramsey-Musolf] 1006.5063 [Zhang et al] 2207.10261
4. Heavy Neutral Leptons

   [Battel, Ghosh, Han, Xie] 2210.09287
5. Light vector bosons with displaced vertices

   [Davoudiasl, Marcarelli, Neil] 2307.00102
6. Heavy Gravitons

   [Hatta] 2311.14470

we: ALPs coupling to gluons and DM!

[Balkin, Coren, Jentsch, Liu, Ovchynnikov Soreq, **Trifinopoulos**] 2601.00068, 2601.XXXXX

Invisible ALPs and Meson decays

- We consider GeV-scale ALPs that act as portals to DM χ: $\mathcal{L}_a \supset \frac{\alpha_s}{4\pi}\frac{a}{f_a}G^{\mu\nu}\tilde{G}_{\mu\nu} + ig_{a\chi}a\bar{\chi}\gamma^5\chi$
- The gluon-coupling induces mixing with the SM pseudo-scalars $P = \{\pi^0, \eta, \eta'\}$. Using the chiral Lagrangian ($m_\pi \lesssim m_a \lesssim 1\text{GeV}$) we may rotate to the physical basis:

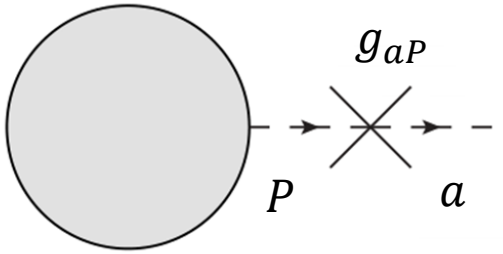

$$a = a_{\text{phys}} + \frac{f_\pi}{f_a}\sum_{P=\pi,\eta,\eta'} g_{aP}P_{\text{phys}}$$

$$g_{a\pi} = \delta_I \frac{m_\pi^2}{m_a^2 - m_\pi^2},$$
$$g_{a\eta} = \frac{2}{\sqrt{6}}\frac{m_\eta^2 - m_\pi^2}{m_a^2 - m_\eta^2},$$
$$g_{a\eta'} = \frac{4}{\sqrt{3}}\frac{m_\eta^2 - m_\pi^2}{m_a^2 - m_{\eta'}^2}.$$

[Balkin, Coren, Soreq, Williams] 2506.15637
[Ovchynnikov, Zaporozhchenko] 2501.04525

- ALPs decay invisibly $\text{BR}(a \to \chi\chi) \approx 1$ when $g_{a\chi} \gtrsim 10^{-3}$.
- The SM mesons may also decay invisibly via off-shell ALPs:

$$\text{BR}(P \to \bar{\chi}\chi) = \frac{m_P}{8\pi\Gamma_P}\left(\frac{f_\pi}{f_a}g_{aP}g_{a\chi}\right)^2\sqrt{1 - \frac{4m_\chi^2}{m_P^2}}$$

Missing-proton-energy (MPE) search

- We consider coherent exclusive electroproduction with invisible final state *X*:

$$p(p_p) + e^-(p_e) \to p(p_{p'}) + e^-(p_{e'}) + X(p_X)$$

- **MEP**: detect electron + forward proton ($\eta_{p'} > 4.5$) with reduced energy ($E_{p'}/E_p < 90\%$)
- *Reducible* background: Leakage of visible states *X* (e.g. $\pi^0 \to \gamma\gamma$, $\rho^0 \to \pi^+\pi^-$, $\varphi \to K\overline{K}$, $\gamma^* \to \ell^+\ell^-$). They can be effectively vetoed if we reconstruct X and require $\eta_X < 4$ (instrumented region).

Signal:

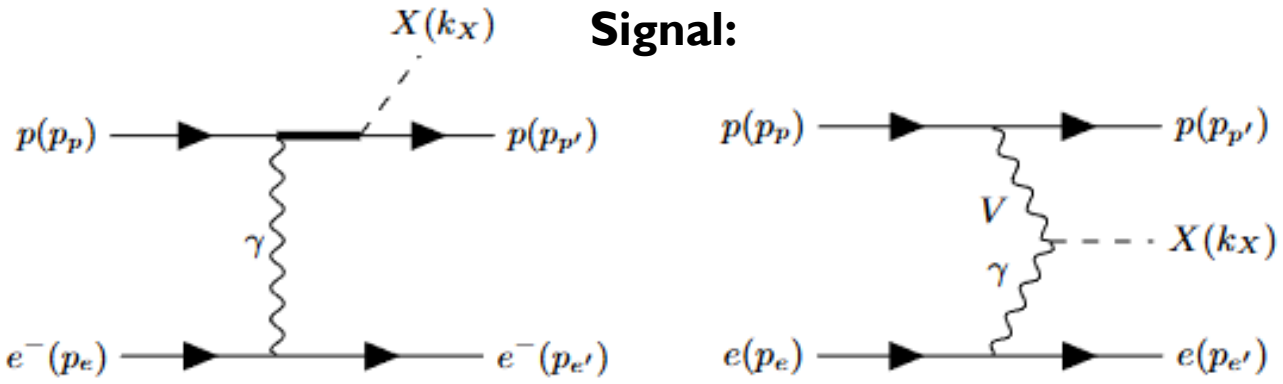

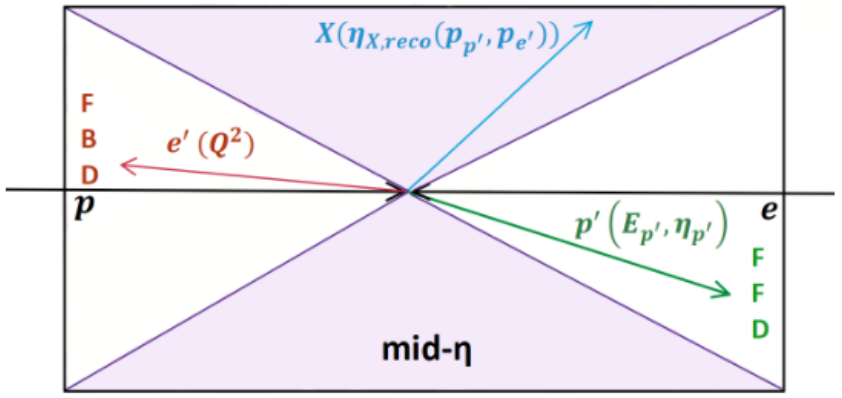

EIC prospects on invisibles

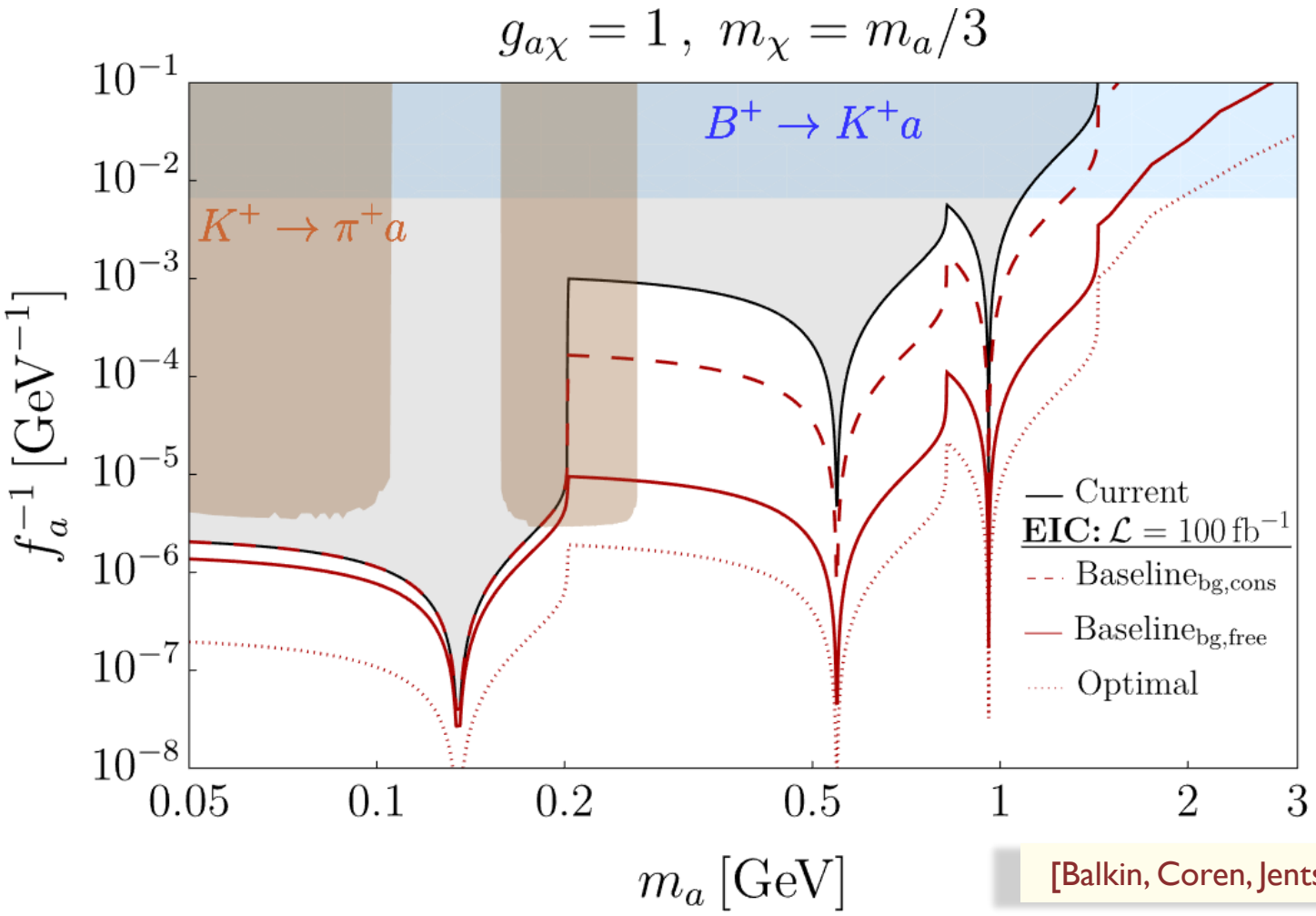

P	$\mathrm{BR}(P \to \mathrm{inv})_{\mathrm{current}}$	$\mathrm{BR}(P \to \mathrm{inv})_{\mathrm{EIC}}$
π^0	4.4×10^{-9} [43]	2×10^{-9} ($\mathrm{Baseline}_{\mathrm{bg,free}}$) 7×10^{-11} (Optimal)
η	1.1×10^{-4} [44]	2×10^{-6} ($\mathrm{Baseline}_{\mathrm{bg,cons}}$) 1×10^{-8} ($\mathrm{Baseline}_{\mathrm{bg,free}}$) 2×10^{-9} (Optimal)
η'	2.1×10^{-4} [44]	2×10^{-5} ($\mathrm{Baseline}_{\mathrm{bg,cons}}$) 8×10^{-8} ($\mathrm{Baseline}_{\mathrm{bg,free}}$) 1×10^{-8} (Optimal)

Selection	**Baseline**	**Optimal**
E_p, E_e	$(100, 10)$ GeV	$(41, 5)$ GeV
p', X	$\eta_{p'} > 4.5,\ 0.5 < E_{p'}/E_p < 0.9,\ \eta_X < 4$	
e'	$10^{-3}\,\mathrm{GeV}^2 < Q^2 < 0.1\,\mathrm{GeV}^2$	–
Bkg	0 (bg,free), Eq. (2) (bg,cons)	0

[Balkin, Coren, Jentsch, Liu, Ovchynnikov Soreq, **Trifinopoulos**] 2601.00068

The next generation lepton-ion colliders

- The EIC is a very powerful machine. But, what comes next?

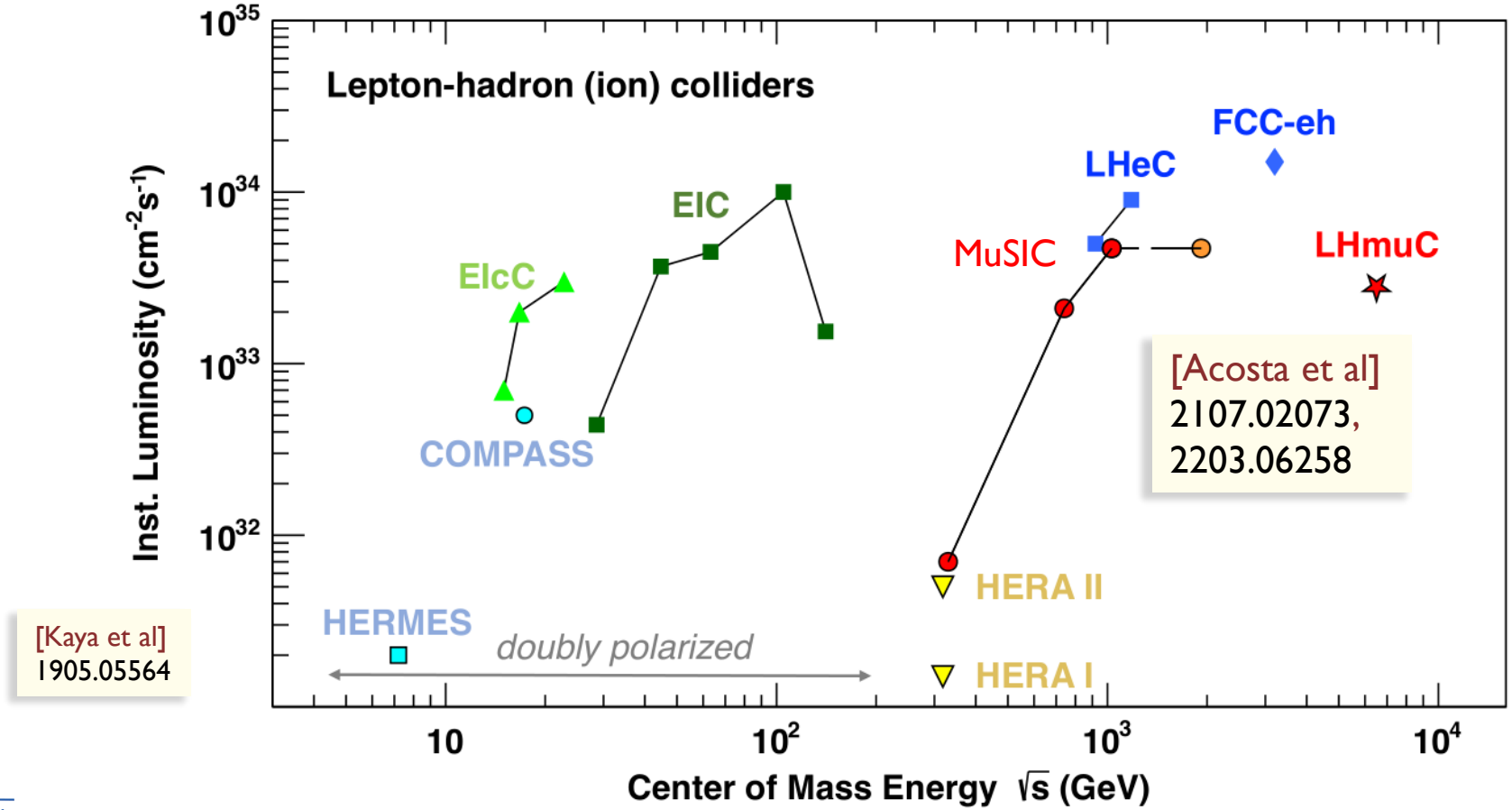

Why should we play MuSIC?

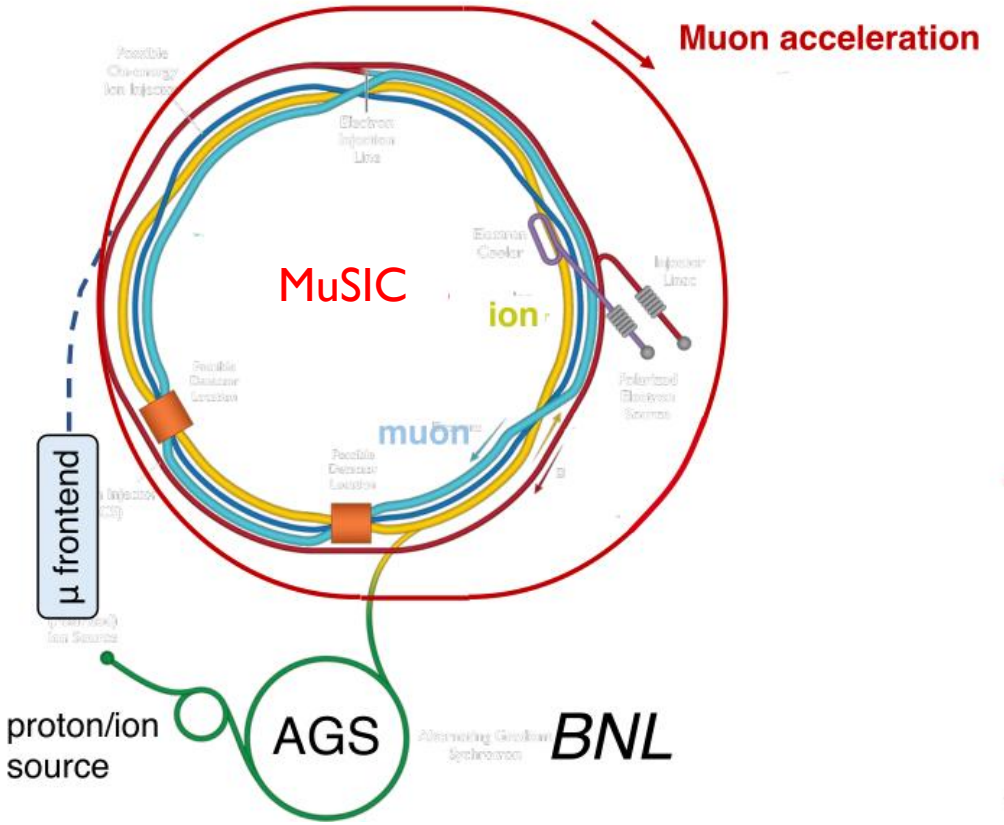

- By utilizing the existing infrastructure at BNL , MuSIC could directly succeed the EIC after its mission is completed (~2040) and reach a center-of-mass energy $\sqrt{s} = 1\ \mathrm{TeV}$.

Re-use of existing infrastructure allays some cost!

- **Dual appeal (and funding?)**: MuSIC establishes a new QCD frontier (nuclear physics), while also facilitating the development of a high-energy muon storage ring on the path towards a future MuC (particle physics).

The MuSIC of ALPs

Signal: 2γ + recoil μ^- + intact Au

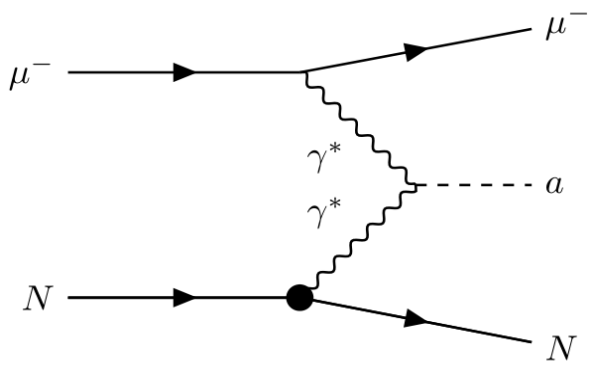

✓ Z^2-enhanced coherent enhancement

Background:

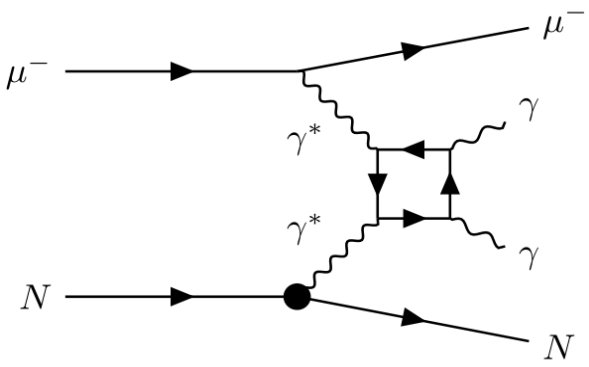

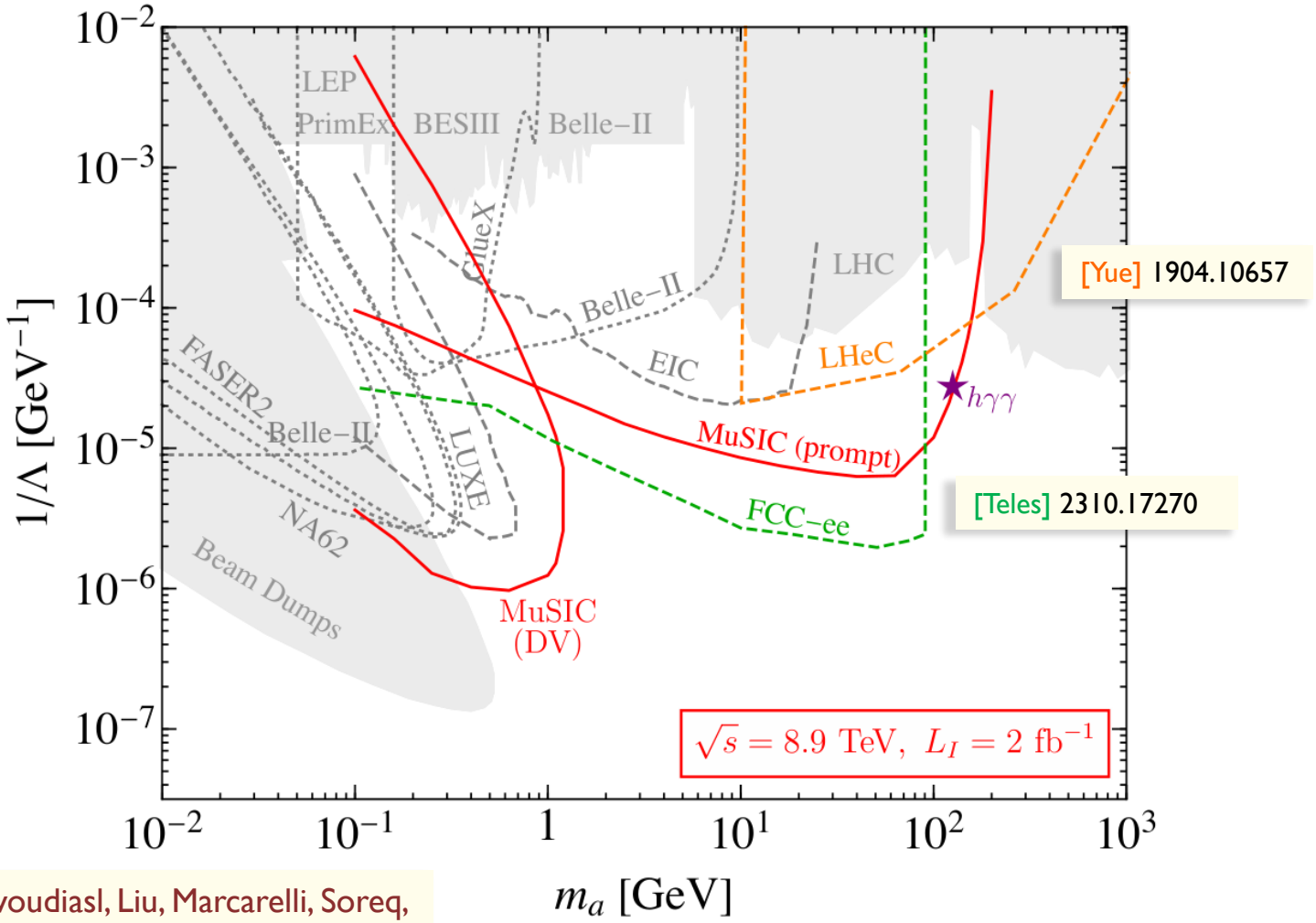

[Yue] 1904.10657

[Teles] 2310.17270

Davoudiasl, Liu, Marcarelli, Soreq, **Trifinopoulos**] 2412.13289

Summary

Methods

Effective Field Theories

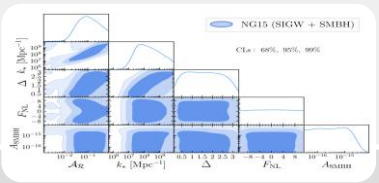

Simulations

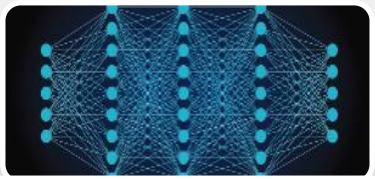

Artificial Intelligence

Fields

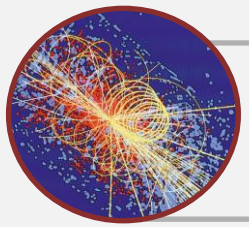

Future Colliders

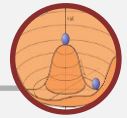

Naturalness

Particle Physics

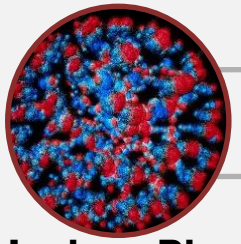

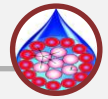

Nuclear Models

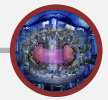

Fusion Experiments

Nuclear Physics

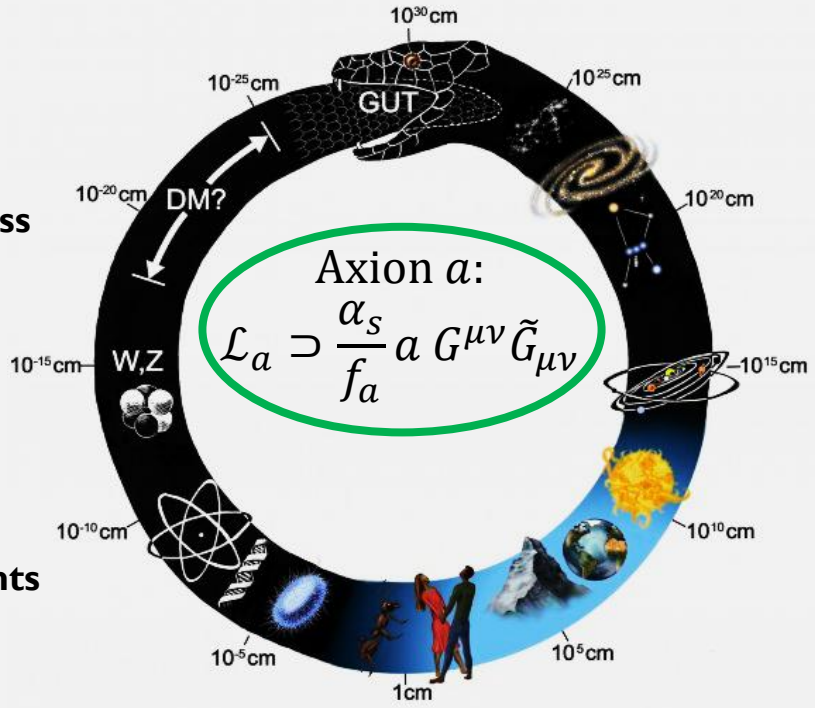

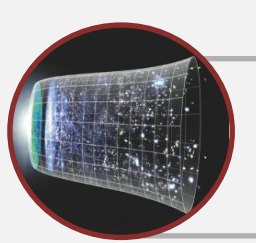

Galaxy Formation

Gravitational waves

Cosmology

Thank you!

Questions?

Backup slides

Outline

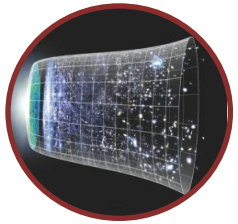

I. Large-Scale Structure bounds

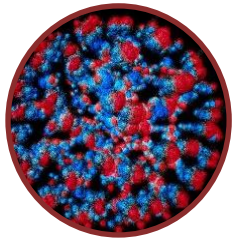

II. Production at Fusion Reactors

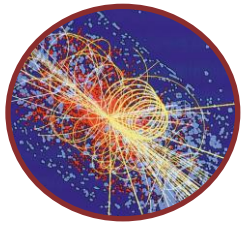

III. Searches at Colliders

Axion Cheatsheet

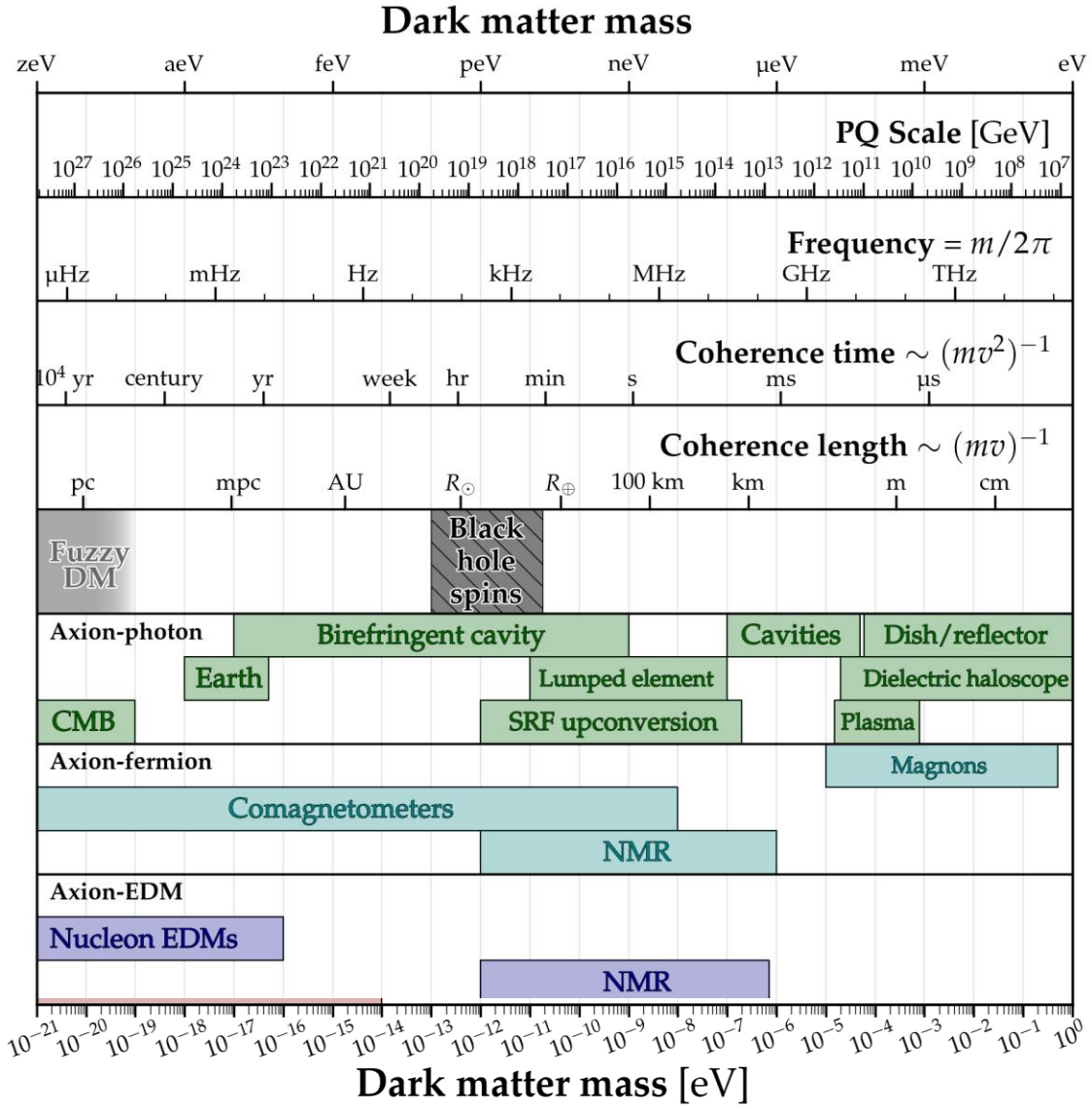

Sokratis Trifinopoulos

Dimensionless Power Spectrum

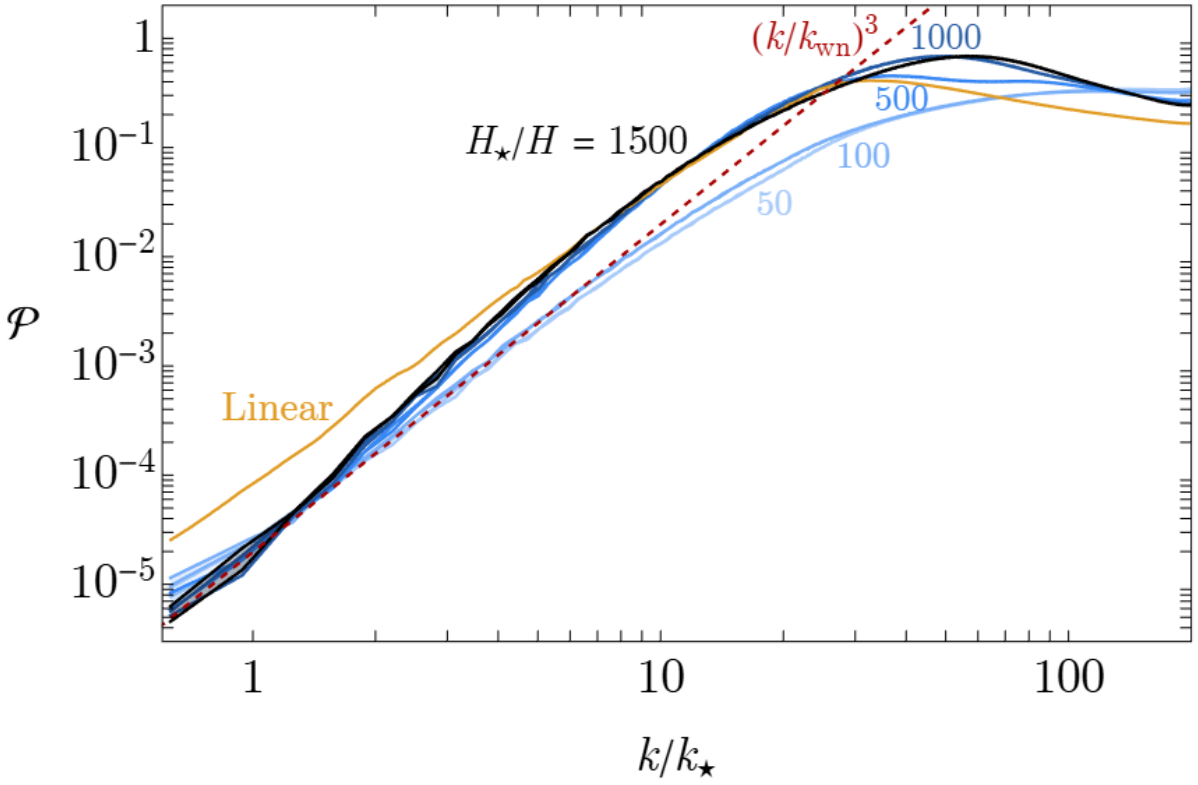

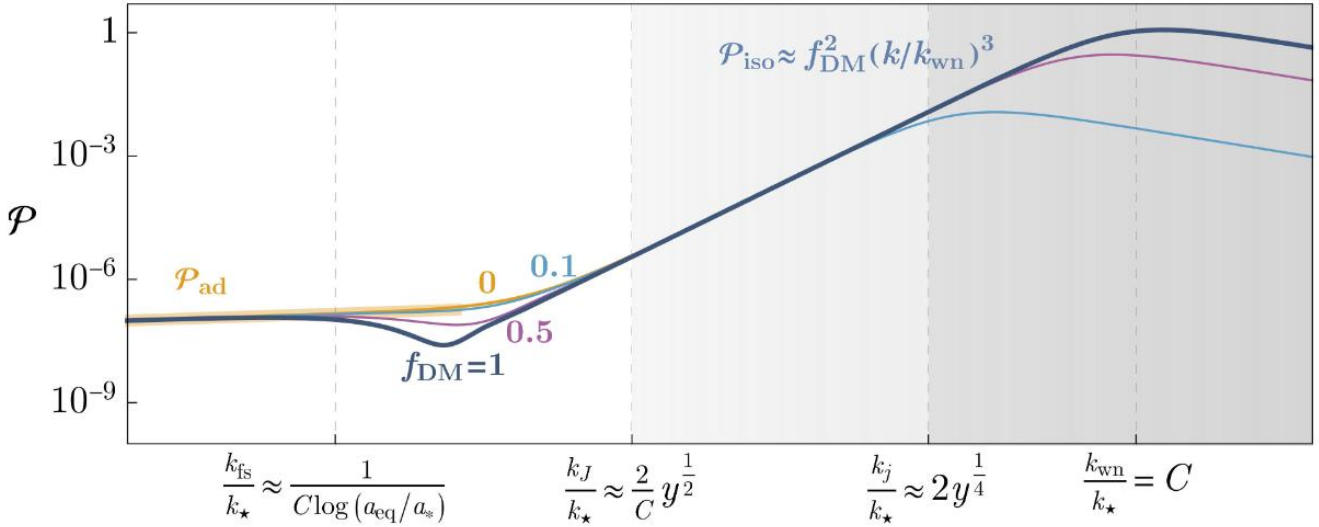

Axion Strings

➢ The strings contain energy which is proportional to $\mu = \underbrace{\pi f_a^2}_{\text{core}} \overbrace{\log \frac{m_r}{H}}^{\text{axion gradient}}$.

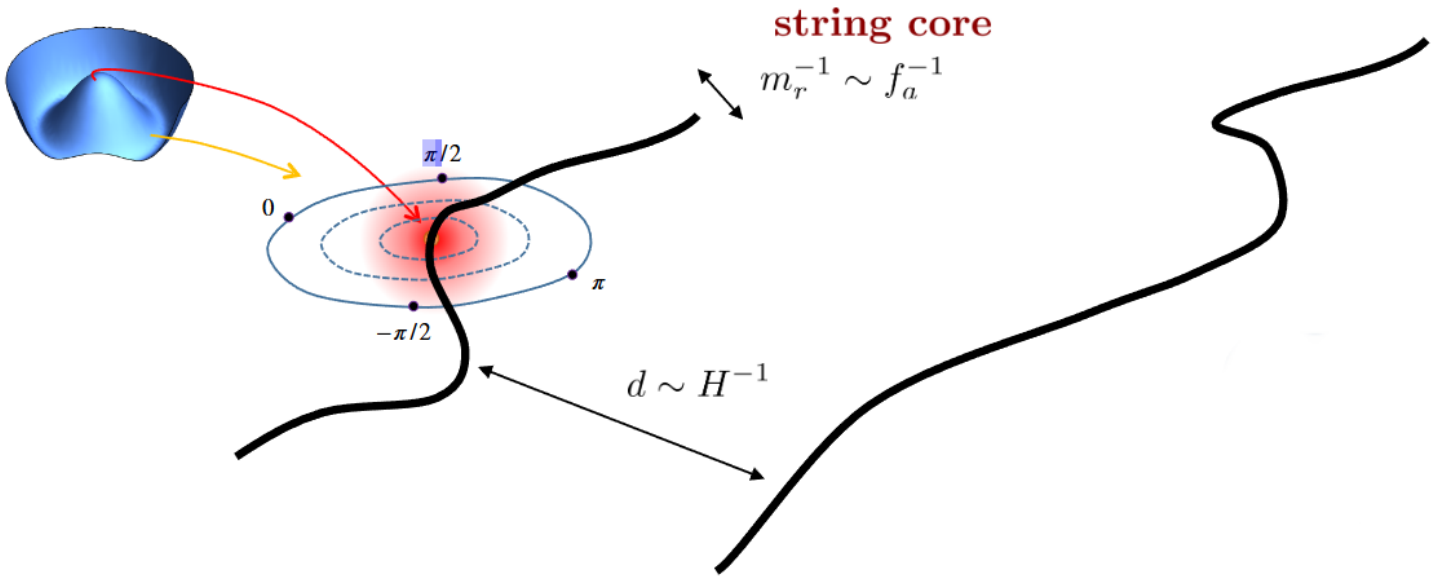

LSS constraints on the isocurvature

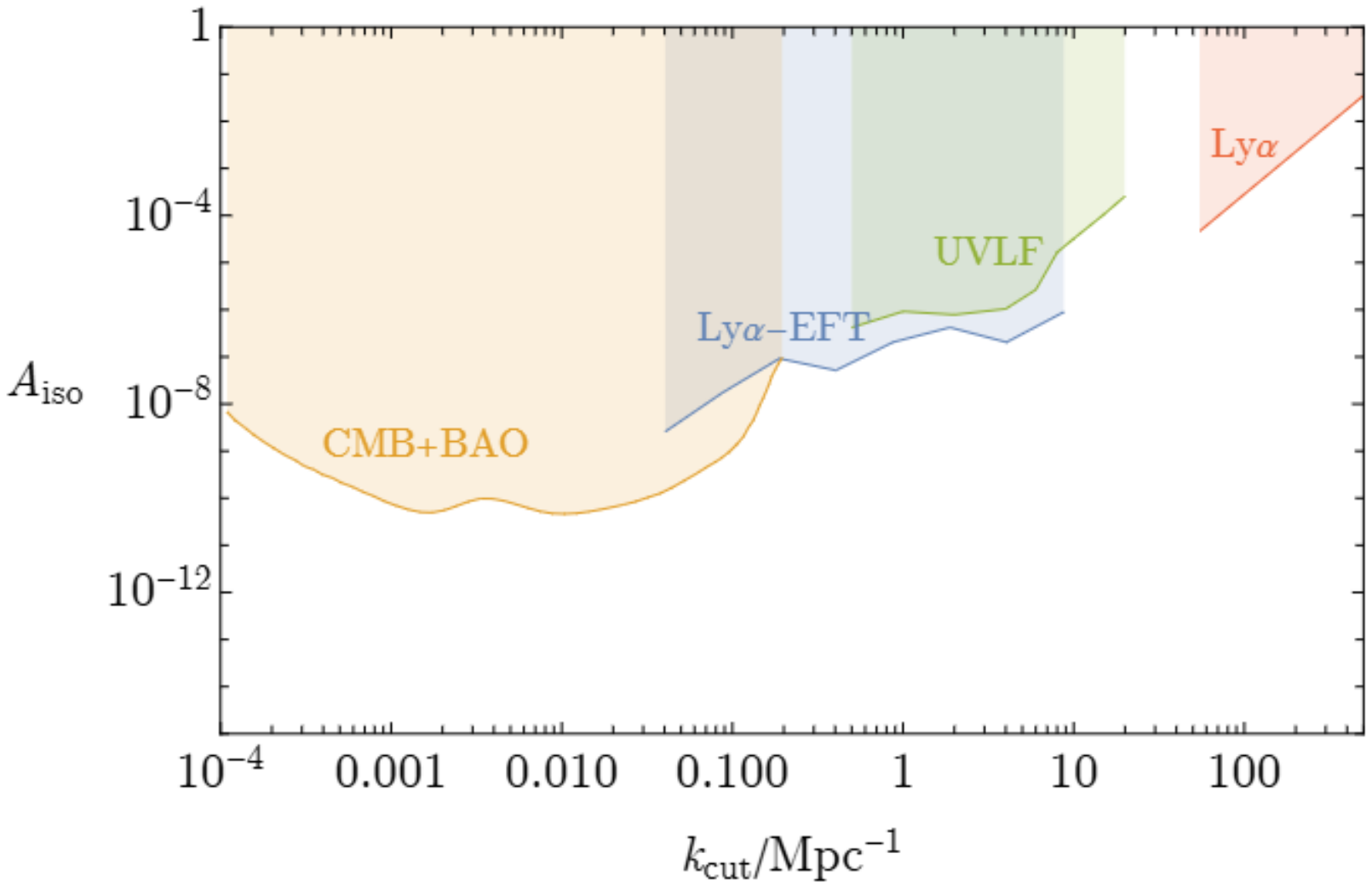

HMF with post-inflationary axions

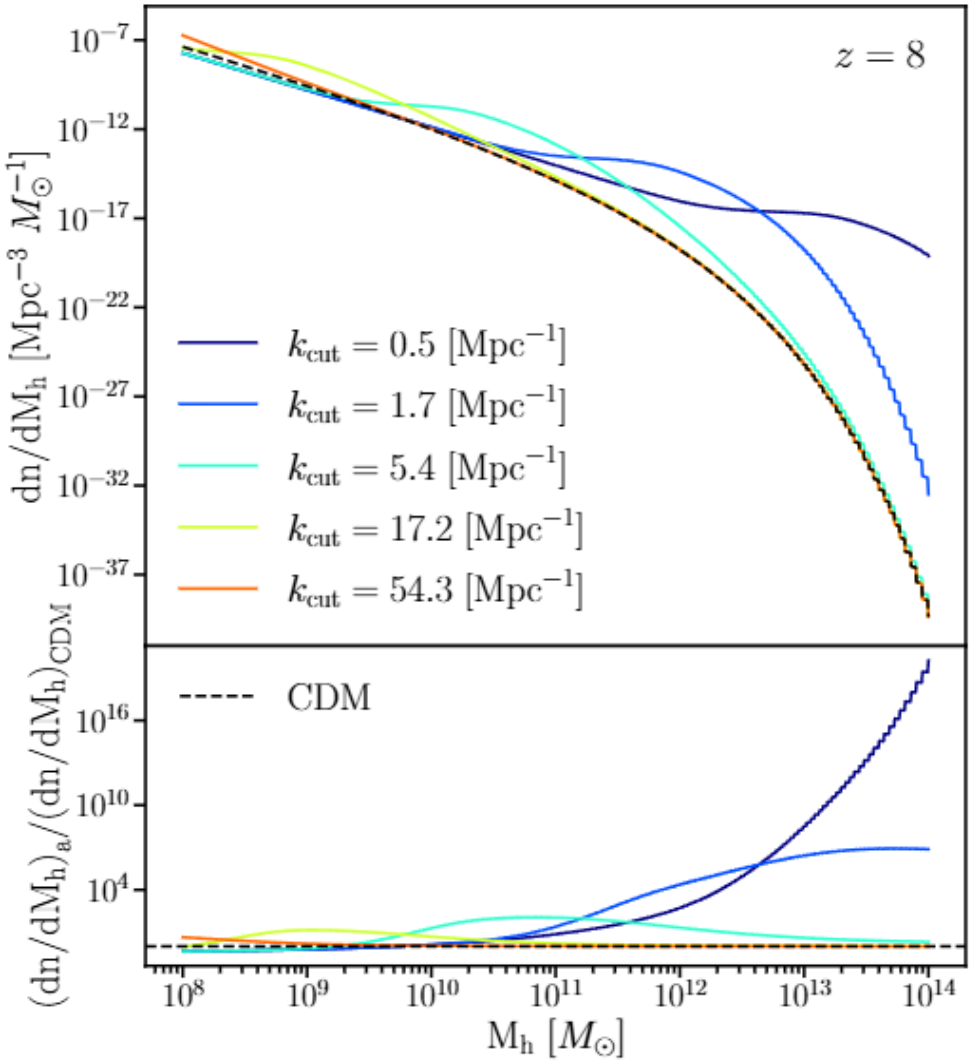

More EFT details

Modeling details. The full EFT model for the 3D Lyman alpha correlations reads

$$P_F^{\rm 3D}\left(k,k_\parallel,z\right) = (b_1 - b_\eta f\mu^2)^2 P(k) + P_{22} + P_{13} - 2k^2 P_{11}(c_0 + c_2\mu^2 + c_4\mu^4)\,, \tag{S2}$$

where $f = \frac{d\ln D_+}{d\ln a}$, $b_1(z), b_\eta(z)$ are linear bias parameters, c_n $(n = 0, 2, 4)$ are higher-derivative counterterms, and

$$P_{22} = \int 2\frac{d^3q}{(2\pi)^3}[K_2(\mathbf{k}-\mathbf{q},\mathbf{q})]^2 P(|\mathbf{k}-\mathbf{q}|)P(q)\ , \quad P_{13} = 6(b_1 - b_\eta f\mu^2)P(k)\int \frac{d^3q}{(2\pi)^3}K_3(\mathbf{k},-\mathbf{q},\mathbf{q})P(q)\,, \tag{S3}$$

and K_n are the Ly-α EFT kernels [44]. We ignore the 3D stochastic contributions. They will be added with the appropriate counterterms when we switch to 1D correlations. Precision measurements of EFT parameters from the ACCEL^2 simulation based on Ref. [49] carried out for the relevant redshift bins $z = 4, 5$ imply the following relations between the EFT parameters:

$$\begin{aligned}
b_\eta &= -0.46107\,b_1 + 0.22784, \quad b_{\eta^2} = -1.66391\,b_1 - 0.59993, \quad b_{\mathcal{G}_2} = -2.56067\,b_1 - 1.82742,\\
b_2 &= -10.01096\,b_1 - 3.23455, \quad b_{\delta\eta} = -5.22520\,b_1 - 1.38922, \quad b_{(KK)_\parallel} = 6.13639\,b_1 + 2.43267,\\
b_{\Pi_\parallel^{(2)}} &= -0.99037\,b_1 + 0.17342, \quad b_{\Pi_\parallel^{(3)}} = -0.35982\,b_1 + 1.32888, \quad b_{\delta\Pi_\parallel^{(2)}} = -3.19383\,b_1 - 2.81066,\\
b_{(K\Pi^{(2)})_\parallel} &= -1.35666\,b_1 - 2.60276, \quad b_{\eta\Pi_\parallel^{(2)}} = -10.61760\,b_1 - 6.93219, \quad b_{\Gamma_3} = -0.11903\,b_1 - 0.24599\,,\\
c_0 &= 0.02827\,b_1 + 0.01177, \quad c_2 = -0.01933\,b_1 - 0.01002, \quad c_4 = 0.00535\,b_1 + 0.00321\,.
\end{aligned}$$

The uncertainties in these relations are negligibly small thanks to an extended range of scales used in the fit at high redshifts, so we ignore them in what follows. We additionally multiply our 3D EFT model with a Doppler broadening kernel,

$$P_F^{\rm 3D}\left(k,k_\parallel,z\right) \to P_F^{\rm 3D}\left(k,k_\parallel,z\right) e^{-k_\parallel^2/k_F^2}\,. \tag{S4}$$

Even more EFT details

The sensitivity to small scales controlled by Λ is renormalized by the 1D stochastic counterterms

$$P_{\rm 1D,\ stoch}(k_\parallel) = \mathcal{C}_0 + \mathcal{C}_1 k_\parallel^2 + \mathcal{C}_2 k_\parallel^4 + \dots \,. \tag{S6}$$

In practice we use $\Lambda = 20\ h{\rm Mpc}^{-1}$ for the linear theory piece and $\Lambda = 12\ h{\rm Mpc}^{-1}$ for the one-loop contribution. These choices are made in order to be conservative and ensure $\Lambda \ll k_{\rm NL}$, which is especially important for the one-loop correction which is more UV-sensitive than the linear theory integrals. Within this scheme, the ACCEL^2 1D data implies the priors

$$\mathcal{C}_0 = 0.82540\, b_1 + 0.13270\,, \quad \mathcal{C}_1 = -0.00725\, b_1 - 0.00133\,, \quad \mathcal{C}_2 = 0.0000050\, b_1 + 0.0000004\,. \tag{S7}$$

In order to be conservative, we additionally marginalize these relations over some width $\Delta\mathcal{C}_n$, estimated from the UV-sensitivity of the theory predictions. We find that increasing the cutoff Λ to $\Lambda' = 30\ h{\rm Mpc}^{-1}$ (and switching off the Doppler broadening) shifts $\mathcal{C}_n$ by

$$\Delta\mathcal{C}_n \simeq 0.05\ h^{-1}{\rm Mpc}/[20\ h{\rm Mpc}^{-1}]^{2n}\ , \tag{S8}$$

which we choose as a prior on $\Delta\mathcal{C}_n$ that we marginalize over independently for every redshift bin.

Halo-Galaxy Connection

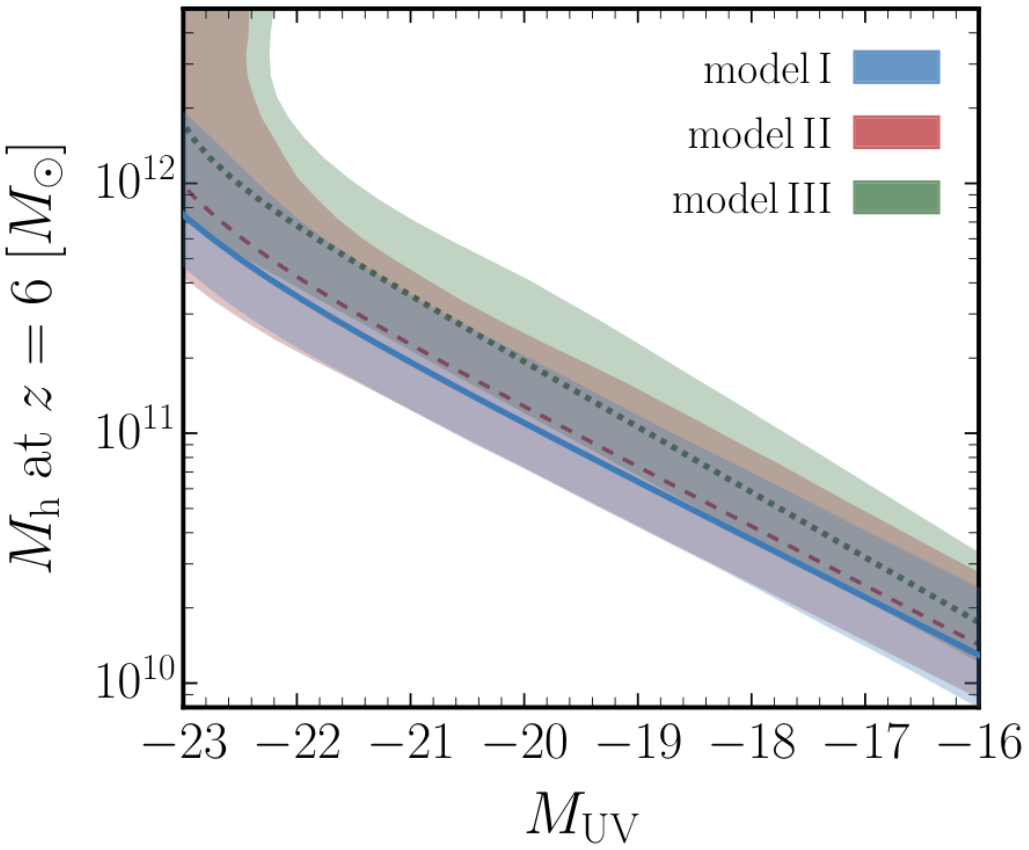

- The SFR and halo-mass accretion are related via a double-power law:

$$\widetilde{f}_* = \frac{\dot{M}_*}{\dot{M}_{\rm h}} = \frac{\epsilon_*}{\left(\frac{M_{\rm h}}{M_c}\right)^{\alpha_*} + \left(\frac{M_{\rm h}}{M_c}\right)^{\beta_*}} \,, \dot{M}_* = \kappa_{\rm UV} L_{\rm UV}$$

derived from a stellar synthesis population models with IMF in $0.1 - 100\, M_\odot$ and with constant SFR.

- Within the AB magnitude system, we have:

$$\log_{10}\left(\frac{L_{\rm UV}}{\rm erg\,s^{-1}}\right) = 0.4\,(51.63 - M_{\rm UV})$$

- In extended PS the accretion rate can be obtained as:

$$\dot{M}_{\rm h} = -\sqrt{\frac{2}{\pi}} \frac{(1+z)H(z)M_{\rm h}}{\sqrt{\sigma^2_{M_{\rm h}}(Q) - \sigma^2_{M_{\rm h}}}} \frac{1.686}{D^2(z)} \frac{{\rm d}D(z)}{{\rm d}z}$$

[Mandau, Dickinson] 1403.0007

fitted with the data using priors motived by simulations

UVLF Priors and Contour Plots

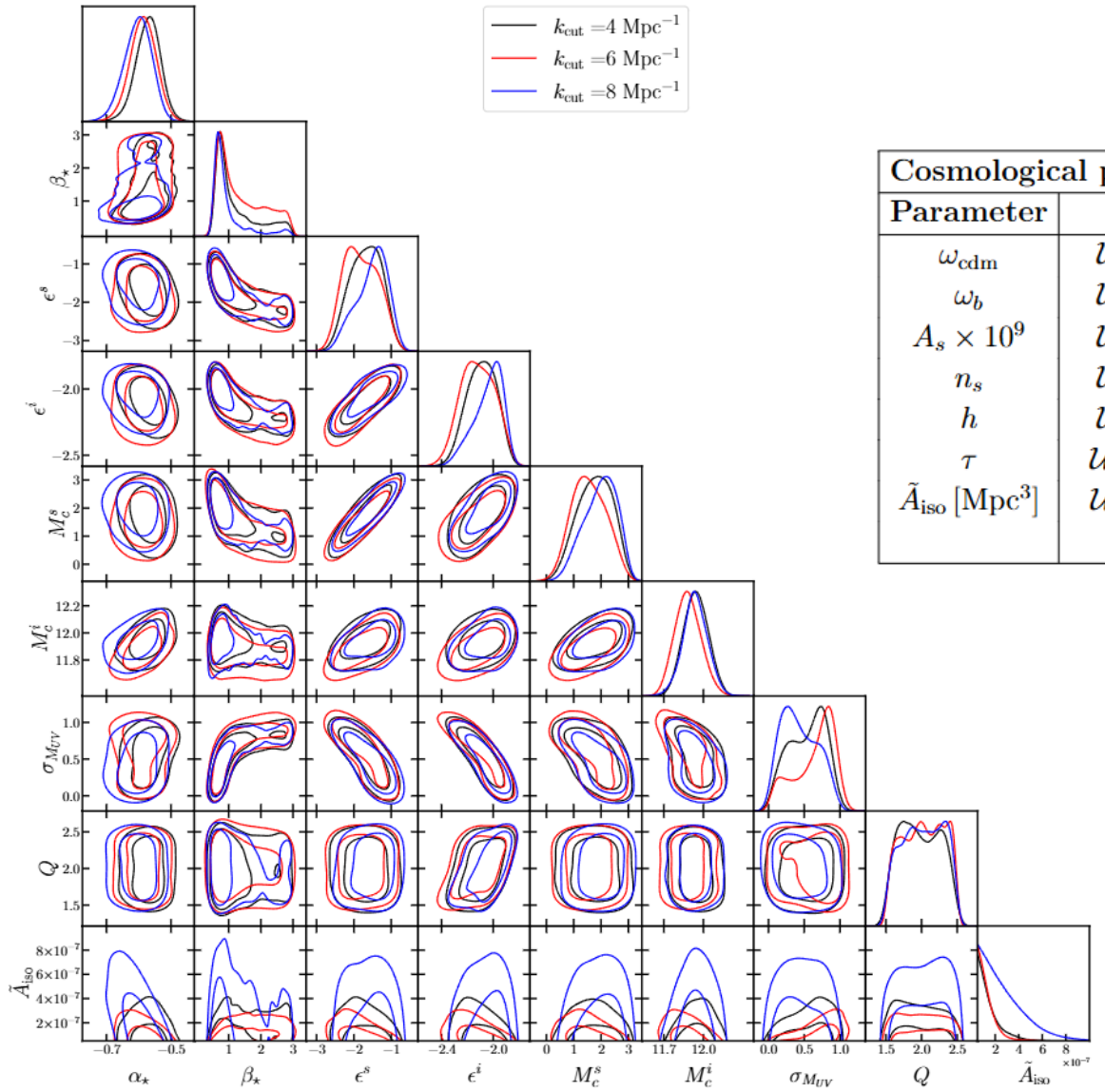

Cosmological parameters		UVLF parameters	
Parameter	Prior	Parameter	Prior
$\omega_{\rm cdm}$	$\mathcal{U}[-\infty, \infty]$	$\alpha_\star$	$\mathcal{N}(-0.557, 0.05)$
ω_b	$\mathcal{U}[-\infty, \infty]$	$\beta_\star$	$\mathcal{U}[0.0, 3.0]$
$A_s \times 10^9$	$\mathcal{U}[-\infty, \infty]$	$\epsilon_s^\star$	$\mathcal{U}[-3.0, 3.0]$
n_s	$\mathcal{U}[-\infty, \infty]$	$\epsilon_i^\star$	$\mathcal{U}[-3.0, 3.0]$
h	$\mathcal{U}[-\infty, \infty]$	M_c^s [$M_\odot$]	$\mathcal{U}[7.0, 15.0]$
τ	$\mathcal{U}[0.004, \infty]$	M_c^i [$M_\odot$]	$\mathcal{U}[7.0, 15.0]$
$\tilde{A}_{\rm iso}$ [Mpc^3]	$\mathcal{U}[0.0, 10^{-4}]$	$\sigma_{M_{\rm UV}}$ [mag^2]	$\mathcal{U}[0.001, 3.0]$
		Q	$\mathcal{U}[1.5, 2.5]$

James Webb Space Telescope

- JWST launched and it is already collecting data!

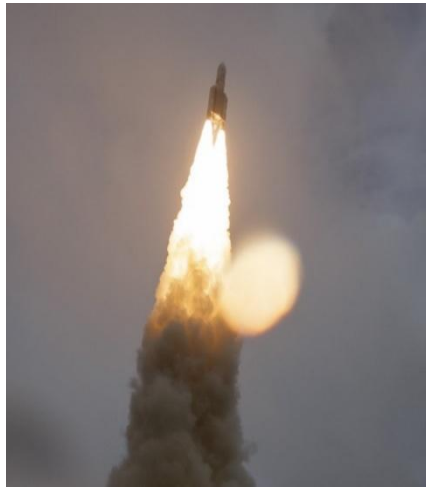

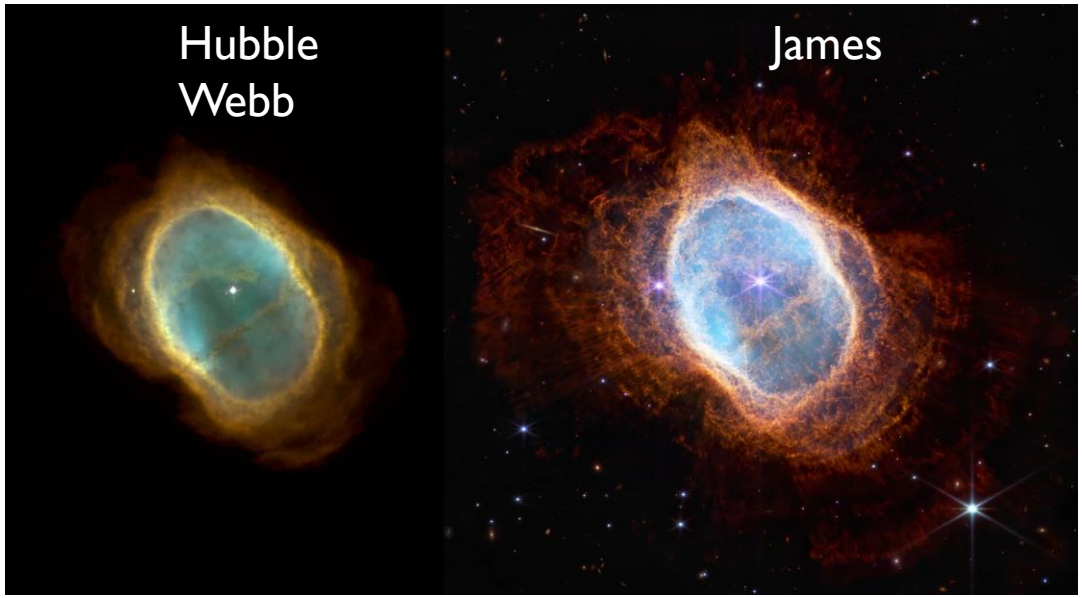

[Xu et al] [STSI/NASA, ESA, CSA, STScI, Webb ERO] Southern Ring Nebula

JWST Early Massive Galaxies

- Initial observations (e.g. JADES & CEERs surveys) have reported photometric evidence of massive galaxies at unexpectedly high redshifts $7 < z < 12$. A large subset of them has been recently spectroscopically confirmed.

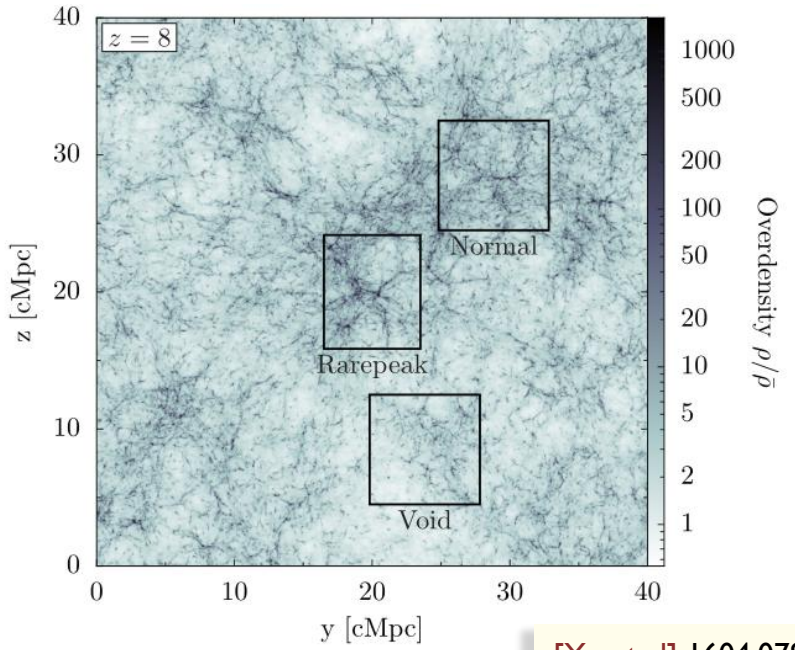

[Xu et al] 1604.07842

[Adams et al] 2207.11217, [Finkelstein et al] 2211.05792, [Naidu et al] 2207.09434

- Large cosmological hydrodynamical simulation demonstrated compatibility with existing models of galaxy formation.

[Keller et al] 2212.12804
[McCaffrey et al] 2304.13755

JWST Early Massive Galaxies: ΛCDM tension?

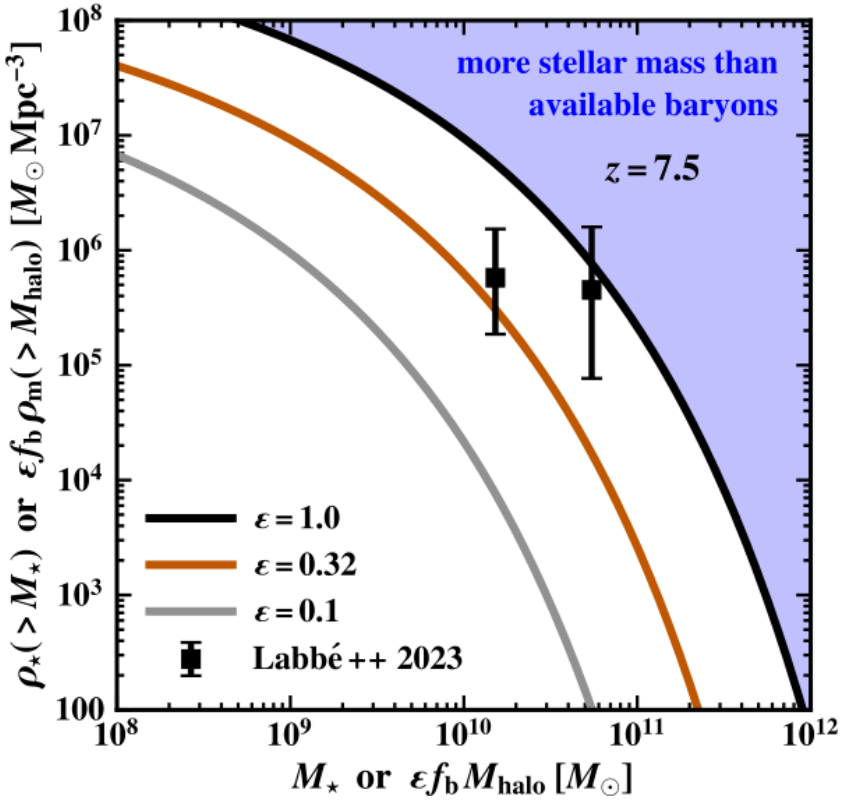

- The status of extreme galaxy candidates with stellar mass as high as 10^{11} $M_\odot$ still remains under investigation. [Labbe et al] 2207.12446

- If those results hold under spectroscopic scrutiny, they would pose a challenge to ΛCDM itself. For $\varepsilon = 0.1$, the current tension amounts to **2.5-3σ** confidence level.

[Boylan-Kolchin] 2208.01611 [Lovell et al] 208.10479 [Wang, Liu,Lu] 2311.02866

Outline

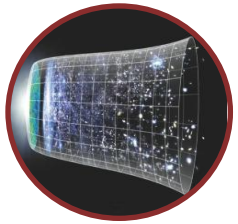

I. Large-Scale Structure bounds

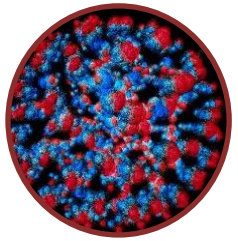

II. Production at Fusion Reactors

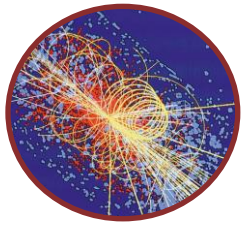

III. Searches at Colliders

Incident neutron flux

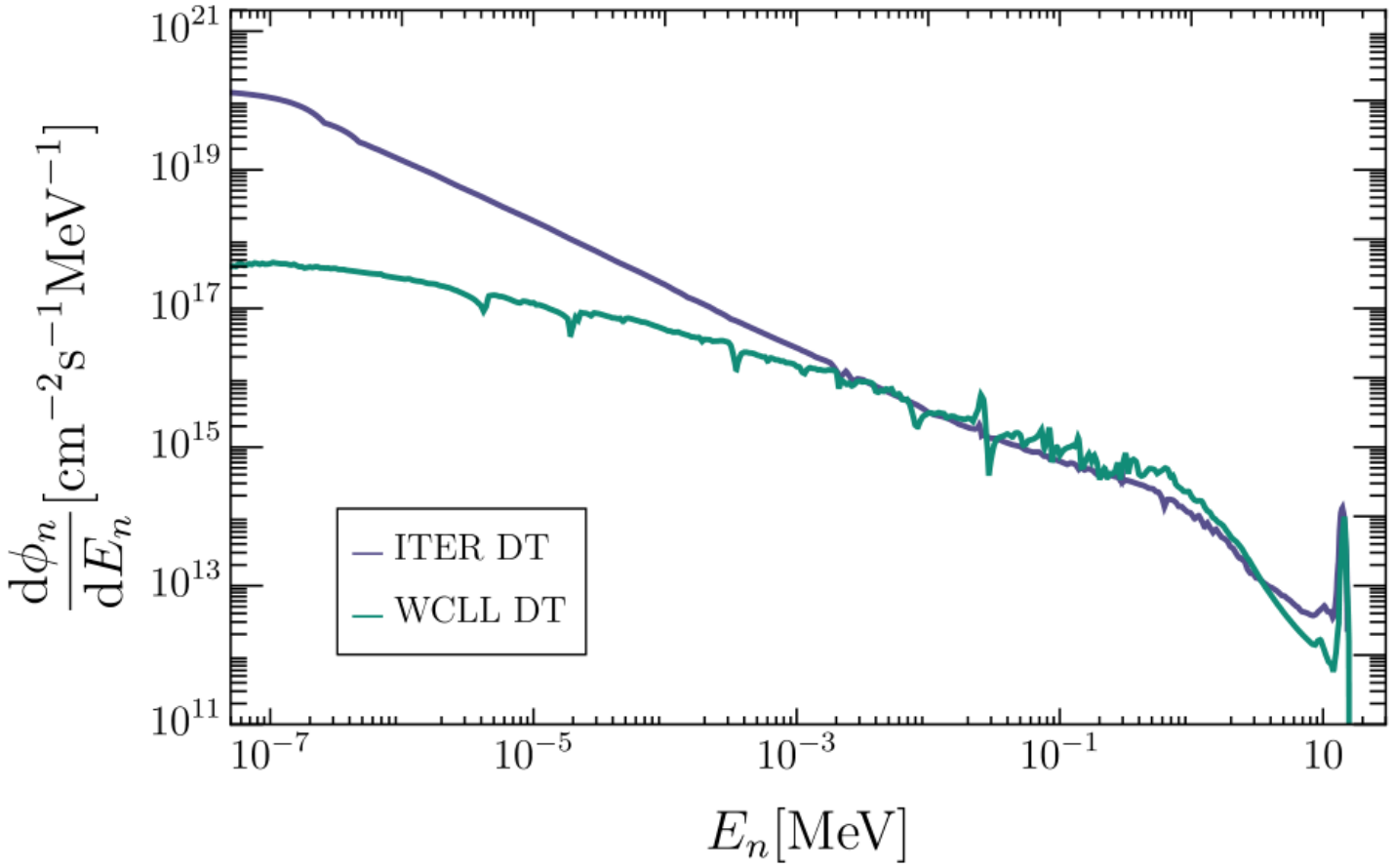

ALP Production and Detection

- Expected flux of produced ALPs:

$$\frac{\mathrm{d}\Phi_\varphi}{\mathrm{d}E_n} = \frac{1}{4\pi L^2} \times \mathcal{P}_{\text{surv.}} \times \frac{\mathrm{d}\dot{N}_\varphi}{\mathrm{d}E_n} \qquad \frac{\mathrm{d}\dot{N}_\varphi}{\mathrm{d}E_n} = \sum_{i,X} N_X \frac{\mathrm{d}\Phi_n}{\mathrm{d}E_n}\, \sigma_\varphi^{i,X}(E_n)$$

$$N_X \approx 2.5 \times 10^{31}\,\mathrm{cm}^3\mathrm{mol}^{-1} \times \rho_{\text{blanket}} \frac{f_X}{m_X} \times \left(\frac{\epsilon_{\text{atten.}}}{0.1}\right) \times \left(\frac{N_{\text{modules}}}{48}\right) \times \left(\frac{V_{\text{module}}}{8.4\,\mathrm{m}^3}\right)$$

- Expected number of dissociation events:

$$N_\varphi^{n\,\text{cap.}} = T N_D \iint \mathrm{d}E_n \mathrm{d}E_\varphi \delta\left(E_\varphi - S_n - E_n\right) \frac{\mathrm{d}\Phi_\varphi}{\mathrm{d}E_n}\, \sigma_{\varphi d \to np}(E_\varphi)$$

$$N_\varphi^{2\to 2\,\text{scat.}} = T N_D \iint \mathrm{d}E_n \mathrm{d}E_\varphi \delta\left(E_\varphi - E_n\right) \frac{\mathrm{d}\Phi_\varphi}{\mathrm{d}E_n}\, \sigma_{\varphi d \to np}(E_\varphi)$$

$$N_D \approx 6 \times 10^{31}$$

$$\sigma_{ad\to np} = \frac{g_{ap}^2}{6m_n} \sqrt{E_a^2 - m_a^2}\, \frac{|\vec{k}|\alpha}{(|\vec{k}|^2 + \alpha^2)^2}\, \frac{(1-\alpha a_s)^2}{1 + |\vec{k}|^2 a_s^2}$$

MeV ALPs interactions

- Starting from the parton-level Lagrangian: $\mathcal{L}_a \supset c_G^a \frac{a}{f_a} \frac{\alpha_s}{8\pi} G^a_{\mu\nu} \tilde{G}^{a\mu\nu} + \frac{\partial_\mu a}{2f_a} \sum_{\psi=u,d,s,e} c_\psi^a \, \bar{\psi}\gamma^\mu\gamma_5\psi$

  we may derive the effective interactions:

$$\mathcal{L}_{a,\text{eff}} \supset -\frac{1}{4} g_{a\gamma} a F^{\mu\nu}\tilde{F}_{\mu\nu} + a \sum_{N=p,n} g_{aN} \left(\bar{N} i\gamma_5 N\right) + g_{ae} a \left(\bar{e} i\gamma_5 e\right)$$

$$g_{ae} = \frac{m_e}{f_a} c_e^a$$

$$g_{a\gamma,\text{eff}} = g_{a\gamma} - \frac{\alpha}{\pi}\frac{g_{ae}}{m_e} B_1(1/\tau_e)$$

$$g_{aN} = \frac{1}{f_a}\left[\sum_{q=u,d,s} F_P^{q/N}(0) c_q^a - F_{\tilde{G}}^N(0) c_G^a\right]$$

Numerical Benchmarks:

p-only: $\quad g_{\varphi p} \neq 0, \quad g_{\varphi e} = g_{\varphi\gamma,\text{eff}} = g_{\varphi n} = 0,$

$pe\gamma$: $\quad g_{\varphi p} \neq 0, \quad g_{\varphi e} = 10^{-3} g_{\varphi p}, \quad g_{\varphi\gamma,\text{eff}} = \frac{10^{-3}}{\text{GeV}} g_{\varphi p}, \quad g_{\varphi n} = 0$

$g_{\varphi e} = (m_e/m_p) \times g_{ap}$

$g_{\varphi\gamma,\text{eff}} = (\alpha/4\pi) \times (1/m_e) \times g_{ae}$

- The decay rates of (pseudo-)scalars are:

$$\Gamma(\varphi \to \gamma\gamma) = \frac{g_{\varphi\gamma,\text{eff}}^2 m_\varphi^3}{64\pi}, \qquad \Gamma(\varphi \to ee) = \frac{g_{\varphi e}^2 m_\varphi}{8\pi}\sqrt{1 - \frac{4m_e^2}{m_\varphi^2}}$$

Prospects for scalar-proton coupling

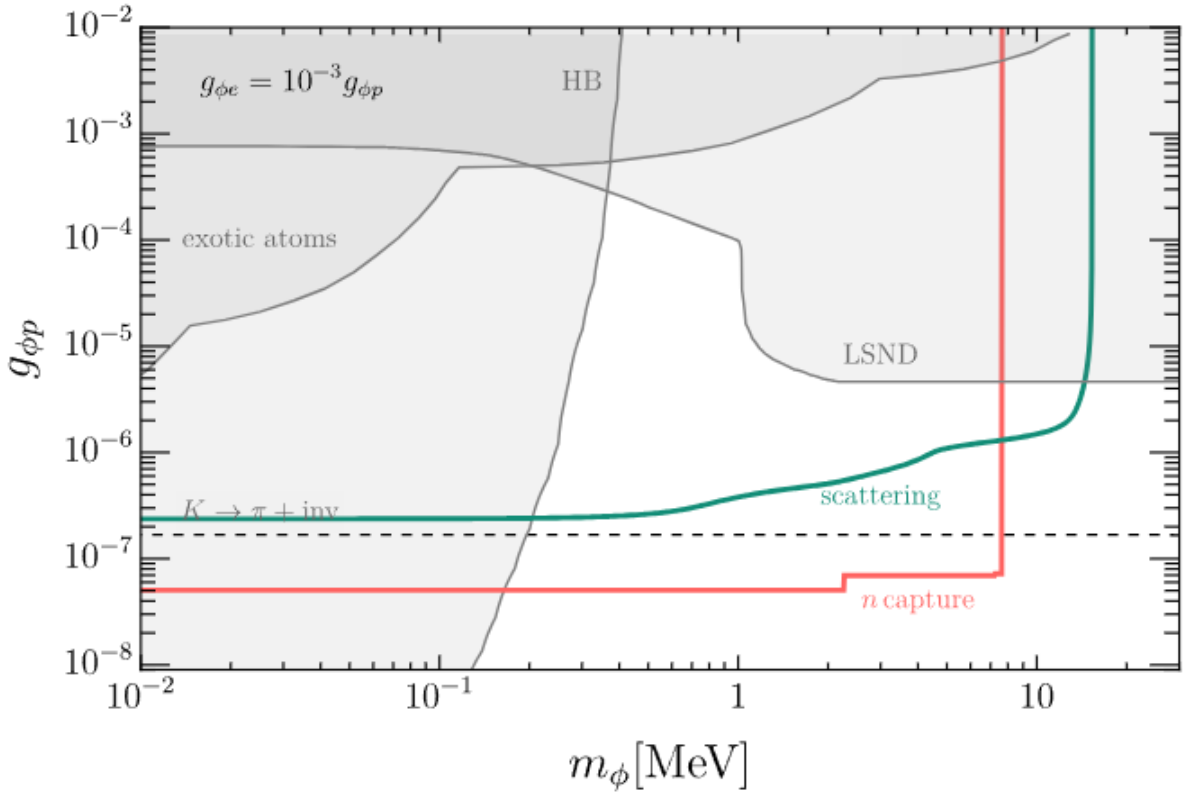

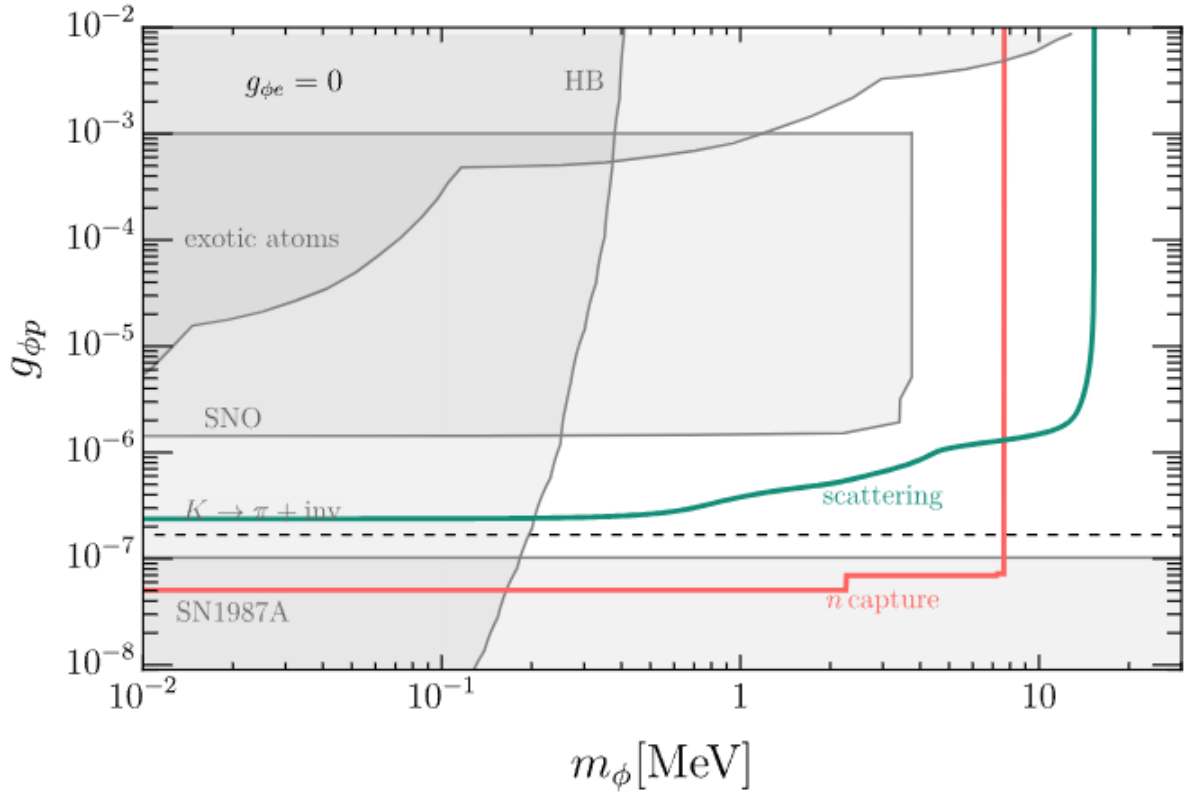

Prospects for ALP-proton coupling ($g_{ae} = 0$)

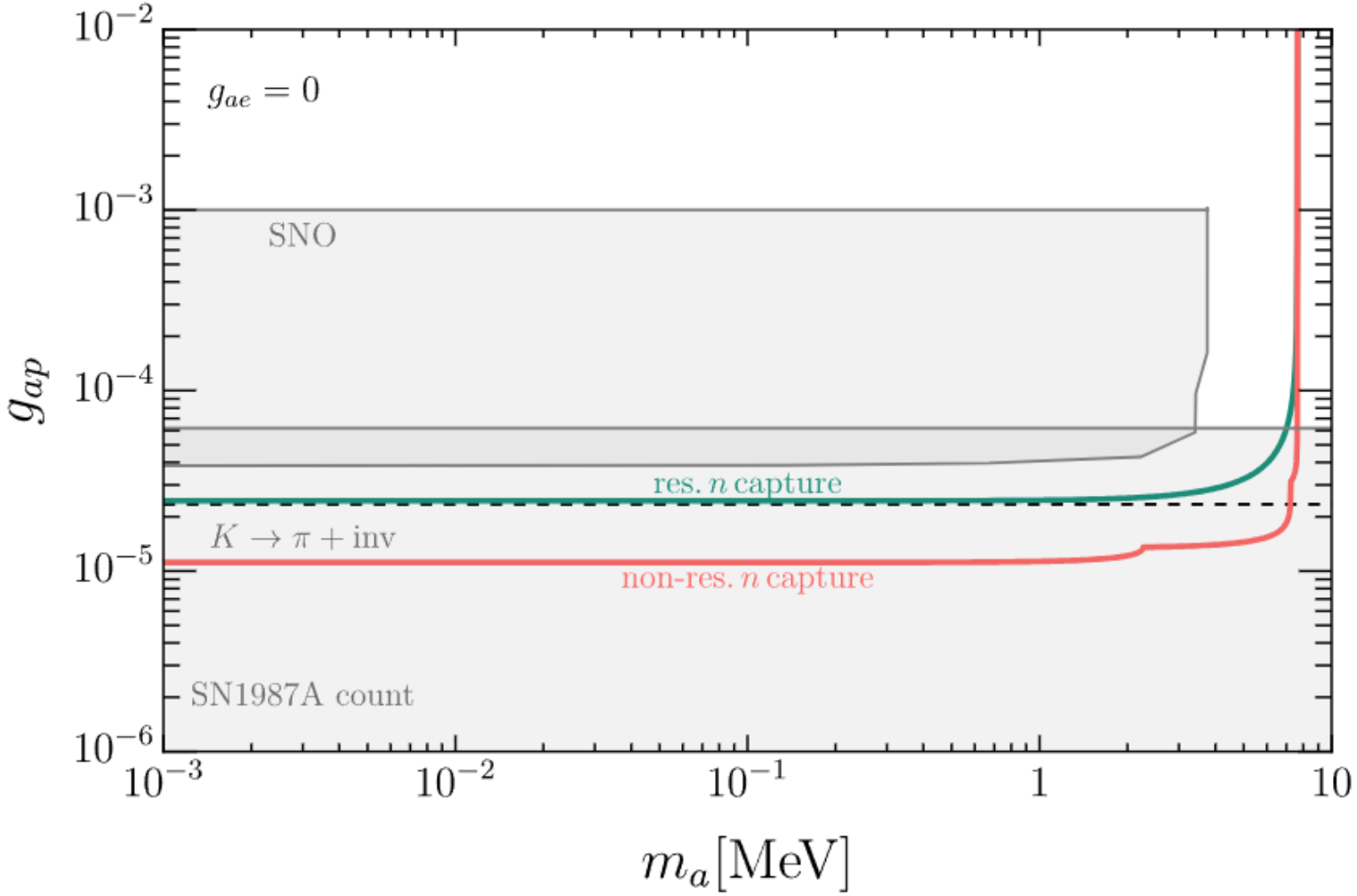

Towards a general-purpose AI for Nuclear Physics

NuCLR is an interpretable deep-learning model that predicts various nuclear observables.

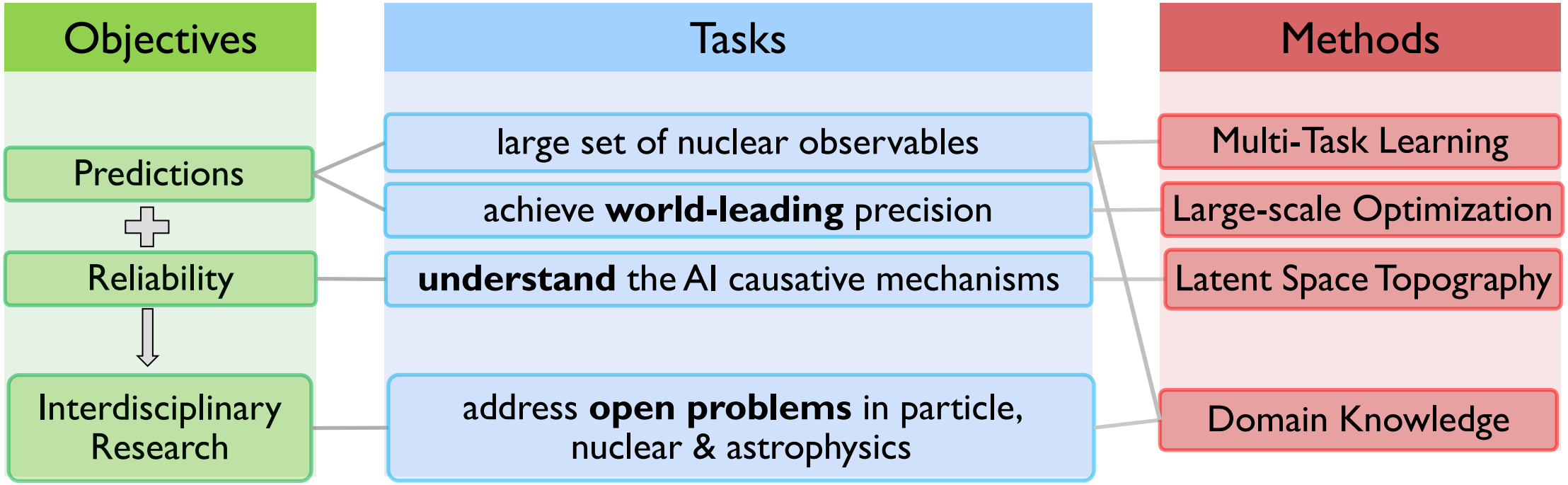

Tasks: nuclear observables

- **Binding energy:** break apart a nucleus into its nucleons, fundamental observable

$$E_B(Z,N) = Zm_p + Nm_n - M(Z,N)$$

- **Charge radius:** root-mean-square radius of the proton distribution.

- **Separation energies:** remove a specific number of nucleons, measure of stability.

$$S_n(Z,N) = M(Z,N-1) + m_n - M(Z,N) \ ,$$

$$S_p(Z,N) = M(Z-1,N) + m_p - M(Z,N) \ .$$

$$Q_\beta(Z,N) = M(Z,N) - M(Z+1,N-1) \ ,$$

$$Q_\alpha(Z,N) = M(Z,N) - M(Z-1,N+1) - m_{^4_2\mathrm{He}} \ .$$

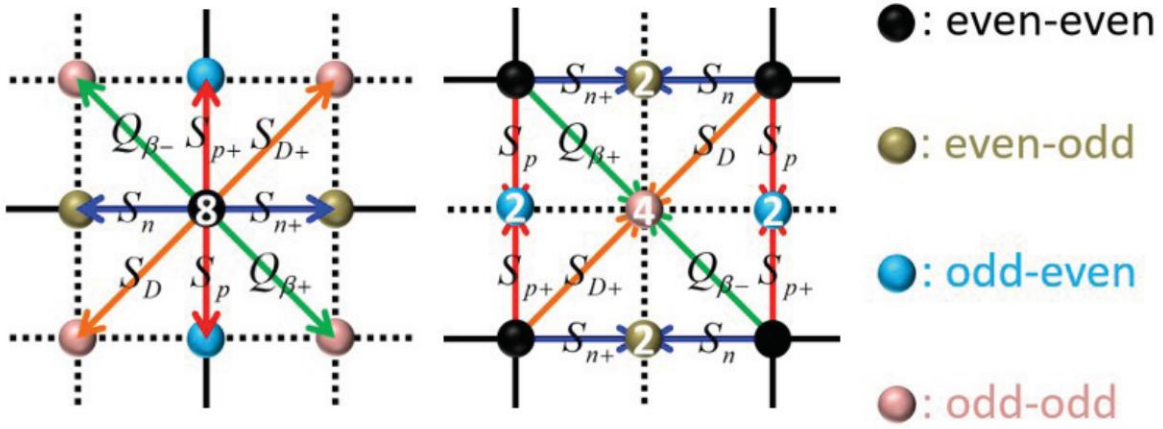

☑ World-leading accuracy

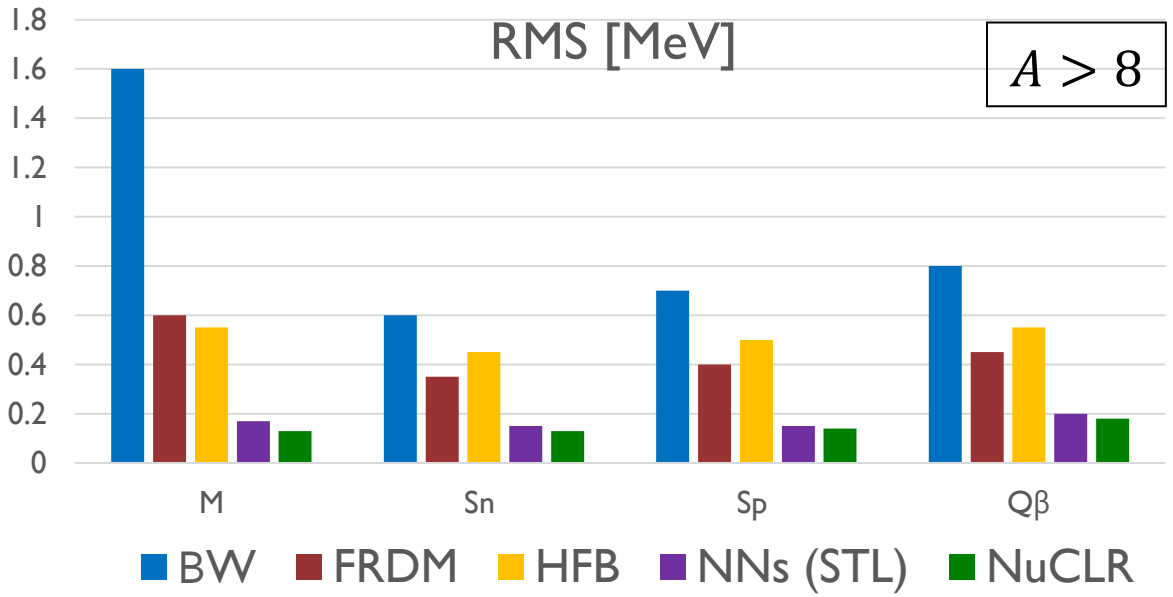

Database (energies): Wang et al (AME2020), Phys. Lett. B, 734: 215–219, 2014

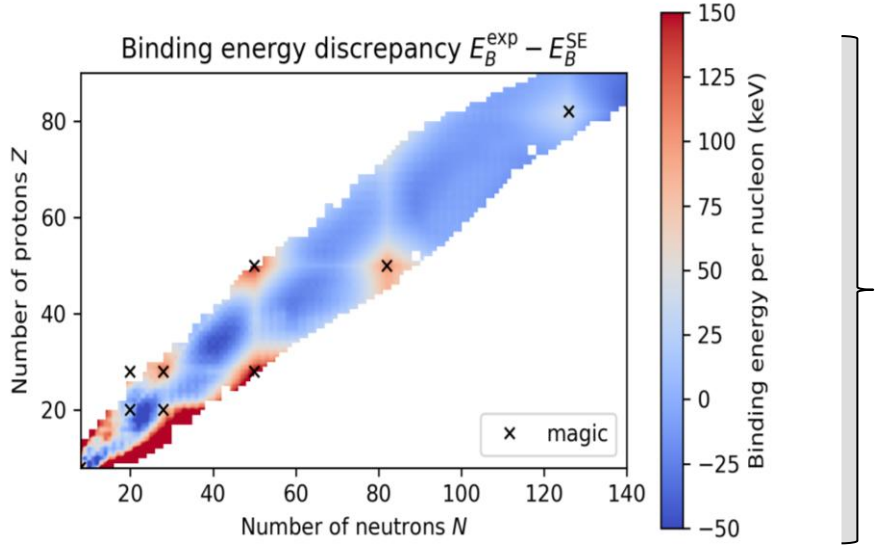

Liquid-drop model

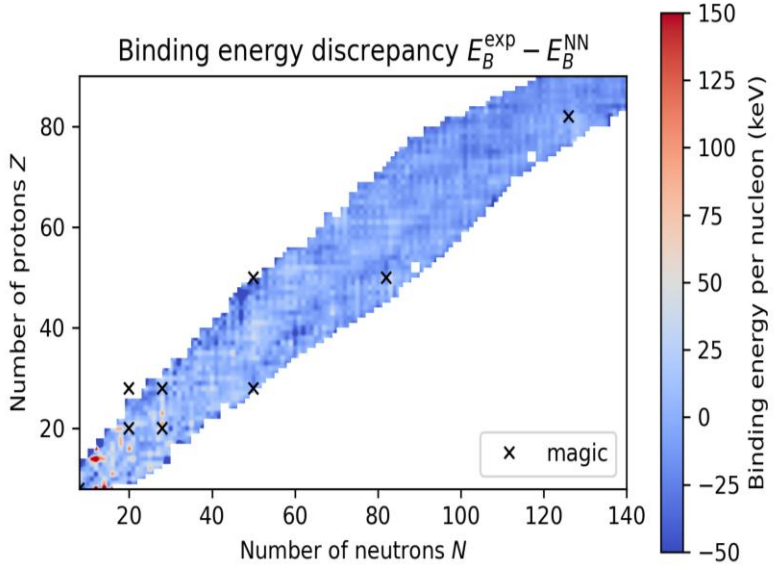

NuCLR

- We find that MTL improves **generalization** compared to single-task training (STL) as it exploits data correlations over multiple tasks a and leverages joint information.

Interpretability by Construction

- The success of MT gives the first hint towards the potential of internalizing the fundamental laws governing the nucleus. BUT we infer this from the RMS score.. is that enough?

When possible, pursue active interpretability, where you control the network architecture and training paradigm.

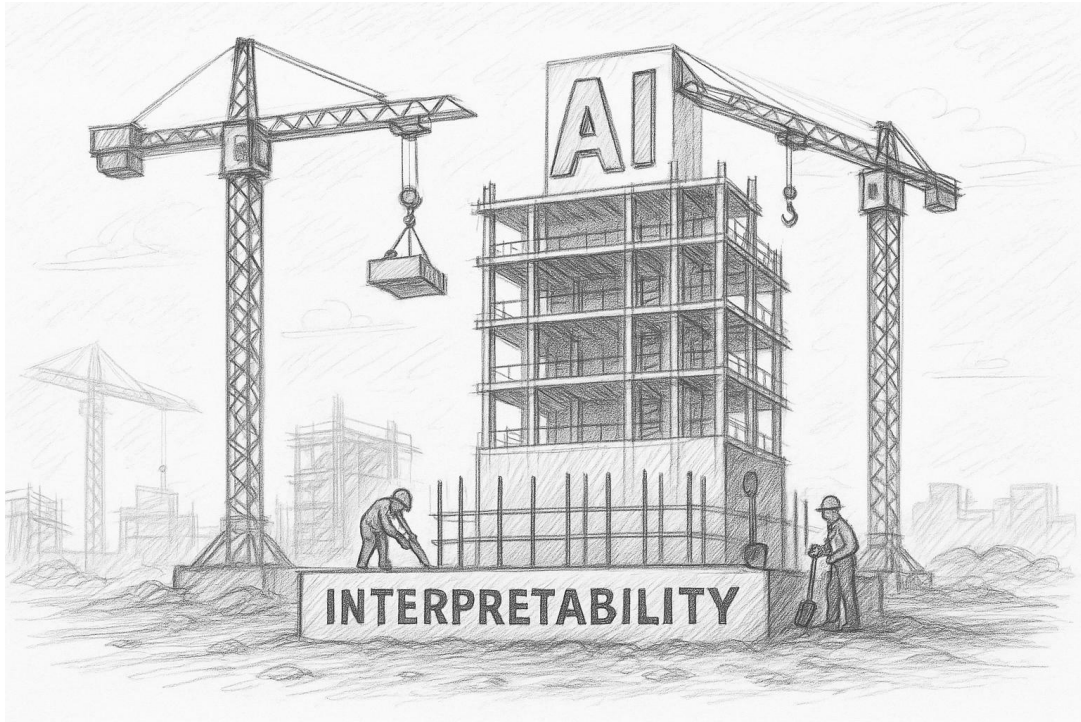

What are NN models actually learning?

- ***Manifold hypothesis:*** Real-world data are expected to concentrate in the vicinity of a manifold of much lower dimensionality, embedded in high dimensional input space. Bengio, Courville, Vincent 1206.5538

- ***Mechanistic Interpretability (MI)*** encompasses techniques of identifying low-rank structures in high-D datasets, and uncovering the algorithms that are implemented.

Interpretable AI via: *Latent Space Topography*

- *Latent space topography* (LST) is an MI procedure which consists of the following steps:

  1) extract high quality features of the NN using a dimensionality reduction method on the latent space,
  2) identify the emergent geometry in the first PC dimensions using domain knowledge,
  3) classify trained networks according to the algorithms they implement.

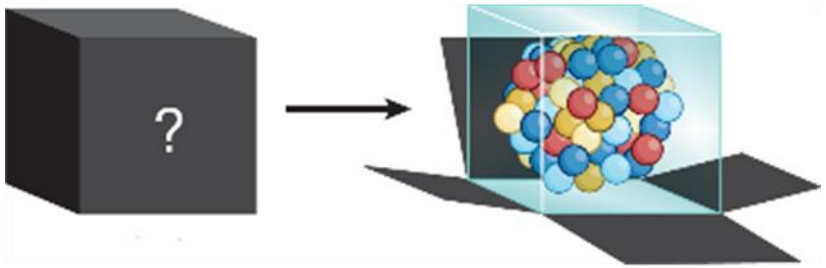

LST on the embedding space

- **NN model:** $N \to \vec{N}, Z \to \vec{Z} \Rightarrow E_b = F_{NN}(\vec{N}, \vec{Z}, \vec{\theta})$, where we consider a simplified case with isospin-symmetric data: $E_b = \underbrace{\alpha_v A}_{\text{volume}} - \underbrace{\alpha_a \frac{(N-Z)^2}{A}}_{\text{assymetry}}$

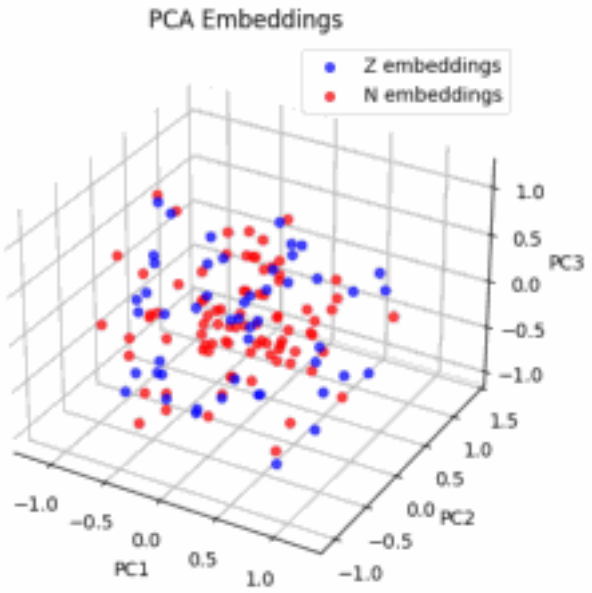

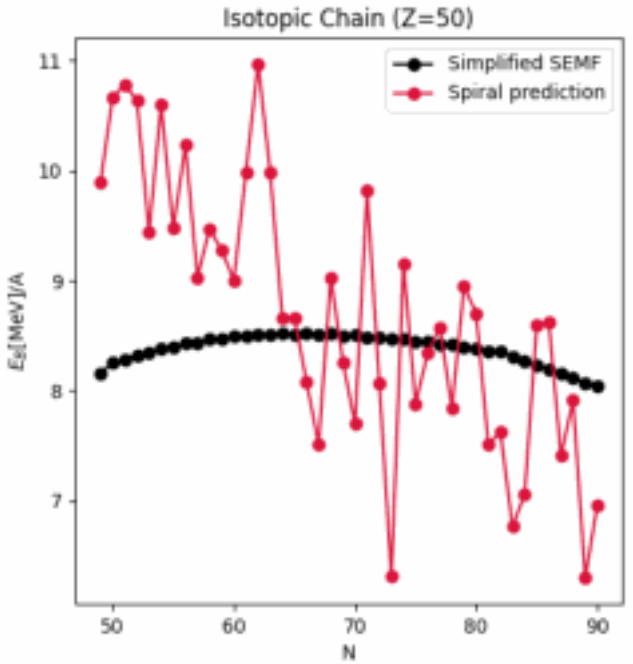

Epoch: 0 RMS: 1.2688

- **LST Step 1:** extract high quality features of the NN using a dimensionality reduction method on the latent space; here: principle component (PC) analysis:

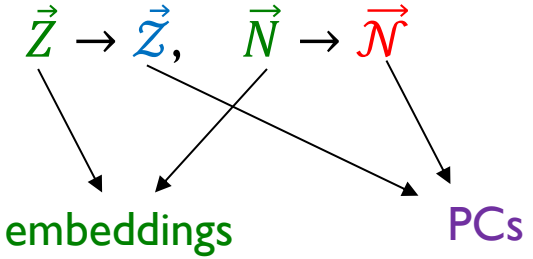

The nuclear *double helix*

LST Step 2: Identify the emergent geometry in the first PC dimensions; here: robust helices that align symmetrically in the 3D PC space.

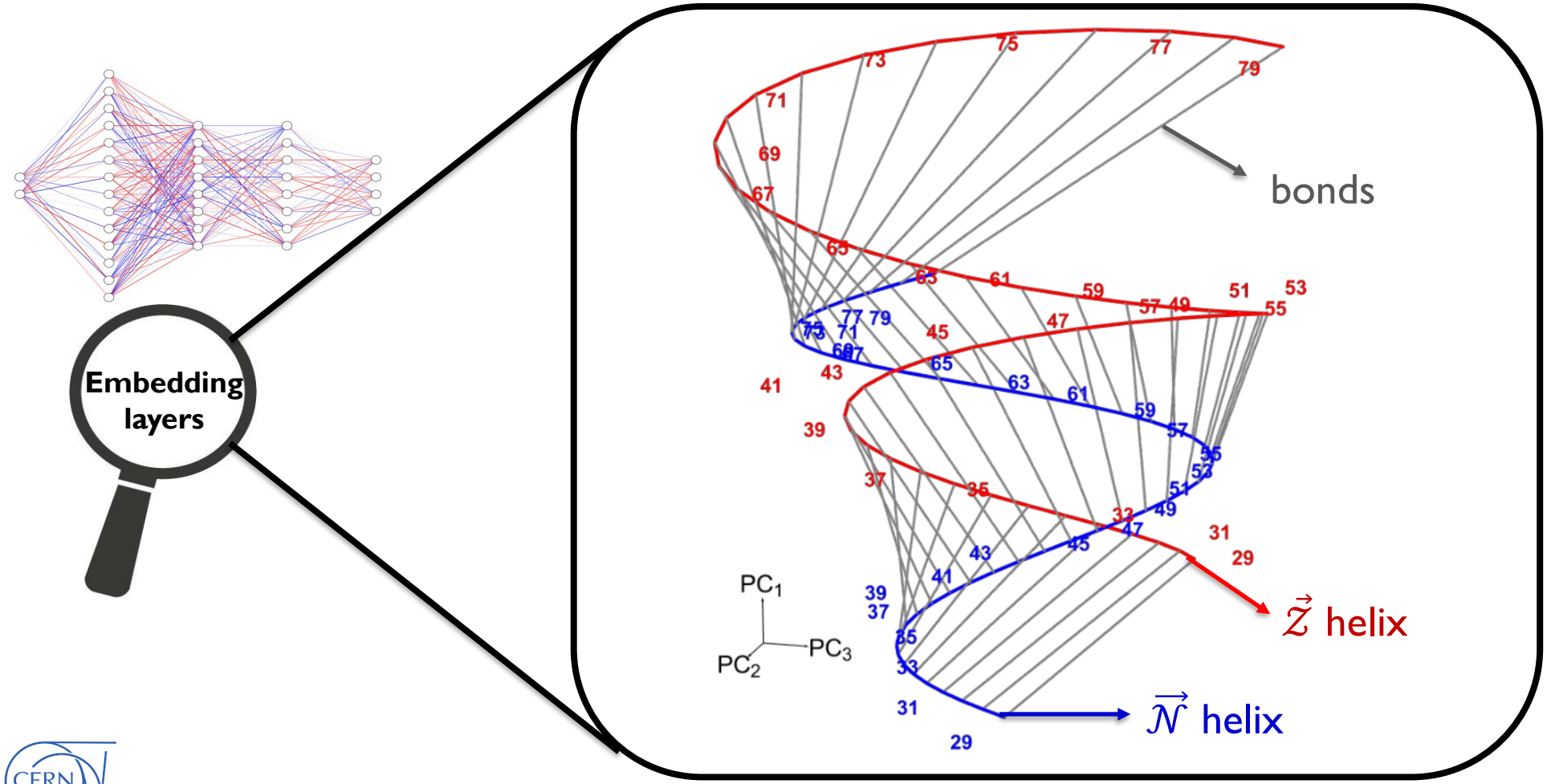

Stability of the nuclear DNA

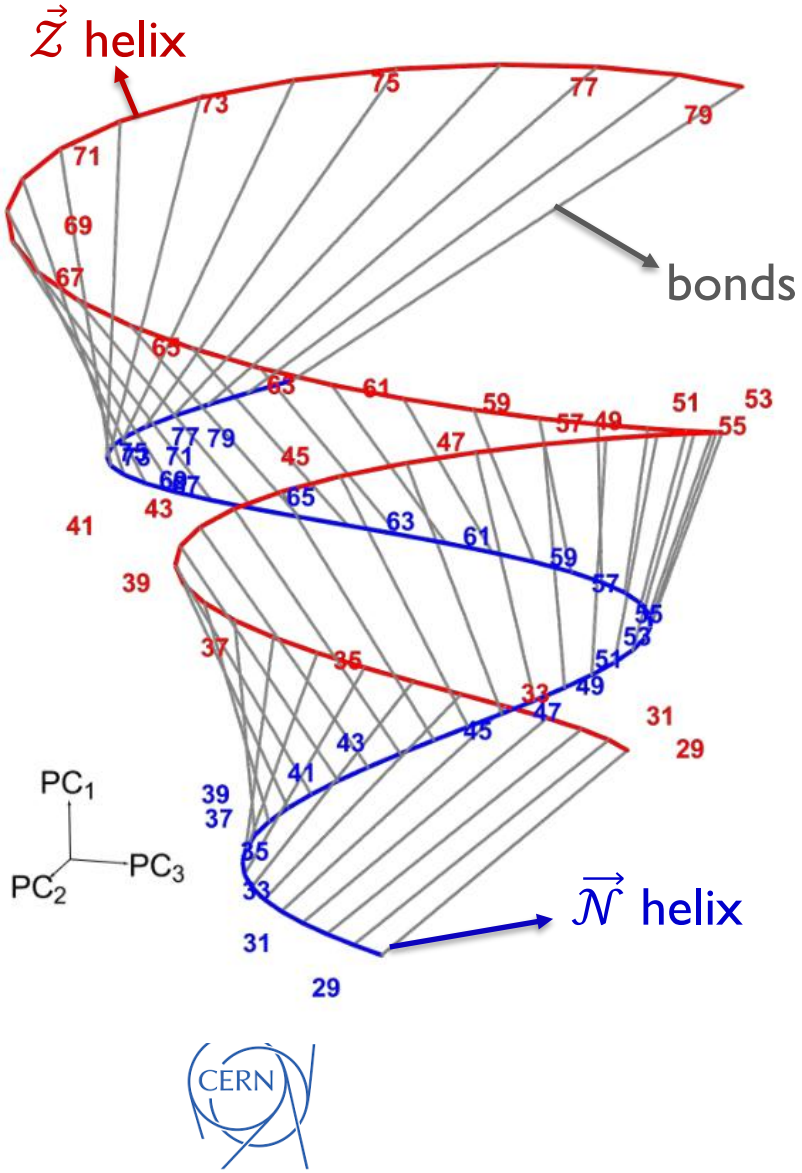

Loss function:

$$\mathcal{L} = \underbrace{\sum_i \left(E^{\text{ex}}_{b,i} - E^{\text{ai}}_{b,i}\right)^2}$$

goodness of fit / van der Waals forces

$$+\lambda \underbrace{\left[\sum_j Z_j^2 + \sum_k N_k^2 + \sum_\ell \theta_\ell^2\right]}$$

regularization / hydrophobic pressure

Deciphering the nuclear helix I

- The volume term is the dominant term. This leads to $\mathcal{Z}_1 \approx \beta Z,\ \mathcal{N}_1 \approx \beta N$.
- **NN prediction:** $F_{NN}(\vec{N}, \vec{Z}, \vec{\theta}) = \frac{\alpha_v}{\beta}(\mathcal{N}_1 + \mathcal{Z}_1) = \alpha_v\, A$. The regularization wants to drive $\beta \to 0$, but the constraint at the loss minimum $F(\vec{\theta}) = \frac{\alpha_v}{\beta}$ prevents this.

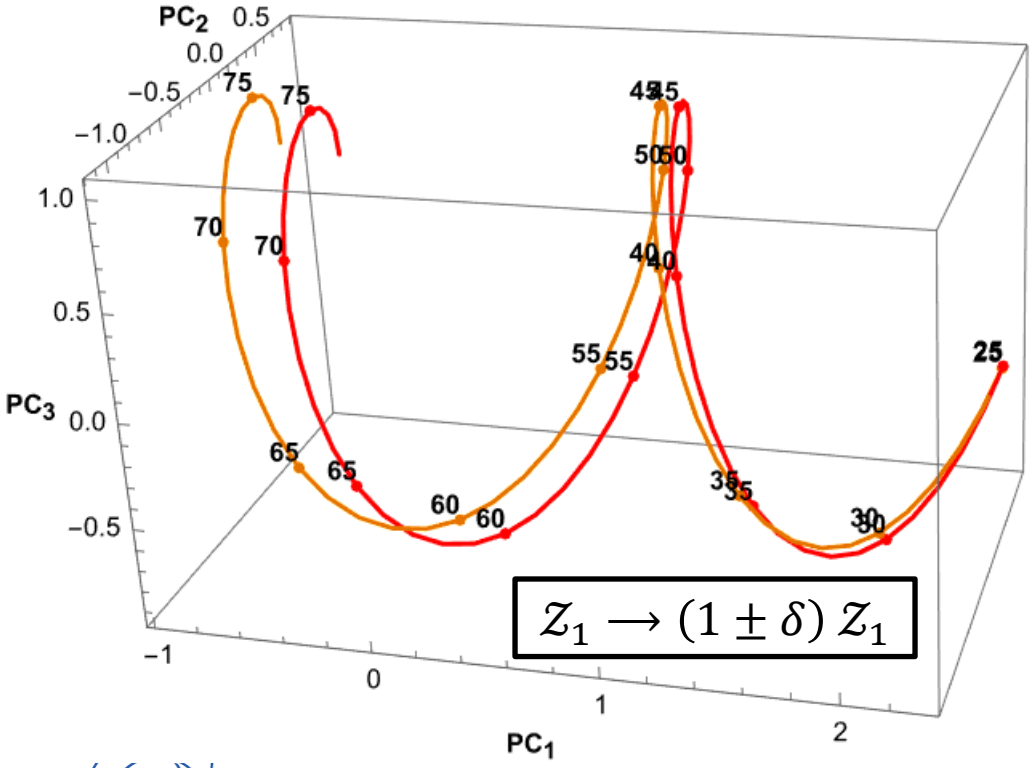

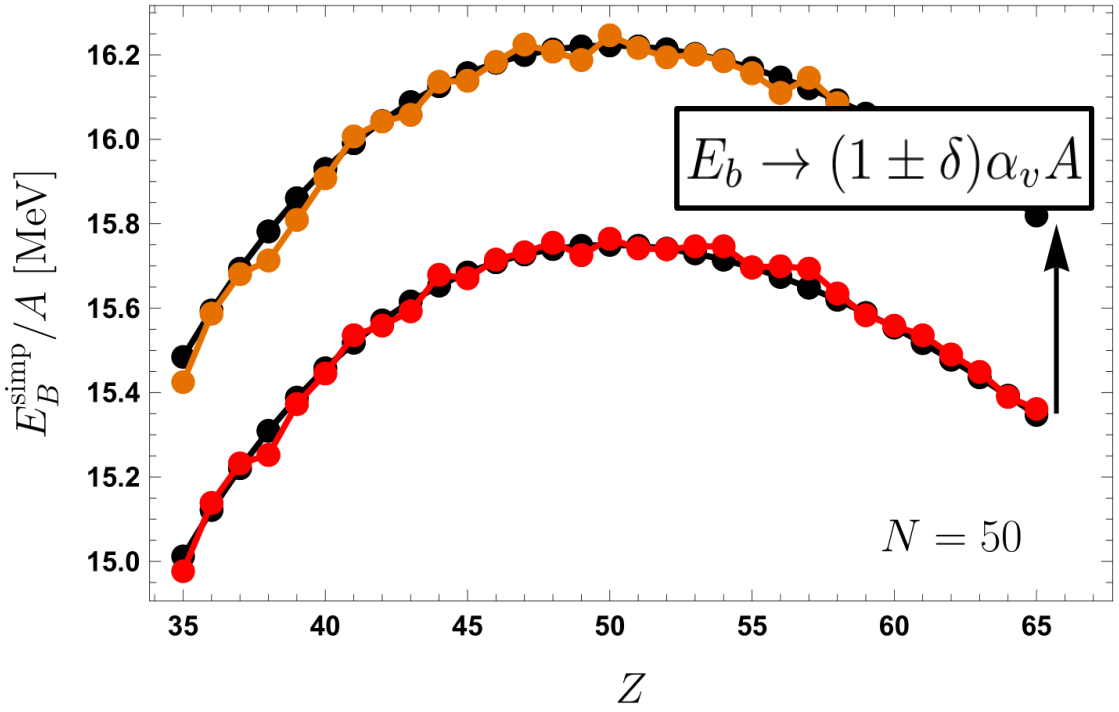

Deciphering the nuclear helix II

- The asymmetry coefficient is encoded in the radius:

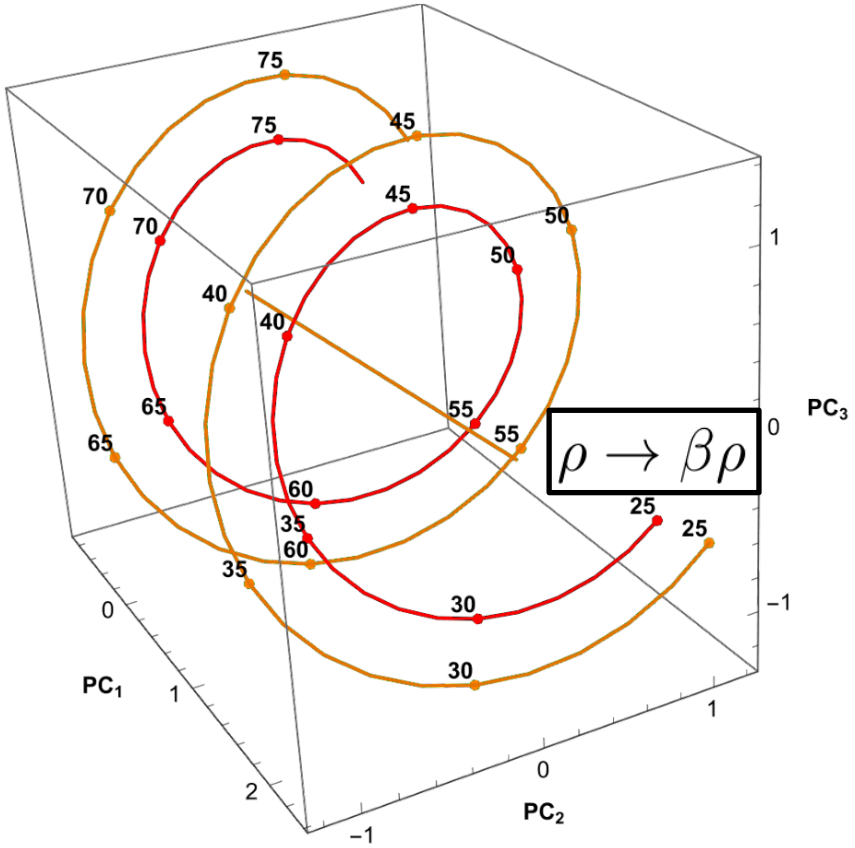

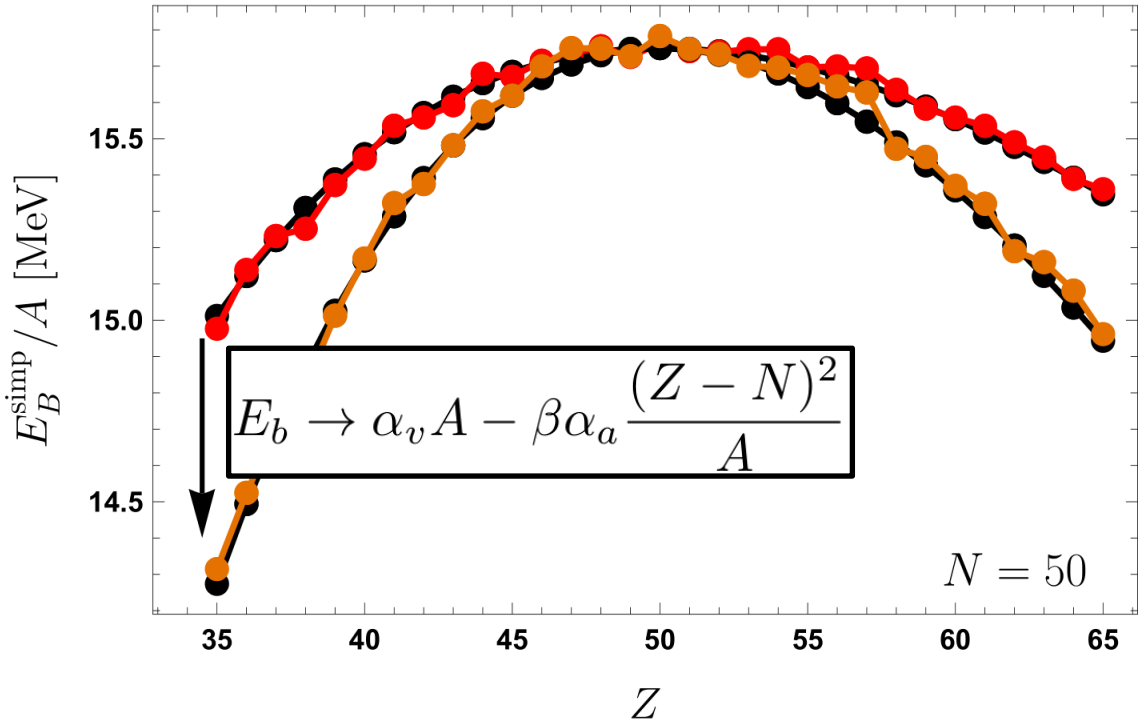

Is the machine thinking (exactly) like humans?

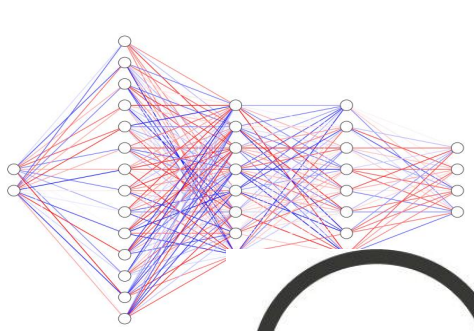

Penultimate layer

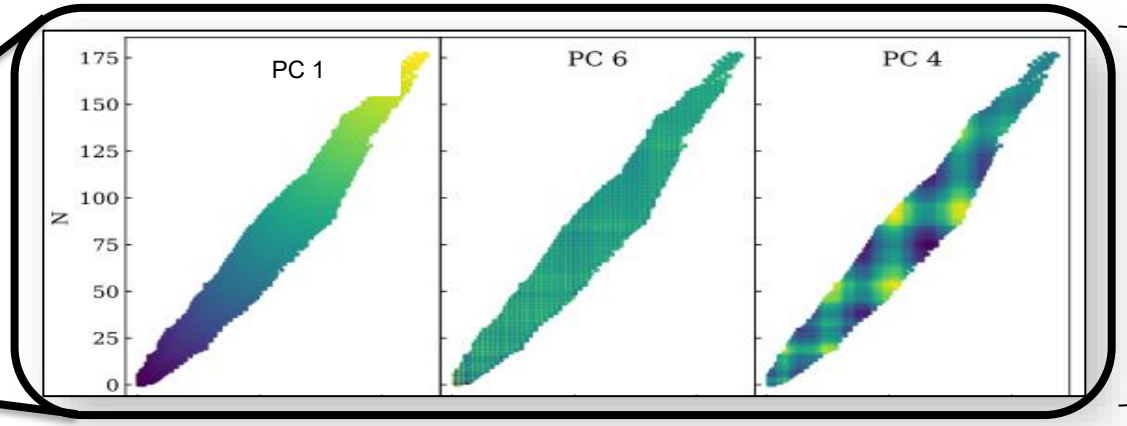

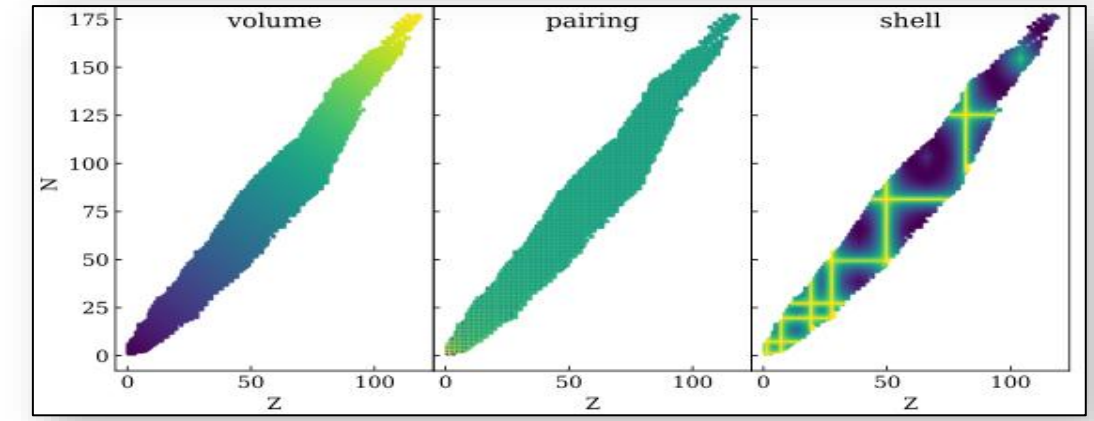

Weizsäcker, Bethe (Nobel 1967)
Gamow, Goeppert-Mayer (Nobel 1963)

Not exactly..

- **First three PCs:** smooth functions; contain most of the information of the LD.

❓ BUT, they do not have to map 1-1 to the human-derived terms.

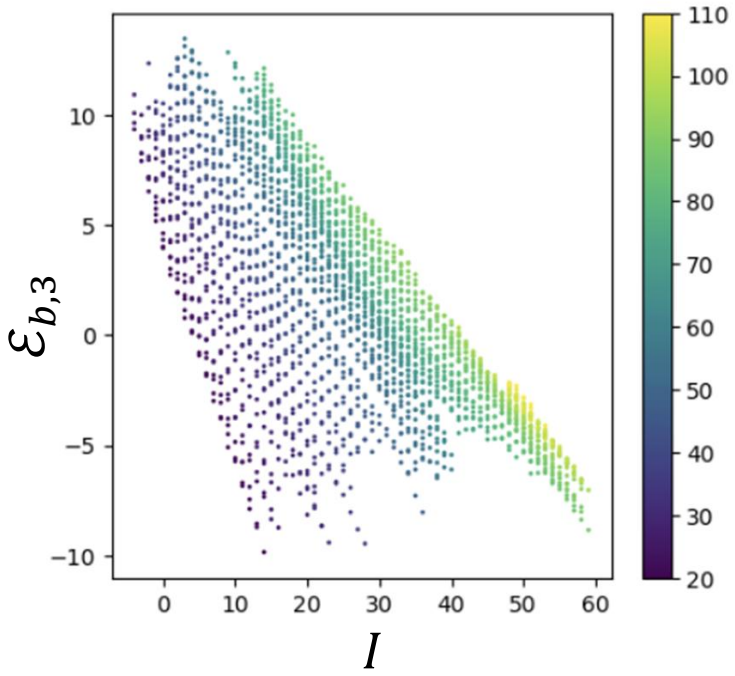

- PC3 plotted against the isospin $I = |Z - N|$ motivates the term: $\mathcal{E}_{b,3} \approx \alpha_3 |Z - N|/A$.

❗ rarely used in popular macroscopic models

- But all the rest of the PCs are discrete functions of Z & N!

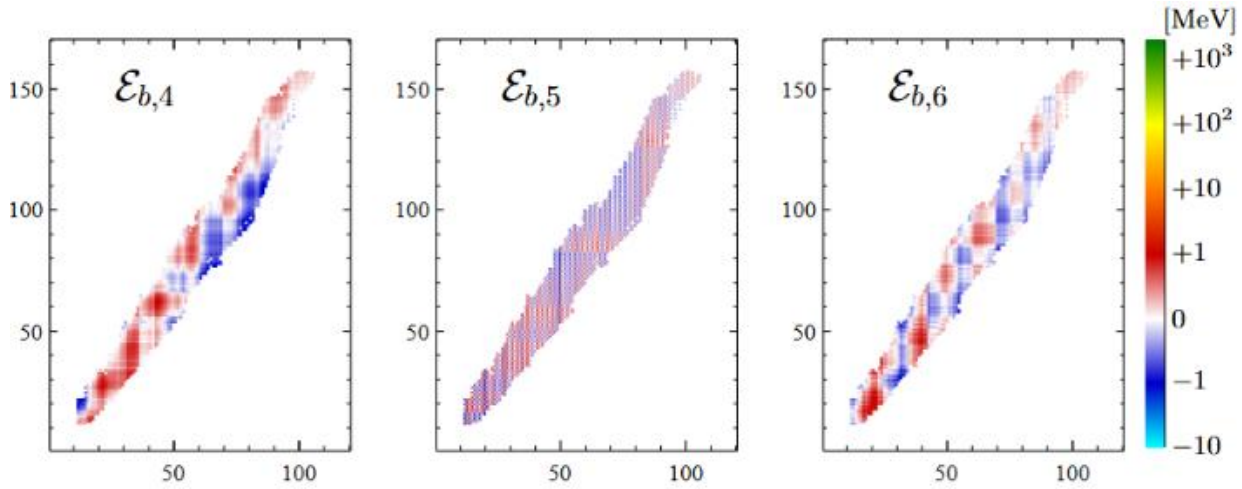

However, it is thinking exactly like Bob Jaffe!

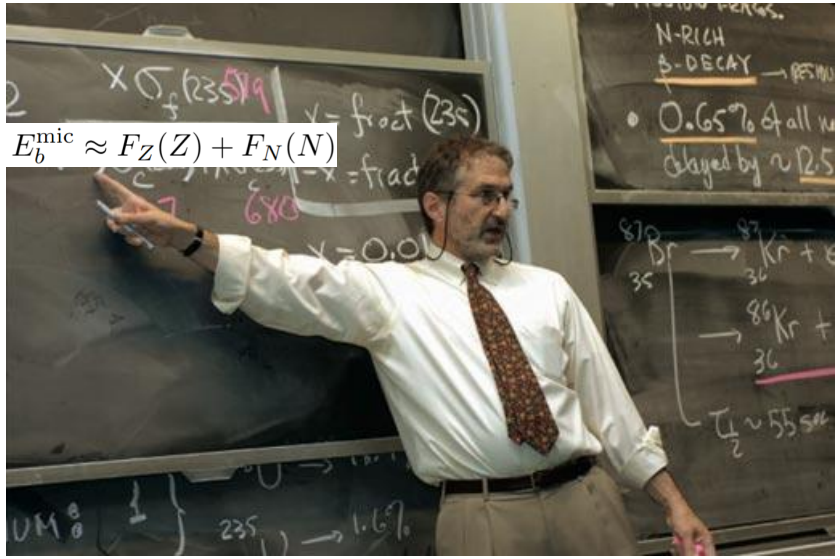

Garvey, Gerace **Jaffe**, Talmi, Kelson *Rev.Mod.Phys.* 41 (1969)
*(Jaffe's Junior Paper in Princeton)

- The lesser PCs can be thought as the microscopic corrections of our analytic model (LD+PC3+DM).
- They take the simple form, we refer to as ***Jaffe factorization***:

$$E_b^{\rm mic} \approx F_Z(Z) + F_N(N)$$

- Consequence of the nuclear-shell model: single-nucleon energy levels do not vary much around small regions of the nuclear plane:

$$E_b(Z+\delta Z, N+\delta N) \approx \sum_i^{Z+\delta Z} E_i^p(Z,N) + \sum_j^{N+\delta N} E_j^n(Z,N)$$

$$E_b(Z+\delta Z, N+\delta N) \Rightarrow F_Z(Z+\delta Z) + F_N(N+\delta N)$$

Garvey-Kelson relations

Jaffe Corrected Models

- Based on the Jaffe factorization we (re)discover the optimal interpolation method.

Isoto(p,n)ic neighbors > distance-based kernels

Correction type	RMS [keV]
WS4 (No corrections)	279
All nearest neighbors	207
Only isoto(p,n)ic nearest neighbors	175
Only isoto(p,n)ic next-to-nearest neighbors	186
Only isoto(p,n)ic (next-to-)nearest neighbors	157

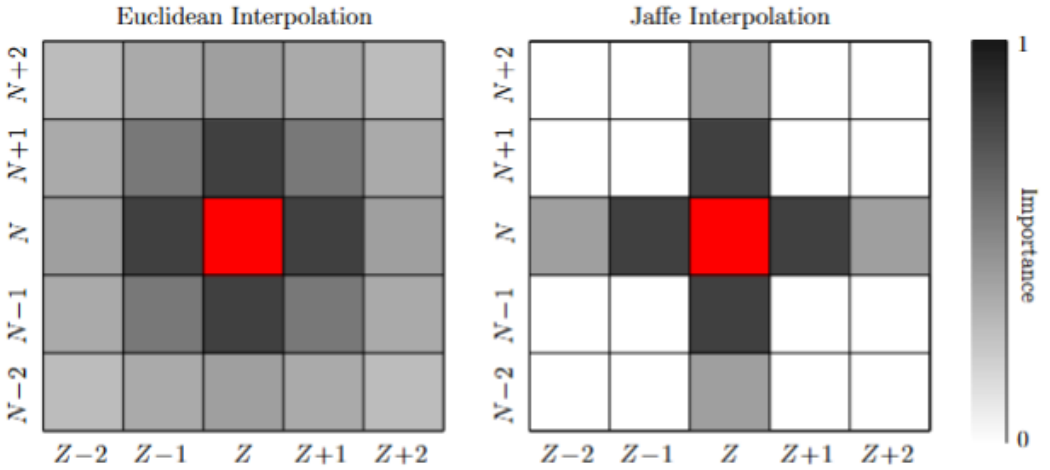

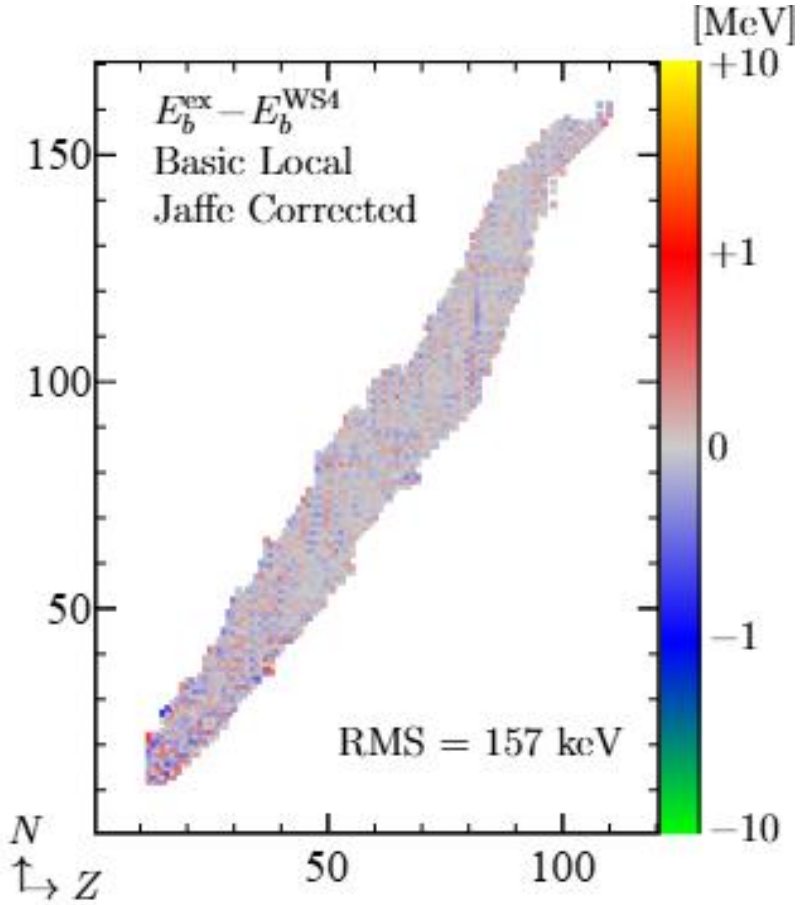

A new symbolic SOTA & the future!

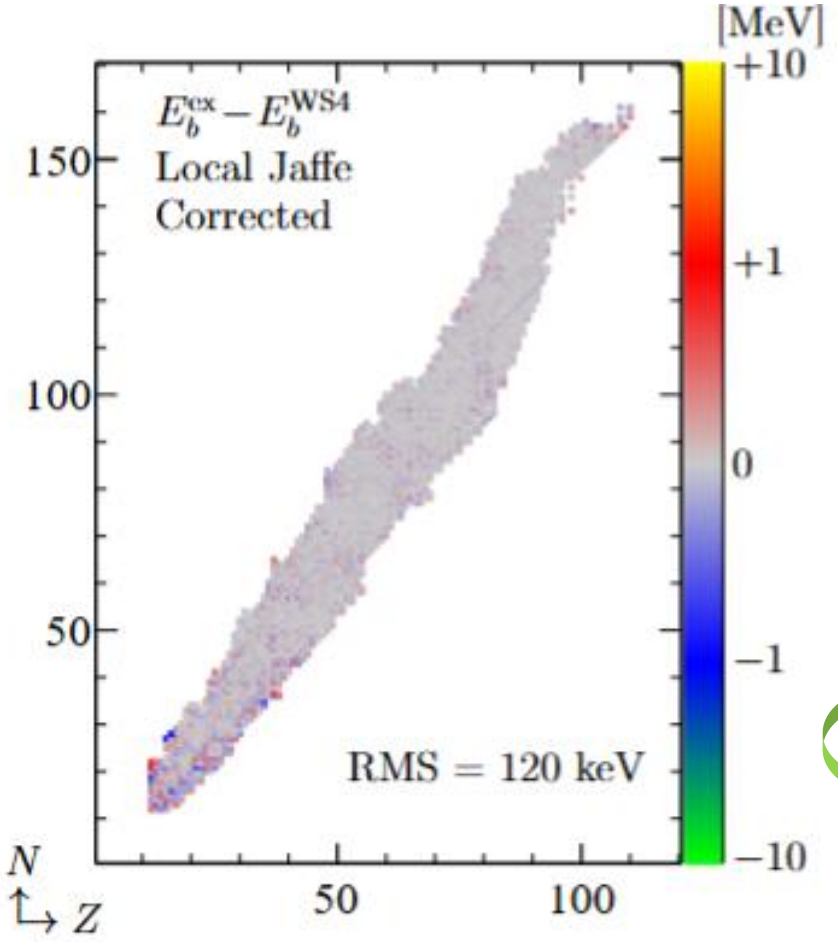

- The AI interpretability study has not sacrificed precision for understanding..

We have achieved both!

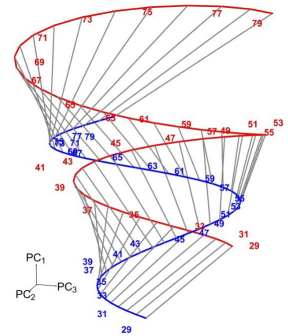

- The most important PCs are ordered hierarchically and are faithful to human knowledge!
- Can we repeat this for other nuclear observables?
  Can we automatize this process?

Symbolic Regression?

Richardson, **Trifinopoulos**, Williams 2508.08370

More Tasks, More Information!

A proof of concept via a *toy model*:

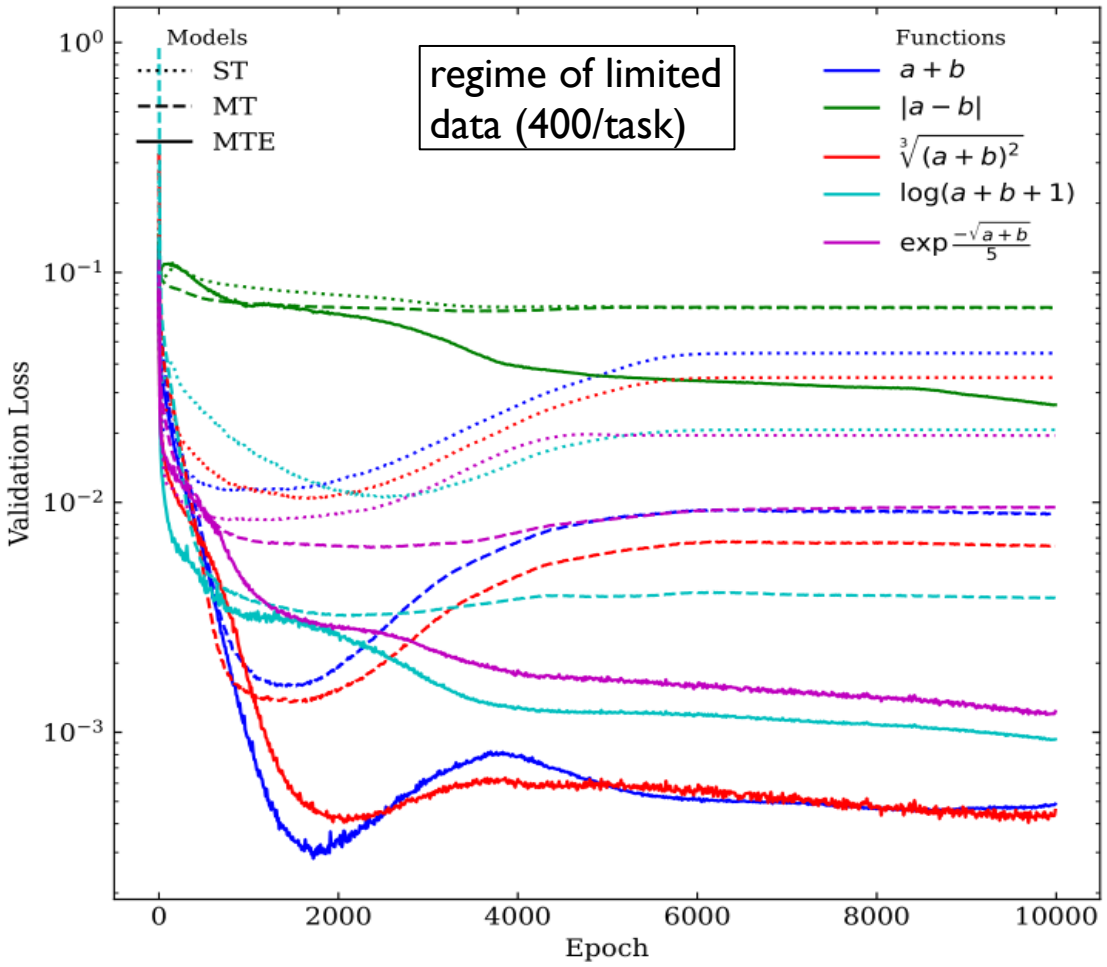

- Training simultaneously on all tasks exploits data correlations over multiple tasks and leverages joint information, improving generalization compared to single-task learning (**MT > ST**).
- Novel: the tasks become also trainable embeddings (**MTE**).
- The embedding space encodes task-independent information!

The model can make inferences for all tasks corresponding to a (Z,N) pair, for which there exist *at least* one task with a measured value.

Principle Component Analysis

- **Goal**: Reduce the dimensionality of data while preserving as much variance as possible.
- **Procedure:**
  1. Center the data ($x_i \rightarrow x_i - \bar{x}$) and calculate the covariance matrix $C = \frac{1}{n-1} \mathrm{X}^{\mathrm{T}}\, \mathrm{X}$.
  2. Solve the EV problem: $C\, \mathbf{v}_i = \lambda_i \mathbf{v}_i$.
  3. Project the data onto the PC space: $\hat{X} = X\, \mathbf{V}$.
- **Interpretation**: The first PC $\mathbf{v}_1$ (with the highest EV λ_1) captures most of the data's variance, i.e. $\mathbf{v}_1 = \underset{\|\mathbf{v}\|=1}{\operatorname{argmax}}(\mathbf{v}^{\mathrm{T}} C \mathbf{v})$, the second captures most of the variance of the transformed data $\hat{X}_1 = X - (X\, \mathbf{v}_1)\, \mathbf{v}_1{}^{\mathrm{T}}$, and so on.

Excurse: Nuclear Models for E_b

- The **liquid drop** (LD) model treats the nucleus as a highly dense incompressible fluid formed by the interplay of nuclear force, electromagnetism, and Pauli Exclusion Principle.

$$E_b^{\mathrm{LD}} = \underbrace{\alpha_v A}_{\text{volume}} - \underbrace{\alpha_s A^{2/3}}_{\text{surface}} - \underbrace{\alpha_c \frac{Z(Z-1)}{A^{1/3}}}_{\text{Coloumb}} - \underbrace{\alpha_a \frac{(N-Z)^2}{A}}_{\text{assymetry}} + \underbrace{\alpha_p \frac{\delta(Z,N)}{A^{1/2}}}_{\text{pairing}}$$

$$R_{\mathrm{ch}} \cong r_0 A^{1/3}$$

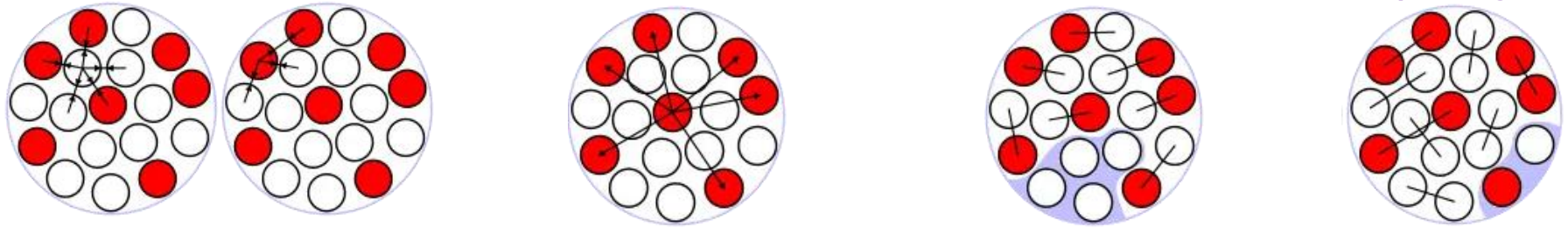

Weizsäcker, Zeitschrift für Physik, 96(7):431–458, Jul 1935.c

- **Micro-macro** models: output of a simplified quantum many-body calculation + symbolic expression; record holder is the Weizsäcker-Skyrme (**WS4**) model with $\mathrm{RMS} = 279\ \mathrm{keV}$.

Wang, Liu, Wu, Meng 1405.2616

Deciphering the nuclear helix

Here: we project the vectors $(\mathcal{N}_2 - \mathcal{Z}_2, \mathcal{N}_3 - \mathcal{Z}_3)$ on the PC_2-PC_3 plane and perform the non-linear transformation of the the clock algorithm: $\vec{\xi} = \begin{pmatrix} \mathcal{Z}_2\mathcal{N}_2 - \mathcal{Z}_3\mathcal{N}_3 \\ \mathcal{Z}_2\mathcal{N}_3 + \mathcal{Z}_3\mathcal{N}_2 \end{pmatrix}$

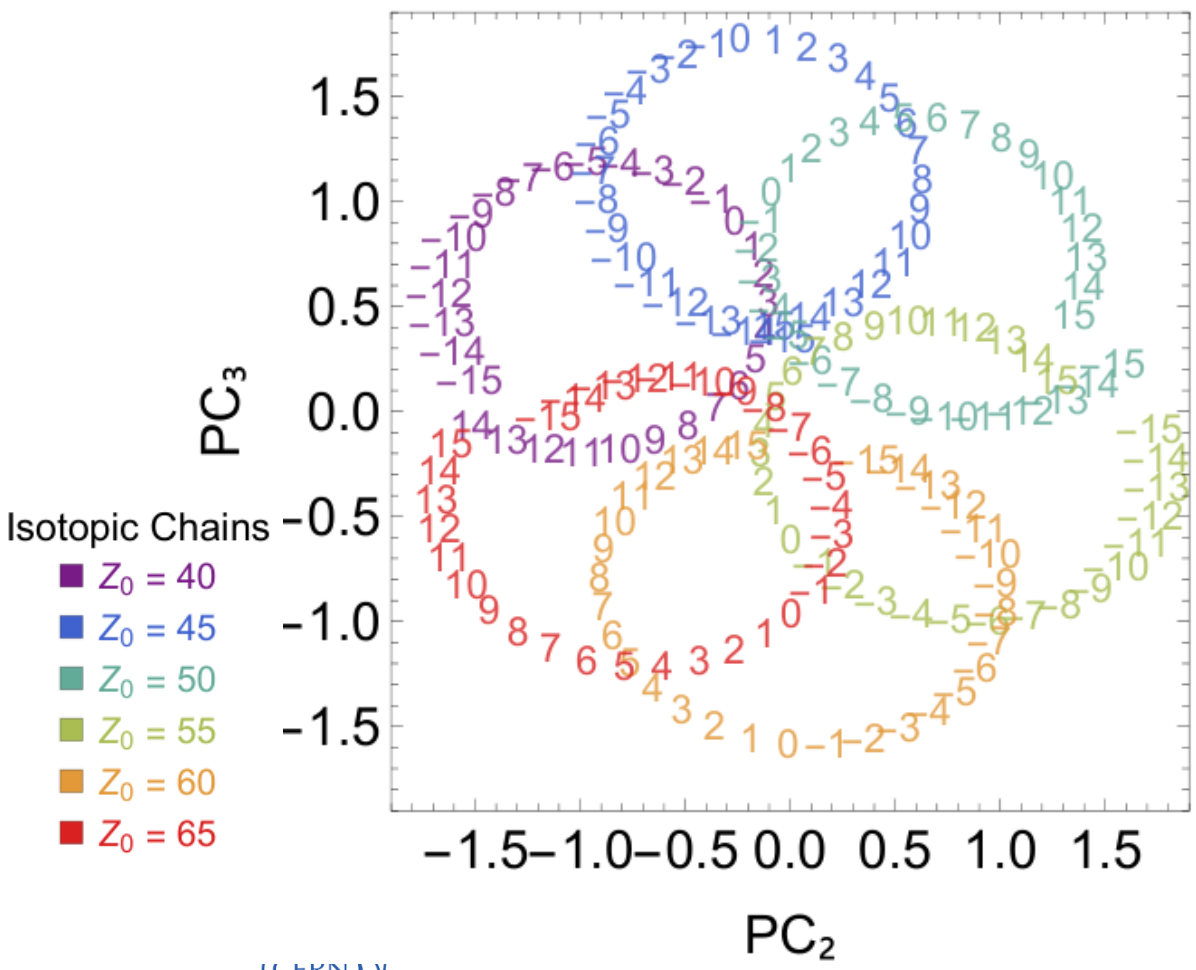

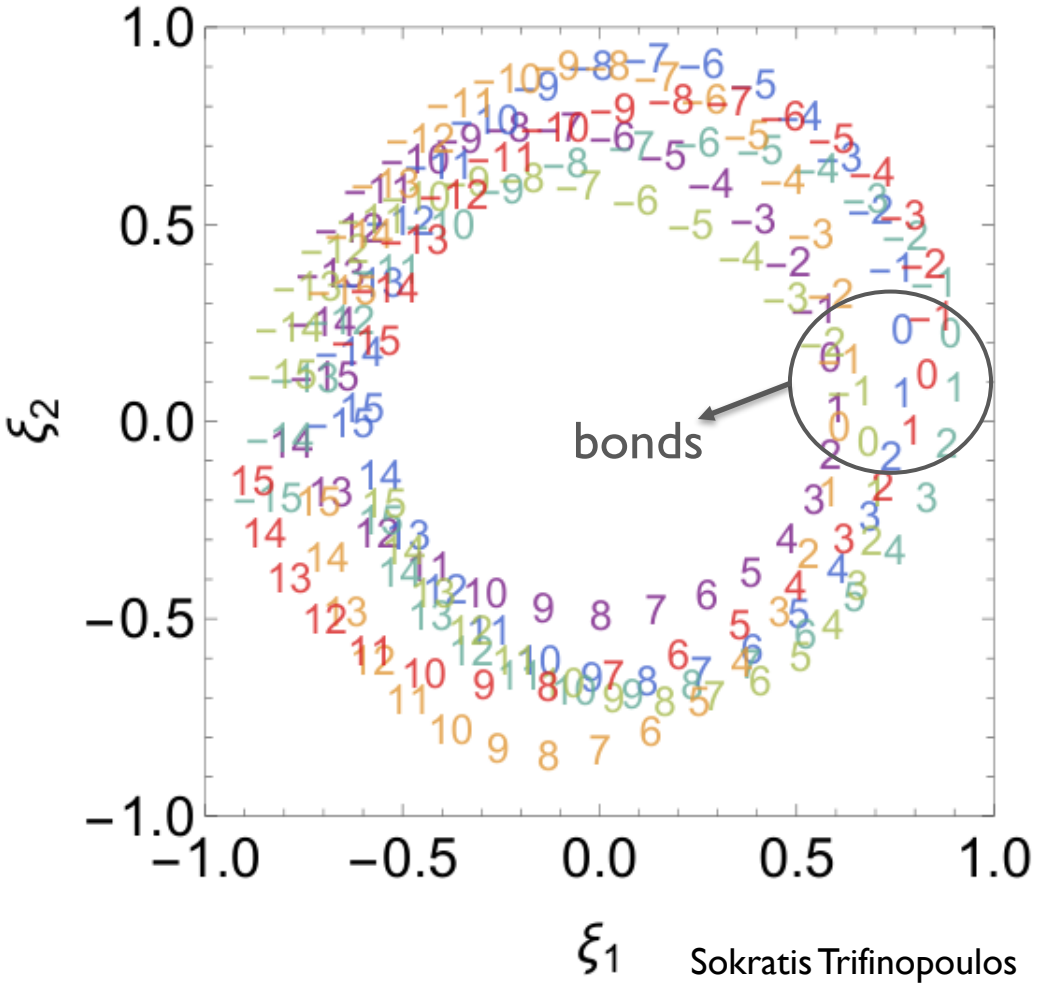

Garvey-Kelson (GK) relations

$$E_b(Z+2,N-2) - E_b(Z+2,N-1) - E_b(Z+1,N-2) + E_b(Z,N-1) + E_b(Z+1,N) - E_b(Z,N) \approx 0$$

$$E_b(Z-2,N+2) - E_b(Z-1,N+2) - E_b(Z-2,N+1) + E_b(Z-1,N) + E_b(Z,N+1) - E_b(Z,N) \approx 0$$

...

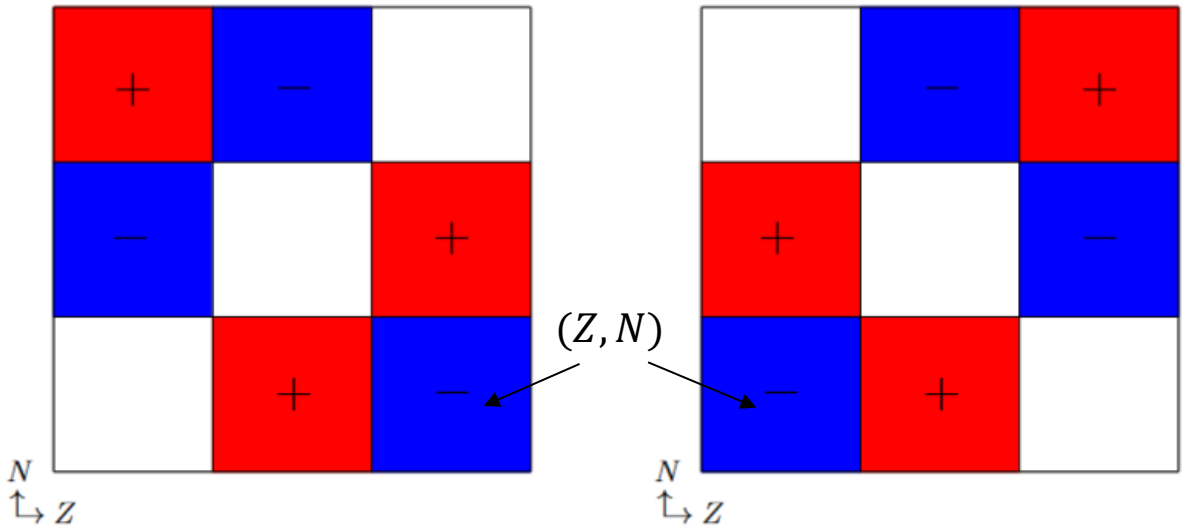

In a small region around (Z,N): $E_b(Z+\delta Z, N+\delta N) \approx \sum_i^{Z+\delta Z} E_i^p(Z,N) + \sum_j^{N+\delta N} E_j^n(Z,N)$

ST & MT architectures

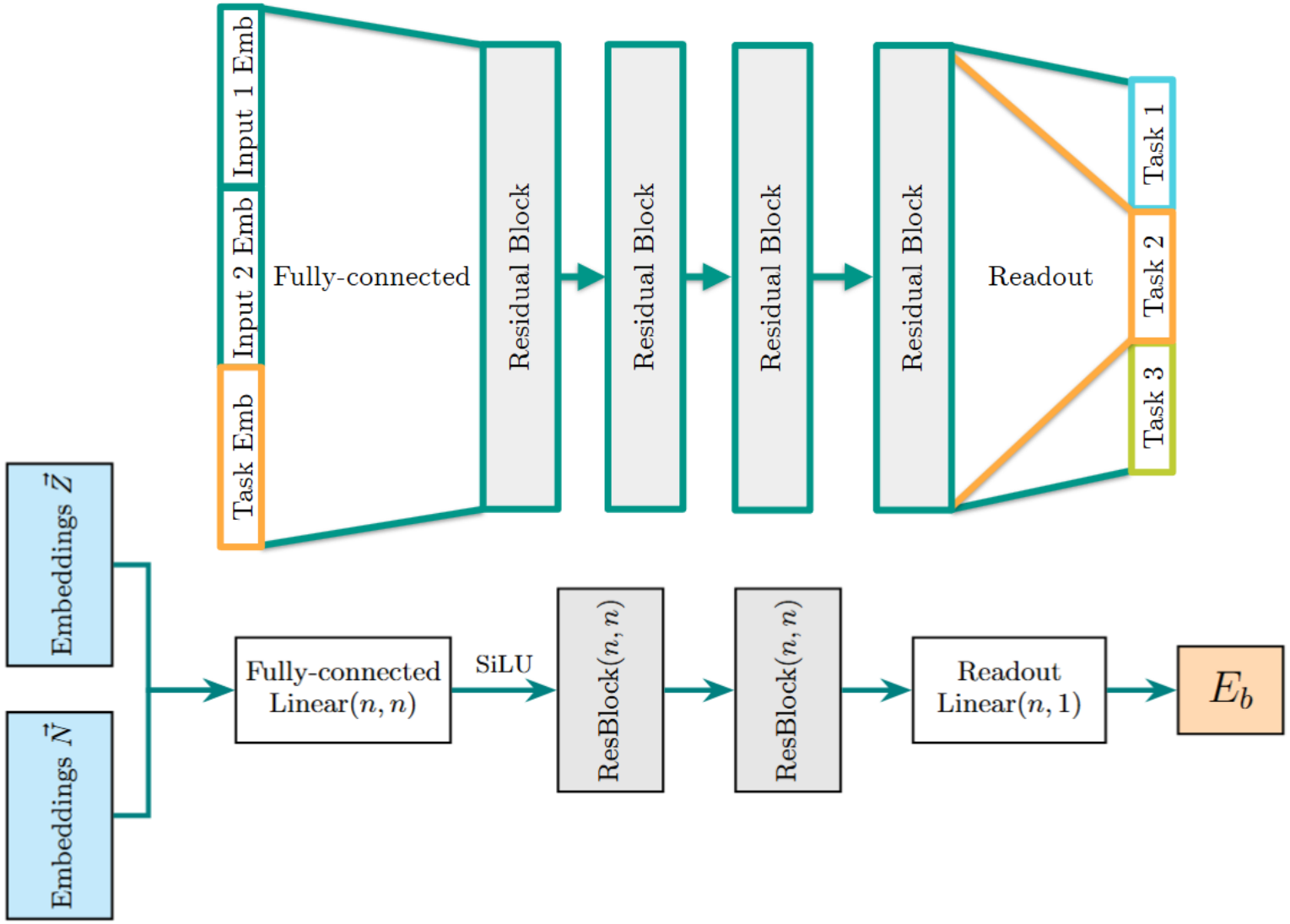

Why we want AI to be "Interpretable"?

- Scientific Reasons:
  - Training data might be biased
  - Overfitting on specific features
  - Generalization away from the specific context
  - Limited ability for independent validation
- Sociological Reasons:
  - Skepticism of statistical reasoning
  - Accountability of decision making
  - Desire to manage unforeseen risks

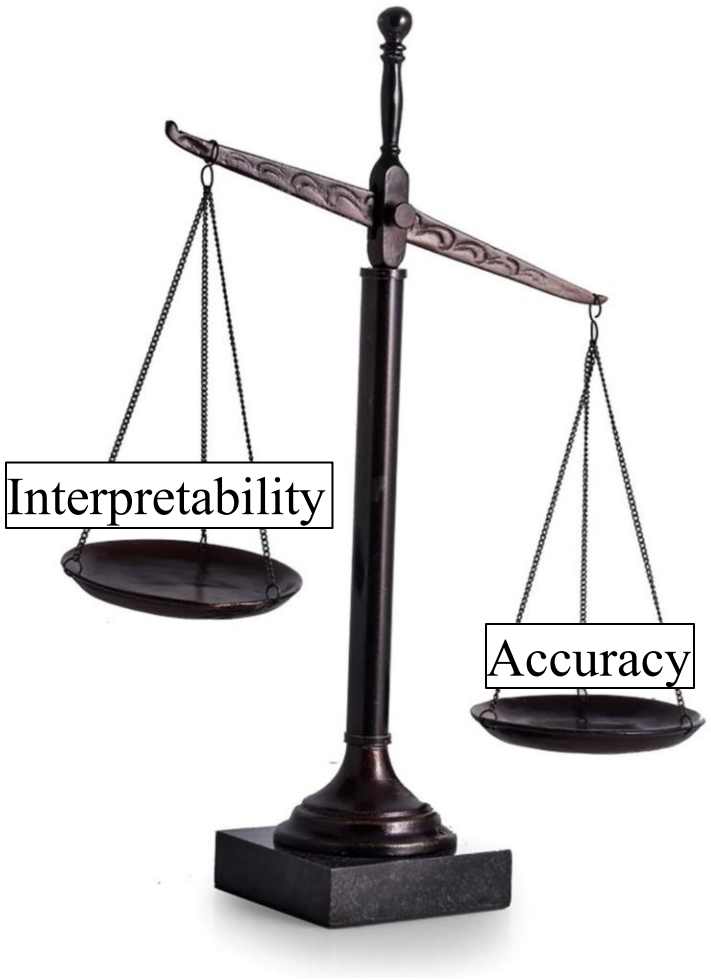

The nuclear *double helix* (real data)

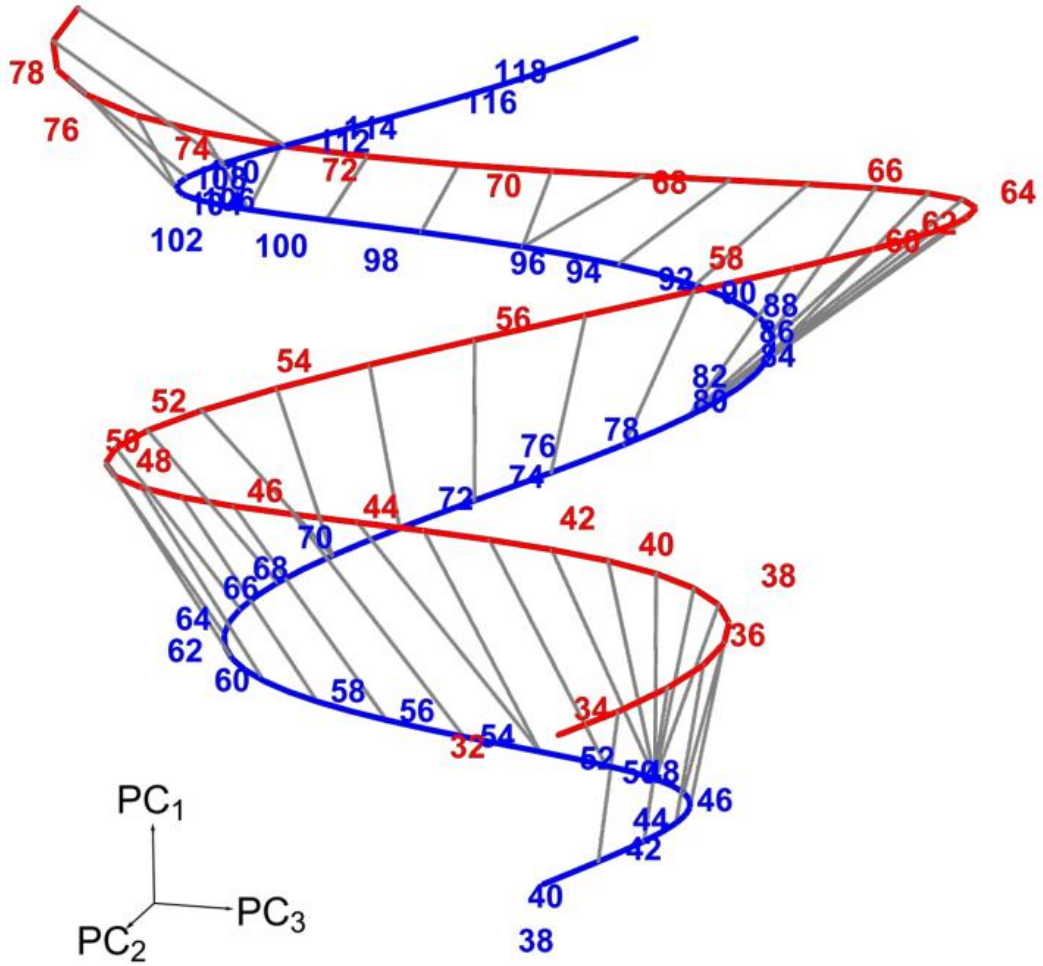

Excurse: Interpretable Algorithms

- **LST Step 3:** Classify trained networks according to the algorithms they implement.
- Let's consider first a toy problem: $(A + B) \bmod p$. Liu et al 2205.10343, Zhong et al 2306.17844
- LST was used to study *grokking*. It was found that: i) generalization coincides with structure formation ii) and identified classes of predictive algorithms that the NN employs.

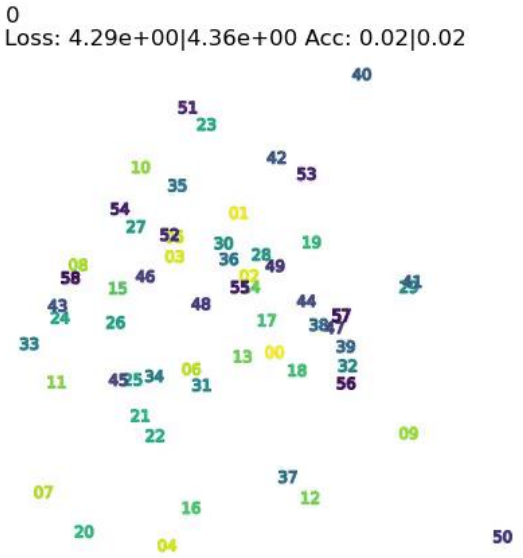

***Clock** Algorithm:*

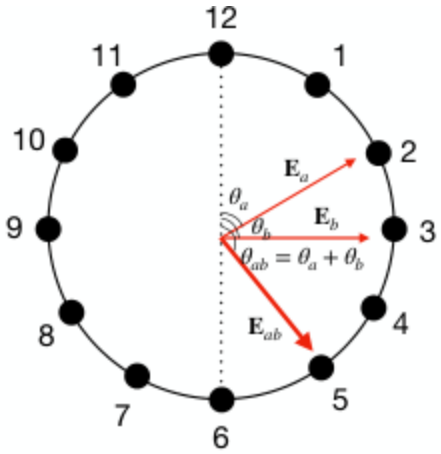

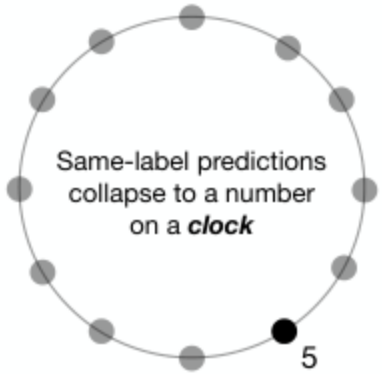

2+3=1+4=12+5=11+6
=10+7=9+8=5 (mod 12)

Meaningful features

- We perform PC analysis also on the penultimate layer. The final prediction is a linear combination of the penultimate layer PCs (**features**).
- The features capture most of the performance!

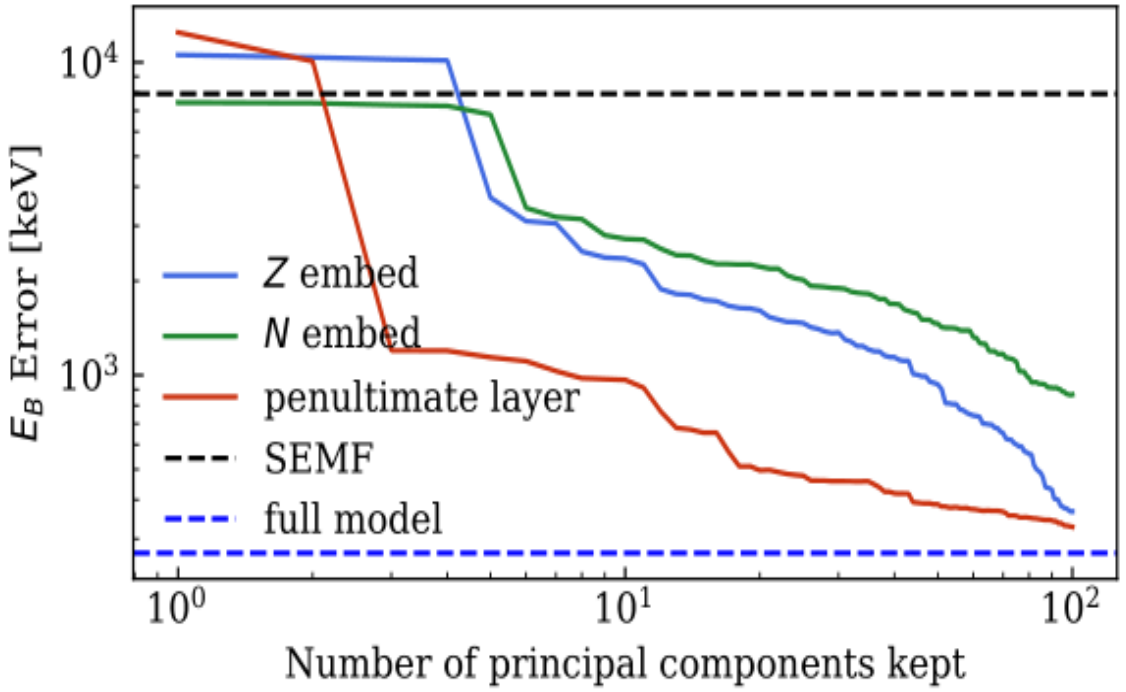

A (personal favourite) application to particle physics

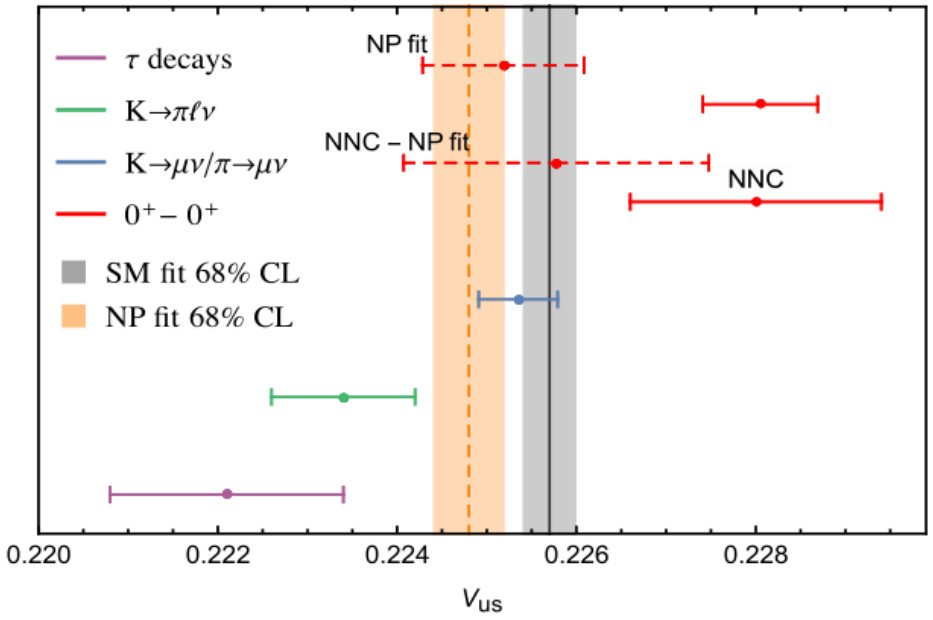

If not nuclear physics then.. New Physics!

Belfatto, **Trifinopoulos** 2302.14097
Marzocca, **Trifinopoulos** 2104.05730

The Cabibbo Angle anomaly: Discrepancies betweena different determinations of V_{us}. [Coutinho et al] 1912.08823 [Grossman et al] 1911.07821

- Depending on the input from nuclear β decays we obtain 1-5σ! Ref. [Seng] 2212.02681 showed that recoil corrections in the tree-level charged weak decay (which scale as ~$q^2 R_{\mathrm{CW}}^2$) could alleviate the tension.
- Limited knowledge of R_{CW}, but it can be inferred from the charge radii of nuclear isotriplets! But, R_{Ch} data are also scarce. → NuCLR can help!

Superallowed β decays

- Superallowed β decays are Fermi transitions (S=0, ΔJ=0) between isobaric analogue states with no parity change ($\Delta\pi$ =1).

$$|V_{ud}|^2 = \frac{2984.432(3)\,\mathrm{s}}{\mathcal{F}t(1+\Delta_R^V)}$$

Universal contribution: EW corrections

$$\mathcal{F}t = ft(1+\delta'_{\mathrm{R}})(1+\delta_{\mathrm{NS}}-\delta_{\mathrm{C}})$$

"corrected" half-life: factoring out nucleus-dependent parts

- What's **new**?

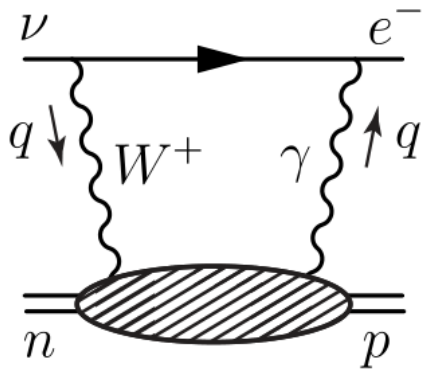

The uncertainty of Δ_R is dominated by the hadronic contribution to the $W\gamma$ box.
New analyses using dispersion relations and hybrid lattice QCD result in a shift of $|V_{ud}|$.

[Seng et al] 1812.03352, 2107.14708 [Czarnecki et al] 1907.06737

Seng's prescription:

1. Define the matrix element

$$\mathfrak{M}_0 = -\frac{G}{\sqrt{2}}\bar{u}_\nu\gamma^\mu(1-\gamma_5)v_e F_\mu(p_f,p_i)$$
$$F_\mu(p_f,p_i) = \langle\phi(p_f)|J_\mu^{W\dagger}(0)|\phi_i(p_i)\rangle = f_+(q^2)(p_i+p_f)_\mu$$

1. Expand the form factor $\bar{f}_+$

$$\bar{f}_+(q^2) = 1 + (q^2/6)R^2_{\mathrm{CW}}$$
$$R^2_{\mathrm{CW}} = -\langle\phi_f|M^{(1)}_{+1}|\phi_i\rangle$$
$$\vec{M}^{(1)} \equiv \int d^3x r^2 \psi^\dagger(x)\frac{\vec{\tau}}{2}\psi(x)$$

1. Relate R^2_{Ch} =

$$\frac{1}{Z_\phi}\langle\phi|\int d^3x r^2\left(\frac{1}{6}\psi^\dagger\psi - \psi^\dagger\frac{\tau^3}{2}\psi\right)|\phi\rangle$$

to R^2_{CW} via nuclear isotriplets:

$$R^2_{\mathrm{CW}} = R^2_{\mathrm{Ch},1} + Z_0(R^2_{\mathrm{Ch},0} - R^2_{\mathrm{Ch},1})$$

[Seng] 2212.02681

Outline

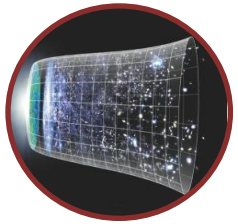

I. Large-Scale Structure bounds

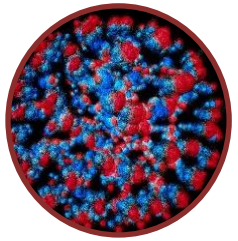

II. Production at Fusion Reactors

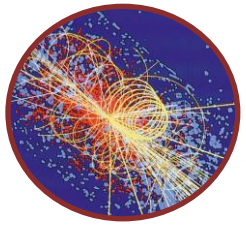

III. Searches at Colliders

Far-forward detector

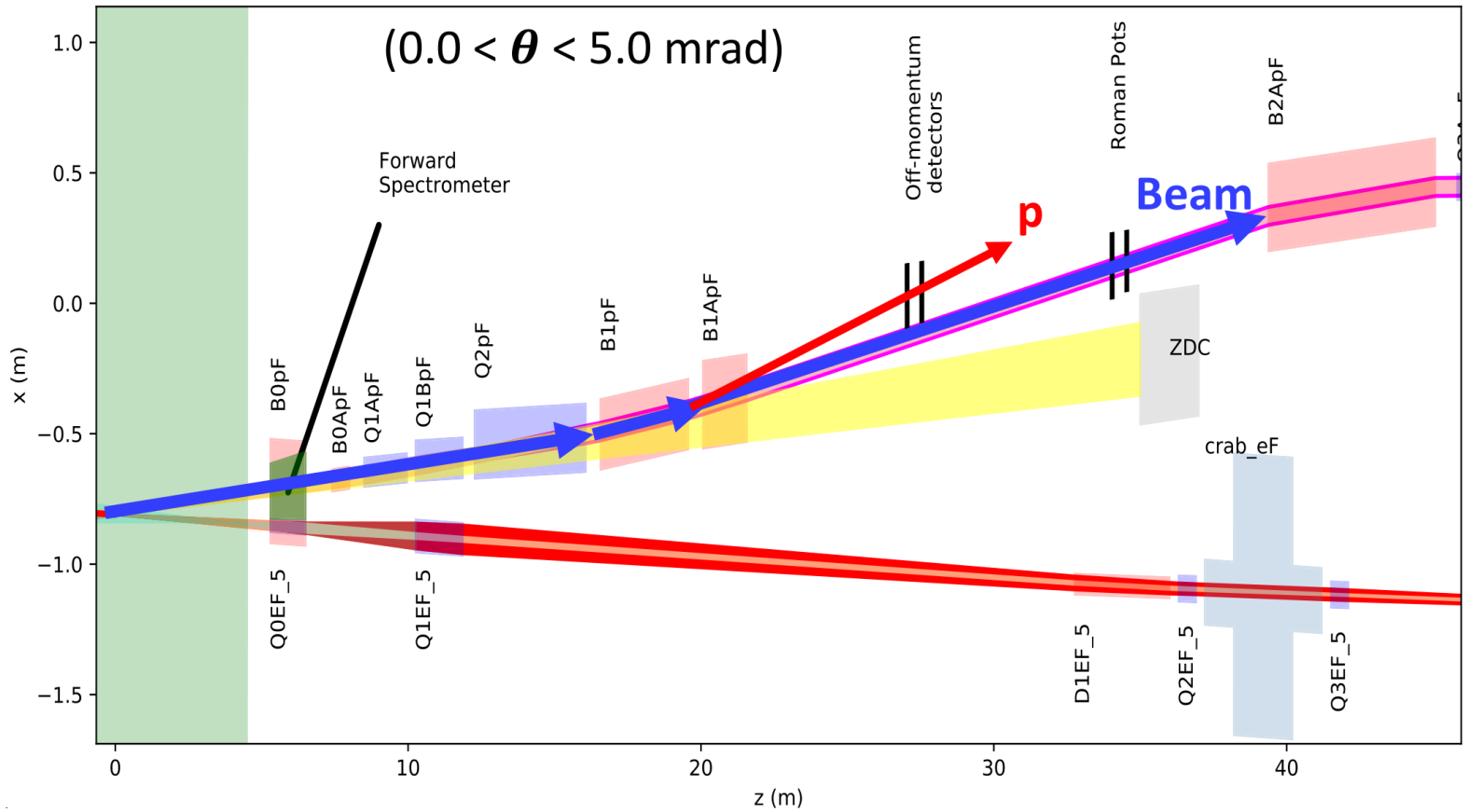

ALP-proton coupling and ALP decay BRs

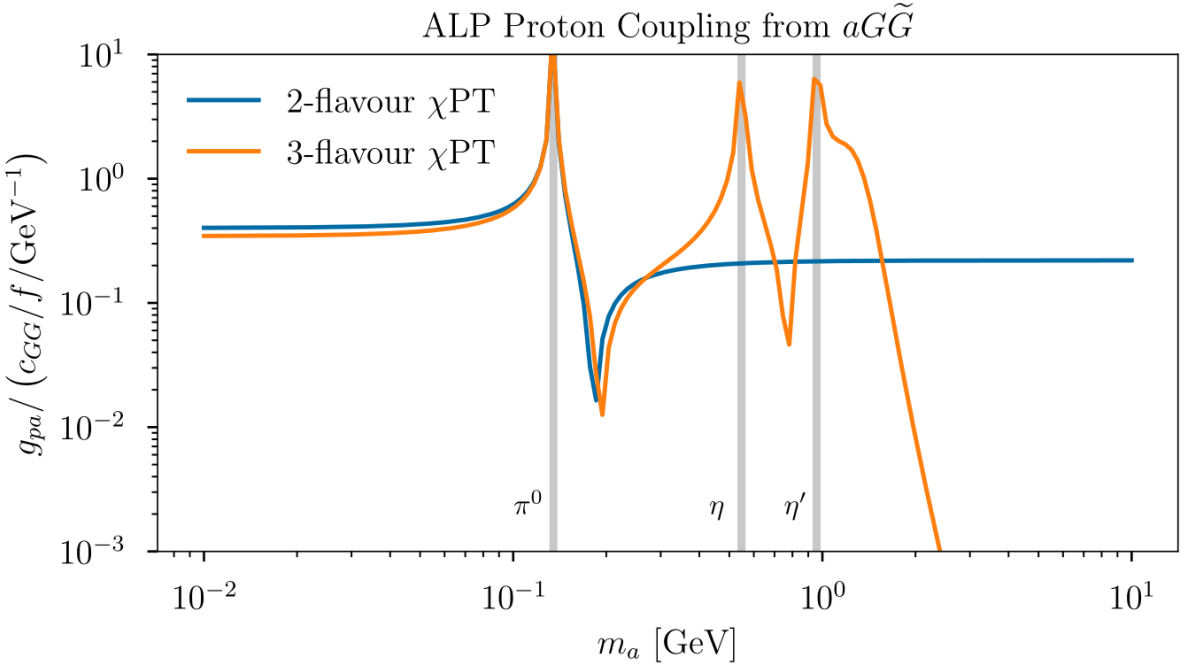

[Blinov, Kowalczyk, Wynne] 2112.09814

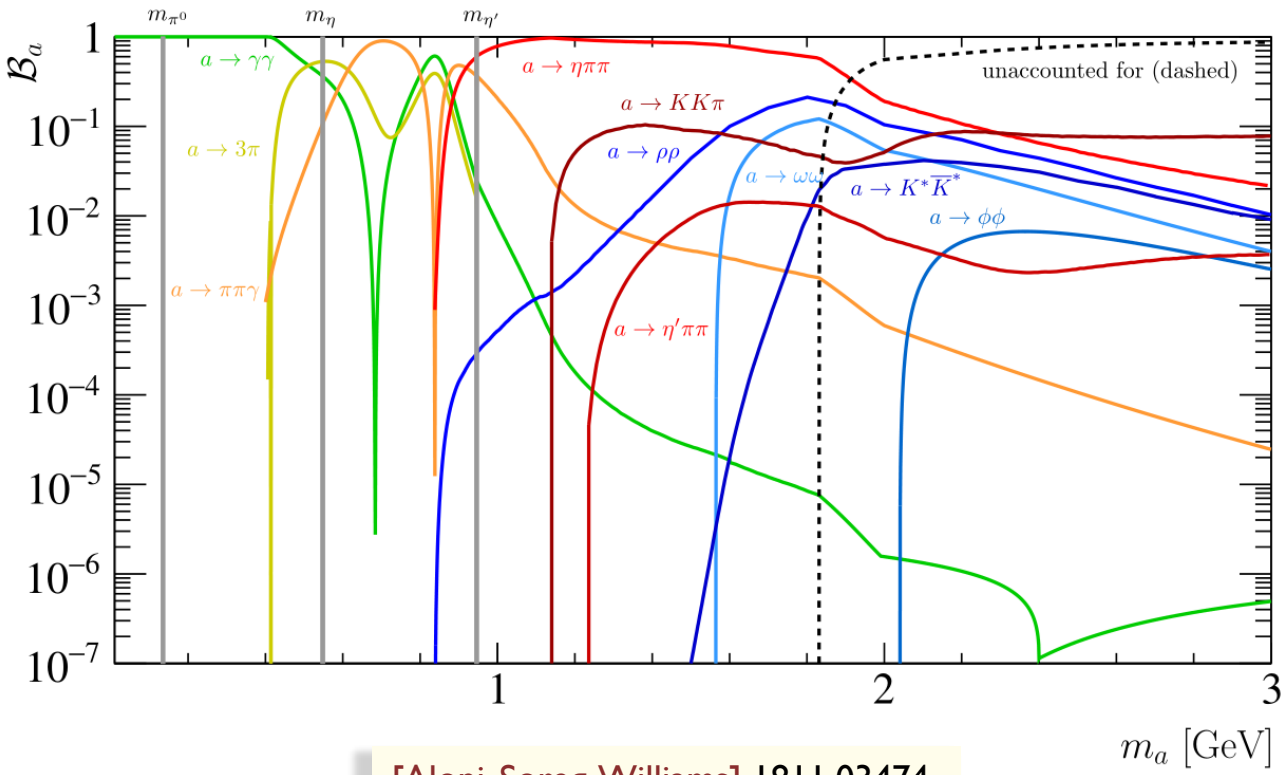

[Aloni, Soreq, Williams] 1811.03474

Production cross section at EIC

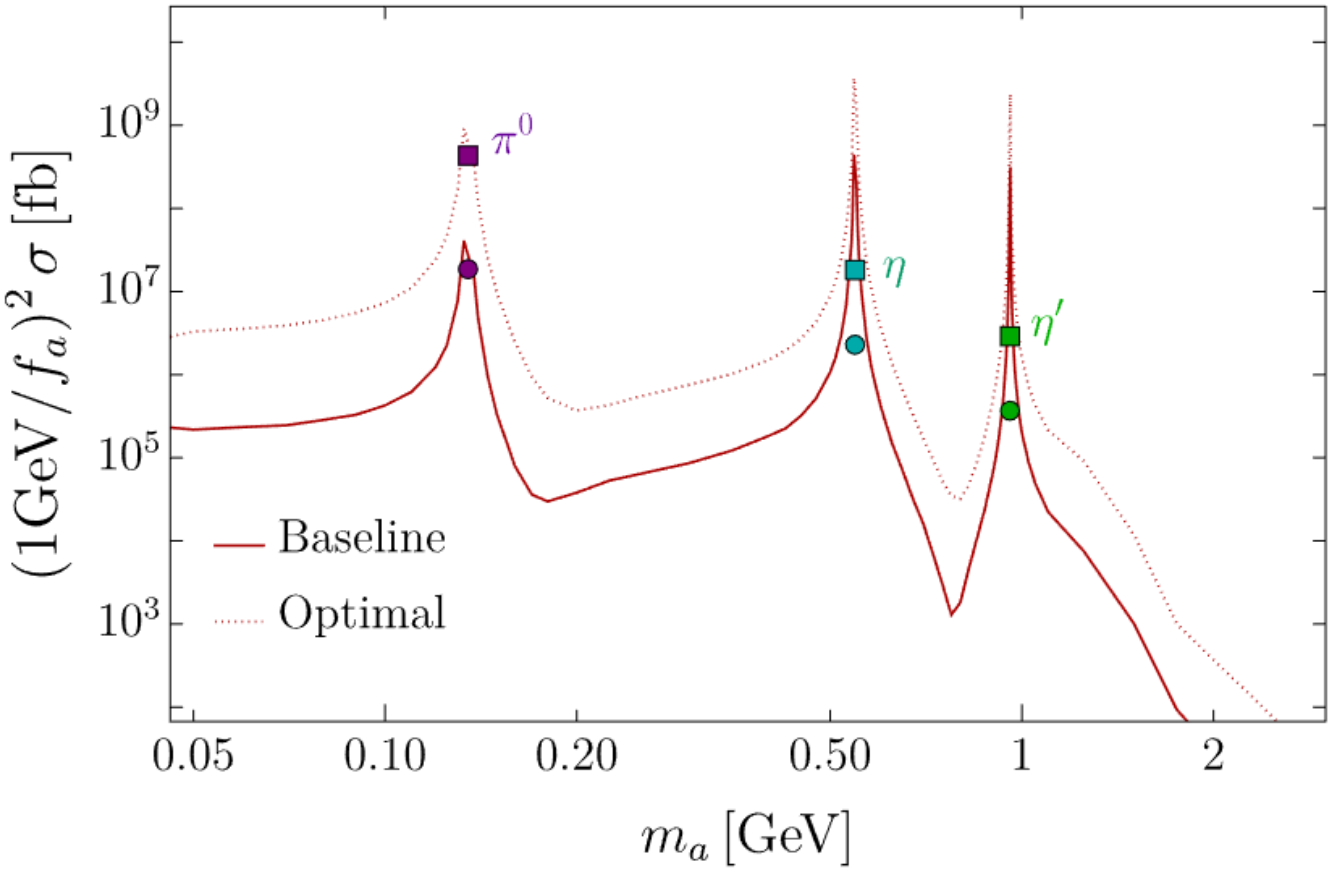

Detector Design Considerations

[Acosta et al] 2203.06258]

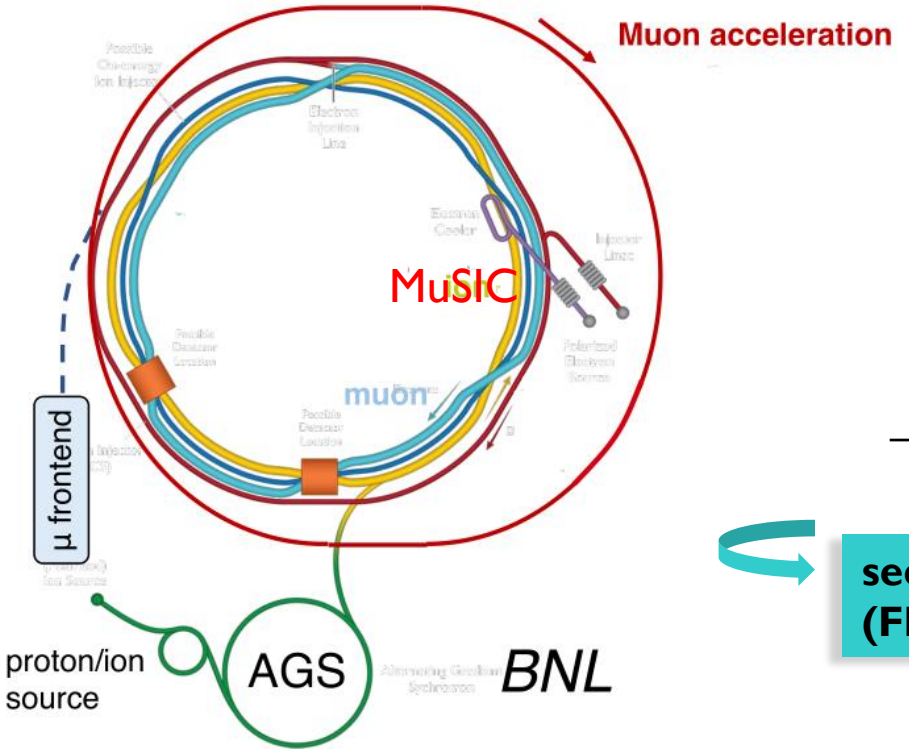

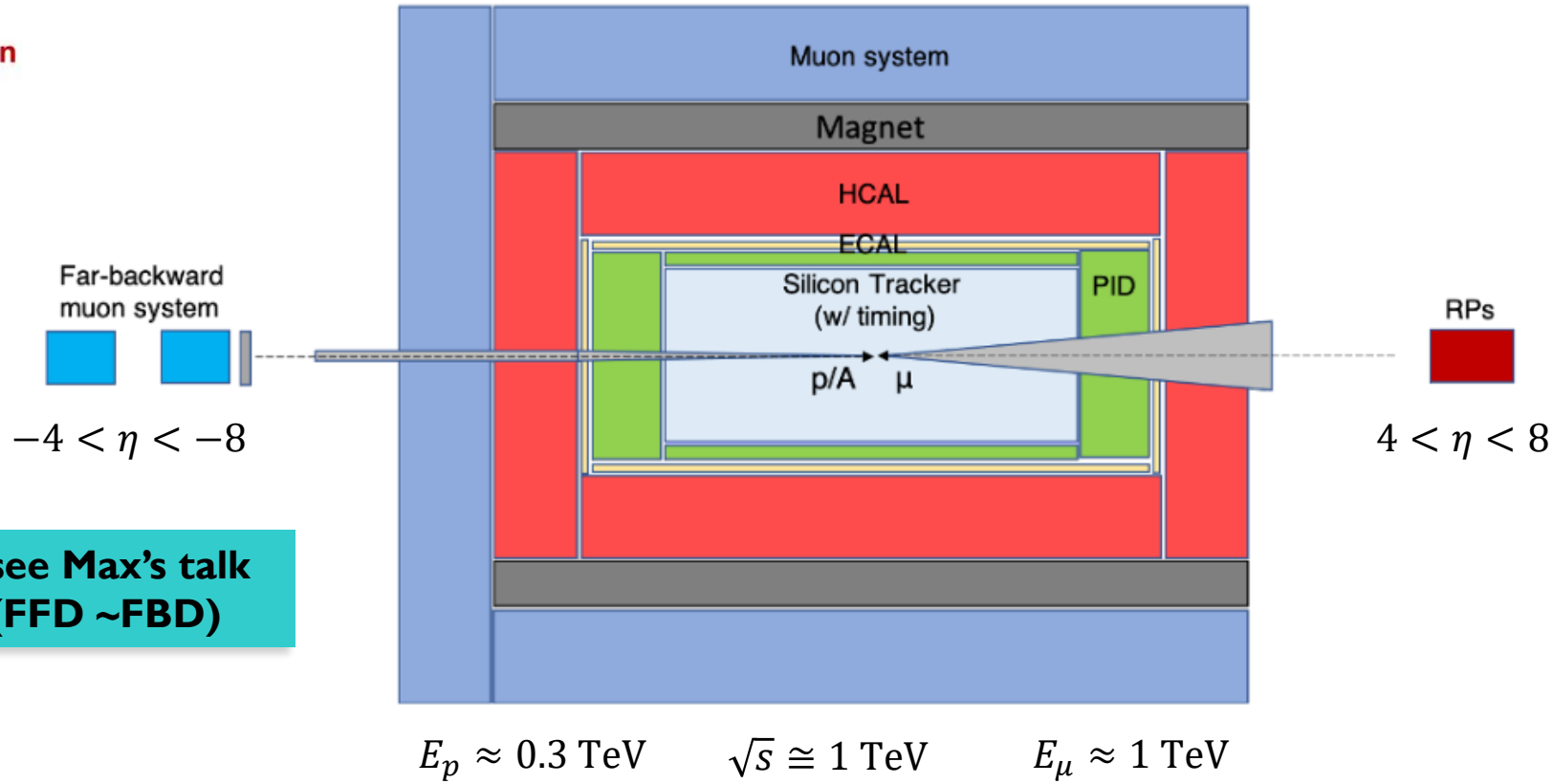

see Max's talk (FFD ~FBD)

BSM Models

We consider four *simplified* BSM models. See also: [Cheung, Wang] 2101.10476 [Hatta] 2311.14470

1. **Leptoquark $U_1 \sim (\mathbf{3}, \mathbf{1}, 2/3)$:** Enables study of $\mu - \tau$ lepton-flavor violation (LFV) at tree-level. U_1 is additionally motivated by *B*-anomalies and as portal to dark matter.

$$\mathcal{L}_{U_1}^{\text{int}} = \lambda_{b\mu} U_1^{\alpha} \left(V_{ib} \bar{u}_L^i \gamma_\alpha \nu_\mu + \bar{b}_L \gamma_\alpha \mu_L \right) + \lambda_{b\tau} U_1^{\alpha} \left(V_{ib} \bar{u}_L^i \gamma_\alpha \nu_\tau + \bar{b}_L \gamma_\alpha \tau_L \right) + \text{h.c.}$$

[Bordone et al] 1712.01368, 1805.09328, [Di Luzio et al] 1708.08450, [Greljo et al] 1802.04274, [Baker, Faroughy, **Trifinopoulos**] 2109.08689

2. **Muonphilic Z':** Light vector gauge boson below the electroweak scale. [He et al] PhysRevD.43.R22

$$\mathcal{L}_{Z'}^{\text{int}} = -g_{Z'}^{\mu} \bar{\mu} \gamma_\alpha \mu Z'^{\alpha}$$

3. **Axion-like Particles:** Theoretically-motivated heavier versions of the QCD axion.

$$\mathcal{L}_a^{\text{int}} = -\frac{a}{4\Lambda} F^{\mu\nu} \tilde{F}_{\mu\nu}$$

[Agrawal, Howe] 1710.04213 [Fitzpatrick et al] 2306.03128 [Takahashi, Yin] 2105.10493

4. **Heavy Sterile Neutrinos:** Accessed via an effective dipole operator: [Ismail, Jana, Abraham] 2109.05032

$$\mathcal{L}_{\text{dipole}}^{(5)} \supset \frac{1}{2} \mu_\nu \bar{\nu} F_{\mu\nu} \sigma^{\mu\nu} N \,, \qquad (\mu_\nu \sim v_{\text{EW}}/\Lambda^2)$$

LFV leptoquark interactions: prompt search

Signal:

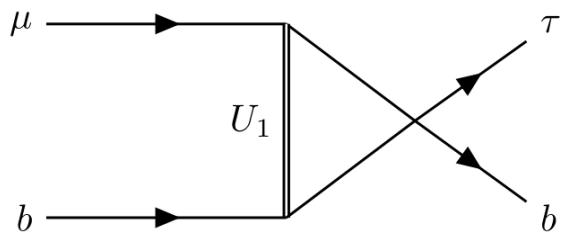

Background:

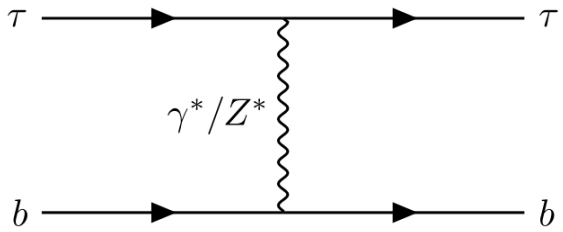

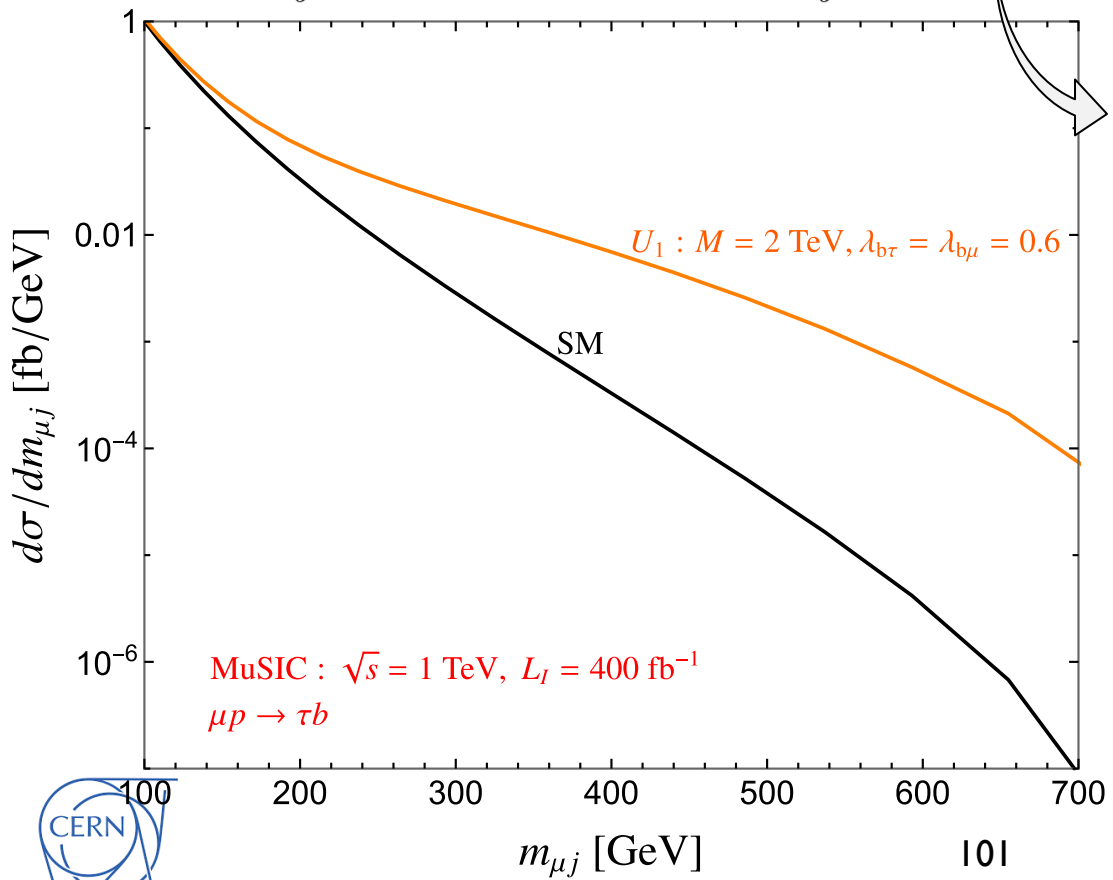

τ content of the muon beam → LePDF

[Han, Ma, Xie] 2007.14300, 2103.09844
[Garosi, Marzocca, **Trifinopoulos**] 2303.16964,
github.com/strifinopoulos/LePDF

- We convolute the PDFs with the differential cross sections and integrate within the central detector rapidity coverage $|\eta| < 3.5$.
- **Acceptance efficiencies**: *b*-tagging 80% , τ-hadronic decays 75% [ATLAS] 2108.07665, 2305.15962

LFV leptoquark reach: MuSIC vs HL-LHC

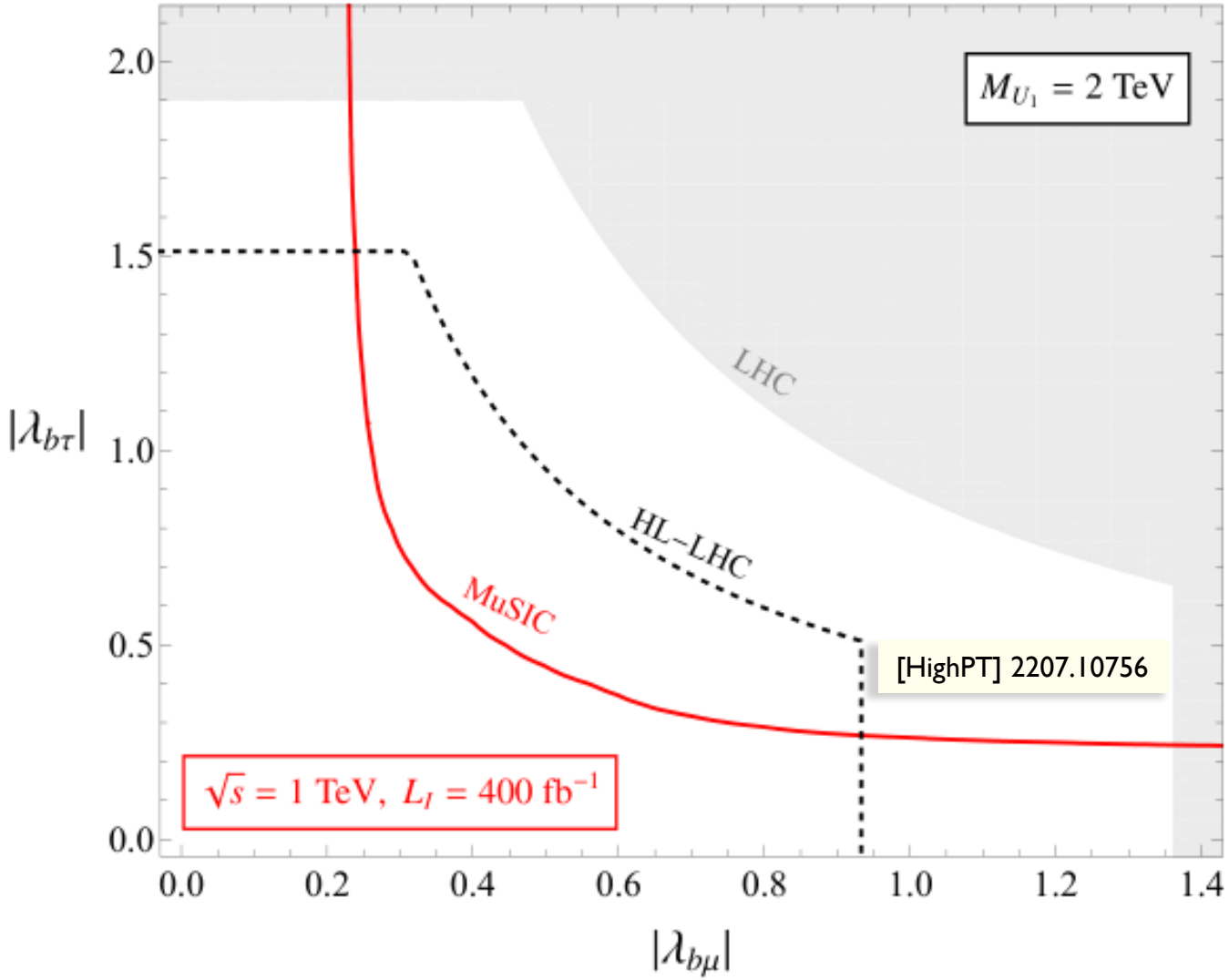

Z' vector boson: displaced vertices

Signal:

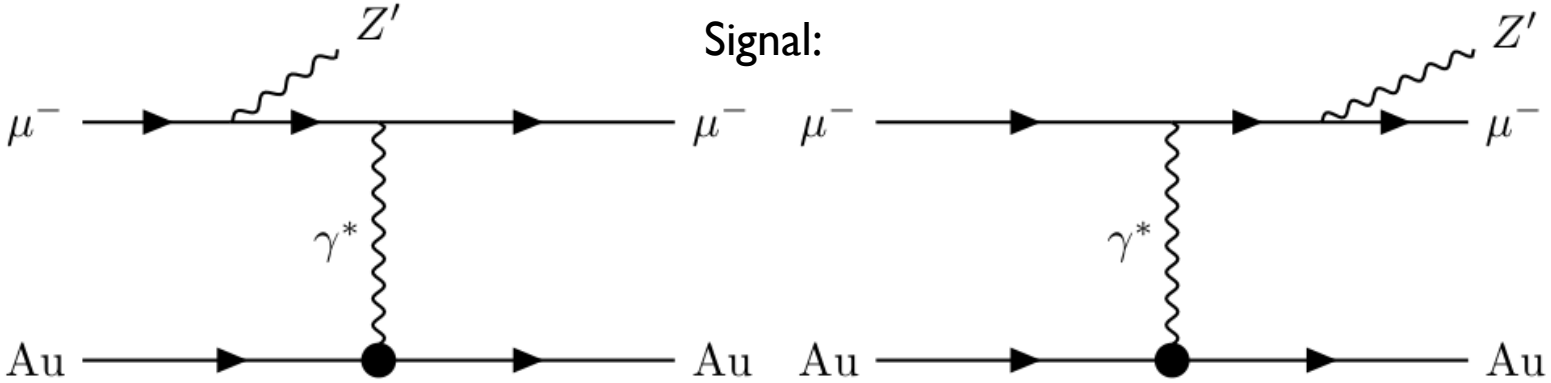

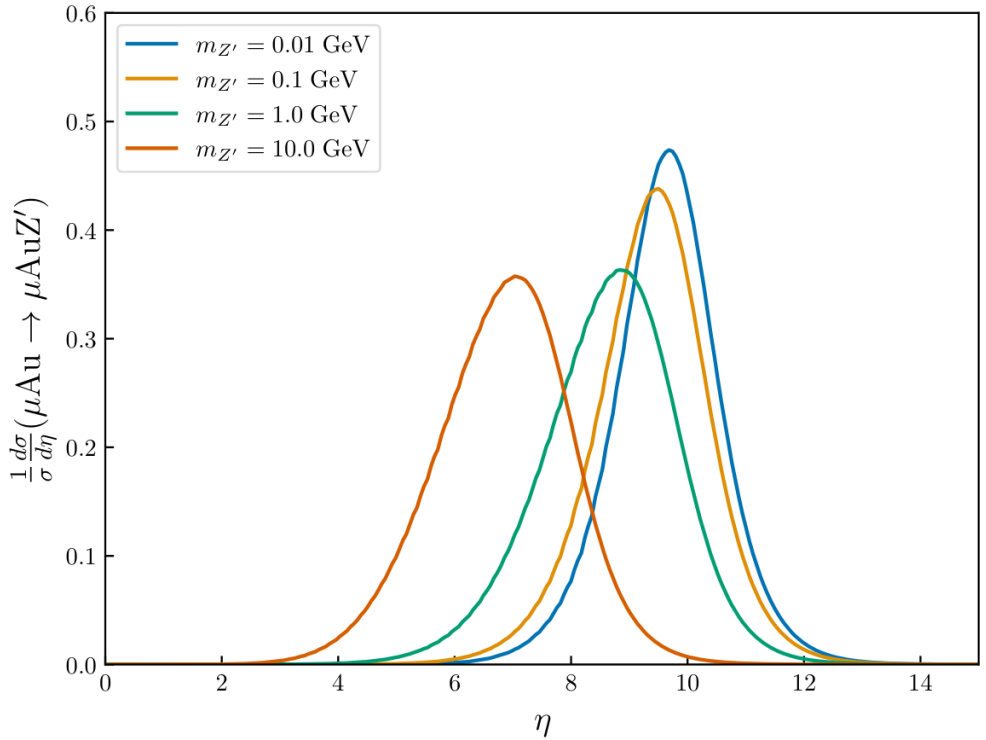

- The cross-section in coherent scattering is Z^2-enhanced.
- The large ion-frame muon energy of $O(100\,\mathrm{TeV})$ leads to highly-boosted Z' in the far-backward direction.
- After traveling some distance ℓ it decays to di-muons with probability:

$$P(\ell) = \frac{e^{-\ell/L_{Z'}}}{L_{Z'}}\,, \qquad L_{Z'} = \beta\gamma/\Gamma_{Z'}$$

boost factor $=|\vec{p}|/M$

- To find the expected number of events, we integrate $P(\ell)$ from $\ell_{\min} = 1\mathrm{mm}$ (veto prompt backgrounds) to $\ell_{\max} = 30\mathrm{m}$ (far-backward muon spectrometer).

Z' vector boson: MuSIC vs Muon Beam Dumps

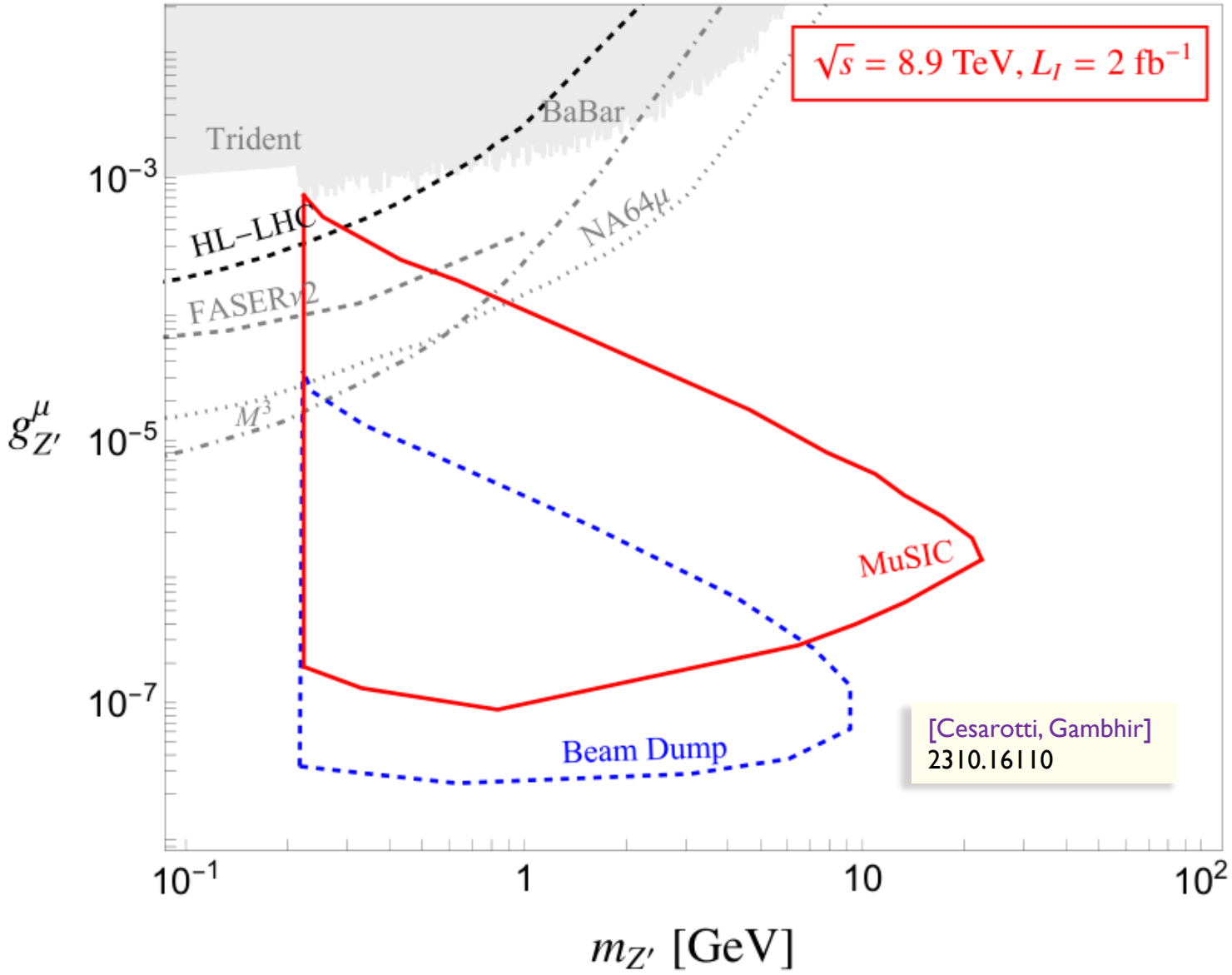

[Cesarotti, Gambhir]
2310.16110

ν_μ magnetic moments: prompt search

Signal:

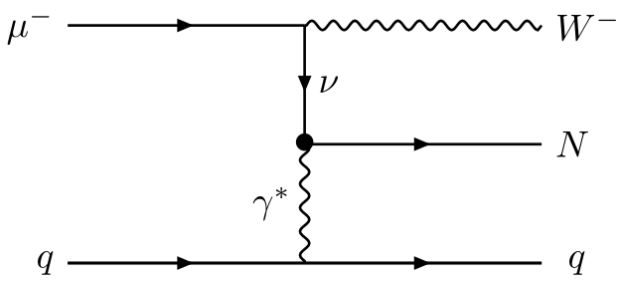

Background:

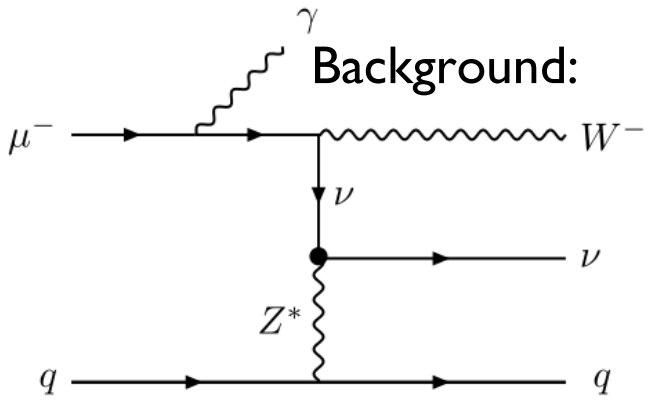

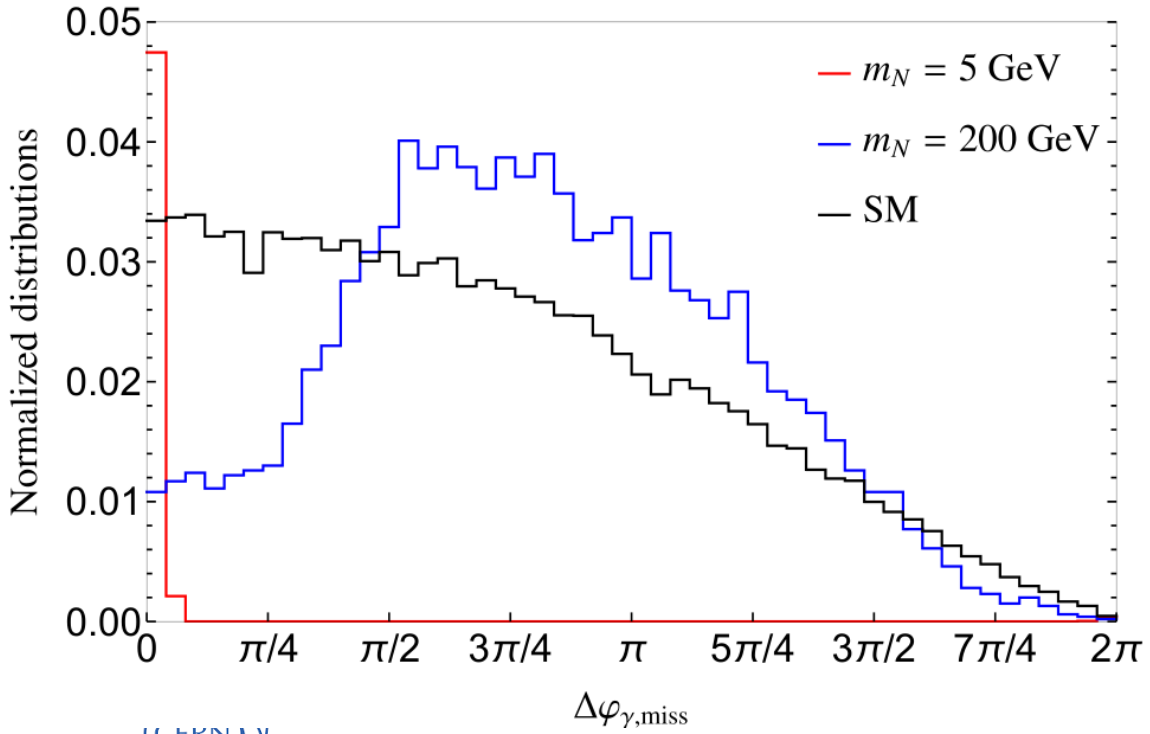

- The HSN is produced via *up-scattering* of SM neutrinos via the dipole operator.
- The HSN subsequently decays to **neutrino+photon**. The missing energy is either collimated or back-to-back with the photon.
- We veto additional neutrinos to suppress the $\nu + \gamma + 3j$ background.

Heavy Sterile Neutrinos: MuSIC vs HL-LHC

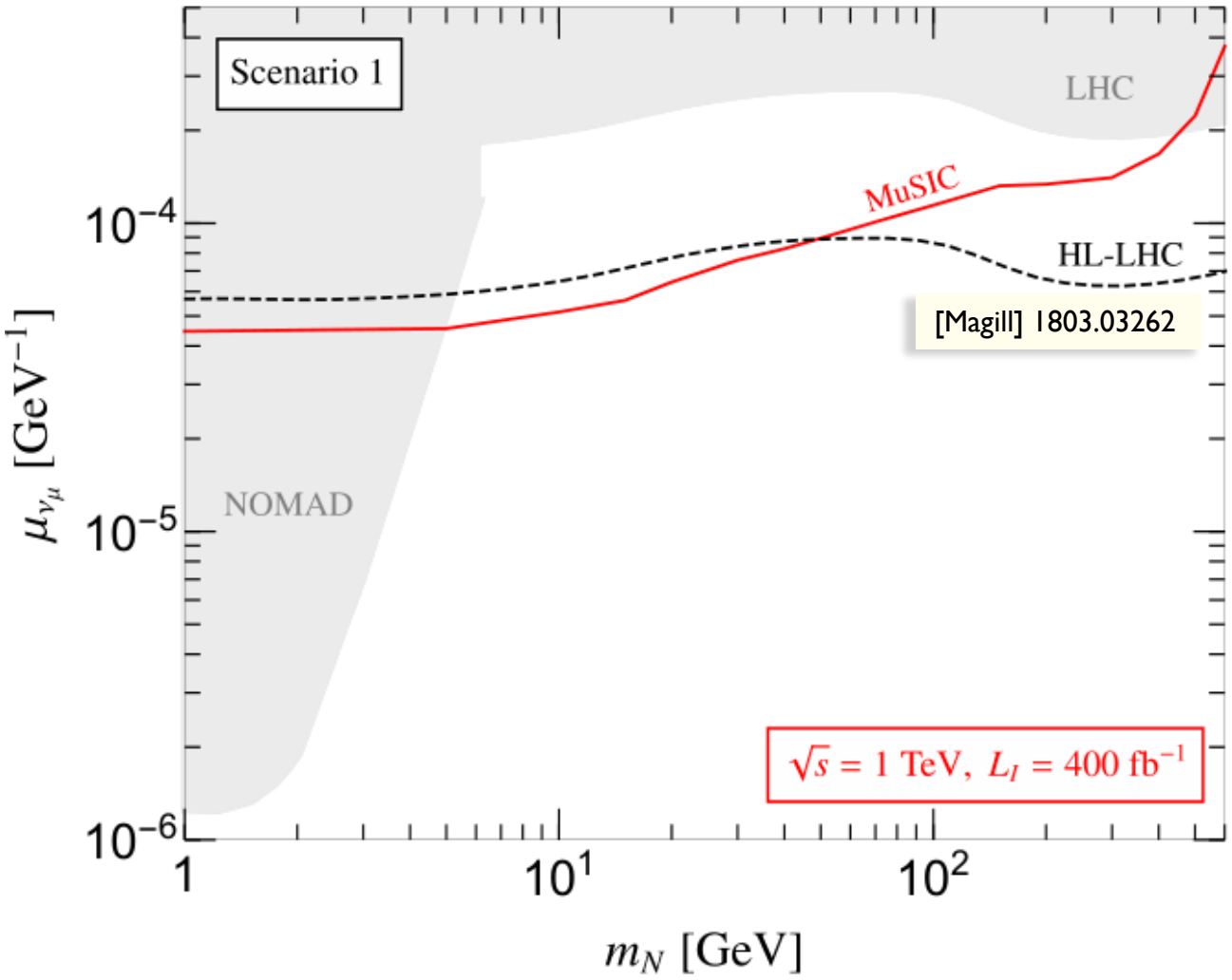

Luminosity Scaling

- Muon Collider:

$$\mathcal{L} \propto \gamma \langle B \rangle \sigma_\delta \frac{N_0}{\epsilon \epsilon_L} f_r N_0 \gamma$$

High energy

High field in collider ring
= small ring
= many collisions

Large energy acceptance
= short bunch
= small betafunction

Dense beam

High beam power

- MuSIC: $\mathcal{L}_{\mu p} = \frac{N^\mu N^p}{4\pi \max[\sigma_x^\mu, \sigma_x^p] \max[\sigma_y^\mu, \sigma_y^p]} \min[f_c^\mu, f_c^p]$

number of particles/beam bunch

bunch frequencies ($f_c^\mu = N_c f_{\text{rep}}$)

$$\sigma_{x,y}^{\mu,p} = \sqrt{\varepsilon_{x,y}^* \beta_{x,y}^* m^{\mu,p} / E^{\mu,p}}$$

amplitude function

transverse emmitance

[Acosta et al] 2203.06258]
[Kaya et al] 1905.05564

MuSIC luminosity estimates

Parameter	Muon	Proton
Energy (TeV)	0.96	0.275
CoM energy (TeV)	1.03	
Bunch intensity (10^{11})	20	3
Norm. emittance, $\varepsilon_{x,y}$ (μm)	25	0.2
$\beta^*_{x,y}$ @IP (cm)	1	5
Trans. RMS beam size, $\sigma_{x,y}$ (μm)	5.2	5.8
Muon repetition rate, f_{rep} (Hz)	15	
Cycles/Collilsions per muon bunch, N_c	3279	
$L_{\mu p}$ ($10^{33}cm^{-2}s^{-1}$)	7	